NACA

RESEARCH MEMORANDUM

EFFECT OF LEADING-EDGE-FLAP DEFLECTION ON THE WING LOADS, LOAD DISTRIBUTIONS, AND FLAP HINGE MOMENTS OF THE DOUGLAS X-3 RESEARCH AIRPLANE AT TRANSONIC SPEEDS

By Earl R. Keener, Norman J. McLeod,
and Norman V. Taillon

High-Speed Flight Station
Edwards, Calif.

NATIONAL ADVISORY COMMITTEE
FOR AERONAUTICS

WASHINGTON
July 15, 1958
Declassified October 28, 1960

NATIONAL ADVISORY COMMITTEE FOR AERONAUTICS

RESEARCH MEMORANDUM

EFFECT OF LEADING-EDGE-FLAP DEFLECTION ON THE WING LOADS, LOAD DISTRIBUTIONS, AND FLAP HINGE MOMENTS OF THE DOUGLAS X-3 RESEARCH AIRPLANE AT TRANSONIC SPEEDS*

By Earl R. Keener, Norman J. McLeod,
and Norman V. Taillon

SUMMARY

Wing loads and load distributions were obtained by differential-pressure measurements between the upper and lower surfaces of the wing of the Douglas X-3 research airplane with various leading-edge-flap deflections. An analysis is presented showing the effect of deflecting the leading-edge flap on the wing characteristics at Mach numbers from 0.55 to 0.9. In addition, the load and hinge-moment characteristics of the leading-edge flap are presented for Mach numbers up to 1.15 with the flap undeflected and for Mach numbers up to 0.9 with the flap deflected.

Deflecting the leading-edge flap affects the chordwise load distribution over about 75-percent chord, and the effects are generally similar at each wing station. The deflected flap delays leading-edge-flow separation to higher angles of attack, and, as a result, the maximum normal-force coefficient is 0.05 to 0.1 greater with flap deflected a nominal 7° at Mach numbers up to 0.76 and about 0.3 greater with the flap deflected a nominal 27° at a Mach number of about 0.55. Below maximum lift, deflecting the flap about 7° does not change the normal-force coefficient appreciably at a given angle of attack; however, the center of pressure is moved rearward over most of the lift range, the rearward displacement increasing with increasing Mach number. No change occurs in the spanwise location of the center of pressure with flap deflection.

Deflecting the flap decreases the flap normal-force and hinge-moment coefficients considerably at a particular angle of attack; however, the maximum normal-force and hinge-moment coefficients increase with flap deflection as a result of the delay in leading-edge-flow separation. The hinge-moment coefficient of the leading-edge flap is an approximately linear function of the normal-force coefficient of the flap.

---

*Title, Unclassified.

Wind-tunnel results from an X-3 model and from models of similar wings show the same effects on the load and pitching-moment characteristics of deflecting the leading-edge flap as are shown by the flight results. The chordwise load distributions from wind tunnel and flight are similar, although at the higher angles of attack the peak loads at the leading edge and flap hinge line are higher for the flight data.

INTRODUCTION

Thin wings used on supersonic aircraft present aerodynamic problems at subsonic speeds as a result of early separation of the flow on the upper surface, beginning at the leading edge (ref. 1). Leading-edge flaps have been shown to improve the landing characteristics of these wings by delaying the leading-edge separation to higher angles of attack, thus increasing the maximum lift (ref. 2). In addition, wind-tunnel tests have shown that a cambered leading edge, such as a deflected leading-edge flap, improves the cruising characteristics of these wings because of an increase in lift-drag ratio for moderate angles of attack (refs. 2 to 4).

As a result of the probable use of leading-edge flaps and cambered leading edges on thin wings, a flight investigation was conducted to determine the effect of deflecting the leading-edge flap on the wing and flap loads and on the detailed load distributions. Utilizing the Douglas X-3 research airplane, the investigation was conducted at the NACA High-Speed Flight Station at Edwards, Calif. The X-3 is a thin wing airplane designed to explore the subsonic and low supersonic Mach number range. The wing is unswept at the 75-percent chord line and has an aspect ratio of 3.09, a taper ratio of 0.39, and a modified 4.5-percent-thick hexagonal section. The leading-edge flap is a plain, constant-chord, full-span flap. References 5 and 6 present an analysis of the wing and flap loads and load distributions obtained by differential-pressure measurements between the upper and lower surfaces of the wing with leading-edge flap undeflected and some preliminary results with leading-edge flap deflected. The data herein supplement the previous data by presenting a more complete analysis of the effects of deflecting the leading-edge flap over a Mach number range of 0.5 to 0.9. In addition, the load and hinge-moment characteristics of the leading-edge flap are presented for Mach numbers up to 1.15 with flap undeflected and for Mach numbers up to 0.90 with the flap deflected. For these tests the flaps were deflected down a nominal 7° at Mach numbers up to 0.9 and a nominal 27° at Mach numbers up to 0.7. A brief comparison with wind-tunnel results is presented.

SYMBOLS

$b/2$	wing semispan, ft
$b'/2$	wing-panel span, spanwise distance from first row of orifices (0.301b/2) to wing tip, ft
C_b'	wing-panel bending-moment coefficient about 0b'/2, $\int_0^1 c_n \frac{c}{c'_{av}} \frac{2y'}{b'} d \frac{2y'}{b'}$
C_{h_f}	leading-edge-flap hinge-moment coefficient, $\int_0^1 c_{h_f} d \frac{2y'}{b'}$
C_m'	wing-panel pitching-moment coefficient about $0.25\bar{c}'$, $\frac{c'_{av}}{\bar{c}'} \int_0^1 c_m' \left(\frac{c}{c'_{av}}\right)^2 d \frac{2y'}{b'}$
C_{N_A}	airplane normal-force coefficient, Wn/qS
C_N'	wing-panel normal-force coefficient, $\int_0^1 c_n \frac{c}{c'_{av}} d \frac{2y'}{b'}$
C_{N_f}	leading-edge-flap normal-force coefficient, $\int_0^1 c_{n_f} d \frac{2y'}{b'}$
C_p	differential-pressure coefficient, $\frac{p_l - p_u}{q}$
c	local wing chord, streamwise, ft
$\bar{c}'$	mean aerodynamic chord of wing panel, $2/S' \int_0^{b'/2} c^2 dy'$, ft
c'_{av}	average chord of wing panel, ft
c_f	local leading-edge-flap chord, streamwise, ft

c_{h_f} leading-edge-flap section hinge-moment coefficient,
$$\int_0^1 C_p\left(1 - \frac{x}{c_f}\right)d\,\frac{x}{c_f}$$

c_m wing-section pitching-moment coefficient about 0.25c,
$$\int_0^1 C_p\left(0.25 - \frac{x}{c}\right)d\,\frac{x}{c}$$

c_m' section pitching-moment coefficient about line perpendicular to longitudinal axis of airplane, passing through $0.25\bar{c}'$, $c_m + 0.50(1 - \bar{c}'/c)c_n$

c_n wing-section normal-force coefficient, $\int_0^1 C_p\,d\,\frac{x}{c}$

c_{n_f} leading-edge-flap section normal-force coefficient, $\int_0^1 C_p\,d\,\frac{x}{c_f}$

g acceleration due to gravity, ft/sec^2

M free-stream Mach number

n normal-load factor, g units

p_l local static pressure on lower wing surface, lb/sq ft

p_u local static pressure on upper wing surface, lb/sq ft

q free-stream dynamic pressure, lb/sq ft

S total wing area, including area projected through fuselage, sq ft

S'/2 area of wing panel (outboard of 0.301b/2), sq ft

W airplane weight, lb

x chordwise distance rearward of leading edge of local chord, ft

x_{cp} chordwise location of center of pressure of wing section, $(0.25 - c_m/c_n)100$, percent c

x'_{cp} chordwise location of center of pressure of wing panel from leading edge of $\bar{c}'$, $(0.25 - C_m'/C_N')100$, percent $\bar{c}'$

y' spanwise distance outboard of $0b'/2$, ft

y'_{cp} spanwise location of center of pressure of wing panel, $(C_b'/C_N')100$, percent $b'/2$

α measured airplane angle of attack, deg

δ_{a_L} left aileron position, deg

δ_f leading-edge-flap position, deg

DESCRIPTION OF AIRPLANE AND WING PANEL

A three-view drawing presenting the overall dimensions of the Douglas X-3 research airplane is shown in figure 1. Photographs of the airplane, including several views of the wing with the leading-edge flap deflected, are shown in figure 2. The physical characteristics of the airplane, wing panel, and leading-edge flap are given in table I. The leading-edge flap is normally used during the landing approach in the full-down position in combination with the trailing-edge flaps.

A drawing of the wing and leading-edge flap is shown in figure 3. The wing has an aspect ratio of 3.09, a taper ratio of 0.39, and zero incidence, dihedral, and twist. The common-chord line at 75-percent local chord is unswept. The wing section is a 4.5-percent-thick modified hexagonal airfoil with vertices at 30- and 70-percent chord. Modifications to the airfoil consisted of a 188-inch radius at 30- and 70-percent chord and a small radius at the leading and trailing edges, as shown in table II. As a result, the wing-section ordinates vary along the span. Table II includes the ordinates of the wing section at five spanwise stations corresponding to the location of the rows of static-pressure orifices. The test panel of the wing over which pressures were measured consists of the portion of the left wing outboard of the first row of orifices $(0.301b/2)$.

The leading-edge flap has a constant streamwise chord of 12.5 inches and extends from the fuselage to the wing tip. Two control-actuator fairings are located on the bottom surface of each wing, as shown in figures 1 and 3. The flap may be deflected to either of two nominal positions; the actual deflection in each position varies slightly under load, generally less than ±2°. During these tests the average deflections for the two positions were 7° and 27°, respectively. Twist in the leading-edge flap is estimated from static tests to be less than 1° with flap undeflected and less than 2° with flap deflected. Structural limitations prohibited the deflection of the leading-edge flap at Mach numbers above 0.7 for 27° deflection and 0.9 for 7° deflection.

INSTRUMENTATION AND ACCURACY

Standard NACA film-recording instruments were used to record the wing differential pressures, indicated free-stream static and dynamic pressures, normal acceleration, angle of attack, angle of sideslip, aileron position, leading-edge-flap position, and rolling and pitching angular velocities and accelerations. The indicated free-stream static and dynamic pressures were obtained from a standard NACA airspeed head mounted on a nose boom, and the static-pressure error was determined in flight. Angles of attack and sideslip were measured by vanes mounted on the nose boom. Leading-edge-flap position was measured at the inboard control actuator. All instruments were correlated by a common timer.

Flush-type static-pressure orifices installed in the left wing were arranged in five streamwise rows. The chordwise locations of the orifices are given in table III, and the spanwise locations are shown in figure 3. The orifices were connected by tubing through the wing to multicell mechanical manometers in the instrument compartment. Lag in the pressure-recording system was determined by the method for photographic instruments presented in reference 7 and was checked in flight by comparing pressure measurements from abrupt and gradual maneuvers. The lag was found to be negligible for the data presented in this paper.

Estimated maximum errors of the pertinent recorded quantities and the resulting coefficients are:

M	±0.01
Differential-pressure measurements, $p_l - p_u$, lb/sq ft	±7
n	±0.05
δ_f and δ_{a_L}, deg	±0.2
C_p	±0.02
c_n	±0.03
c_m	±0.01
c_{n_f}	±0.05

c_{h_f}	± 0.03
C_{N_A}	± 0.02
$C_N{}'$	± 0.04
$C_m{}'$	± 0.02
C_{N_f}	± 0.07
C_{h_f}	± 0.05

TESTS

The data presented were obtained from wind-up turns at Mach numbers from 0.71 to 1.14 at an altitude of about 30,000 feet and from level-flight stall approaches at an altitude of about 20,000 feet during which the Mach number decreased from 0.65 to 0.45. Tests with the leading-edge flap deflected were conducted to the maximum Mach number prescribed by structural limitations. Reynolds number based on the mean aerodynamic chord of the wing varied between 16×10^6 and 26×10^6.

DATA REDUCTION AND PRESENTATION

Automatic digital computing equipment was used to obtain pressure coefficients from the recorded data and to perform the chordwise and spanwise integrations necessary to obtain the normal-force and pitching-moment coefficients. The leading-edge-flap normal-force and hinge-moment coefficients were obtained by integrating the load distributions ahead of the hinge line. Since the orifice rows are streamwise, the flap section characteristics are for sections that are not normal to the hinge line as is usually desired; however, the differences between the values obtained for the streamwise sections and the values that would be obtained for normal sections are considered to be negligible. Finally, it should be noted that for $\delta_f \approx 27^\circ$ an appreciable error occurred in the wing-section normal-force coefficient obtained by integrating the differential pressures. As a result, a correction was made by resolving the normal force of the flap to its component normal to the wing chord. A similar correction was made to the wing-section pitching-moment coefficient. The error for $\delta_f \approx 7^\circ$ was considered to be negligible.

The pressure coefficients and aerodynamic characteristics obtained from the wing differential-pressure measurements are tabulated in tables IV to VI for $\delta_f = 0^\circ$, 7°, and 27° at $M \approx 0.55$. These data were obtained from stall approaches in which the actual Mach number decreased from about 0.65 to 0.45. Tables VII and VIII present the data for $\delta_f \approx 7^\circ$ at $M \approx 0.85$ and 0.90, respectively. Data for $\delta_f = 0^\circ$ at Mach numbers of 0.71 to 1.15 and for $\delta_f \approx 7^\circ$ at $M \approx 0.71$, 0.76, and 0.80 are tabulated in reference 6. The leading-edge-flap normal-force and hinge-moment coefficients are presented in tables IX to XI.

RESULTS AND DISCUSSION

Chordwise Load Distributions

Representative chordwise load distributions selected from the tabulated data for leading-edge flap deflected are presented as oblique projections in figure 4. This figure will be used throughout the discussion to explain some of the results. Included in figure 4 are the load distributions for $\delta_f = 0^\circ$ to show the effect of deflecting the leading-edge flap.

$\delta_f \approx 7^\circ$.- At Mach numbers of approximately 0.55 and 0.71 (figs. 4(a) and (b)) only a moderate change is evident in the chordwise load distributions over most of the lift range when the leading-edge flap is deflected about 7°. However, at $\alpha \approx 3^\circ$ ($M \approx 0.71$) the loading at the leading edge is noticeably reduced when the flap is deflected, and the loading at the hinge is increased. Deflecting the flap produces similar results at all wing stations, except for some flap end effect at the leading edge of the inboard station. The deflected flap affects the pressures over about 75 percent of the local chord.

At $M \approx 0.90$ (fig. 4(c)) deflecting the flap causes a larger change in the leading-edge loading at the lower angles of attack; however, at $\alpha = 9^\circ$ the effect is greatly reduced. Data for $\delta_f \approx 7^\circ$ were not obtained above $\alpha = 9^\circ$ at $M \approx 0.90$.

$\delta_f \approx 27^\circ$.- When the leading-edge flap is deflected about 27° at $M \approx 0.55$ (fig. 4(a)), a larger change occurs in the chordwise load distributions than for $\delta_f \approx 7^\circ$. At the lower angles of attack a large negative load occurs at the leading edge, changing rapidly to a large positive load as a result of the expansion of the flow over the hinge line. As the angle of attack increases, the loading near the leading edge becomes positive and increases continuously to the maximum angles of attack measured. As for $\delta_f \approx 7^\circ$, the result of deflecting the flap is similar at all wing stations, and the deflected flap affects the pressures over about 75 percent of the local chord.

Leading-edge-separation boundary.- The effects of leading-edge-flow separation on the characteristics of the X-3 wing are discussed in reference 6, and an approximate boundary for separation with leading-edge flap undeflected is presented. It is shown that the leading-edge-flow separation starts at low angles of attack and results in low values of maximum lift at Mach numbers up to about 0.9; however, above this Mach number the flow around the leading edge remains attached up to high angles of attack and results in high values of maximum lift.

A similar boundary illustrating the effect of leading-edge-flap deflection on leading-edge separation is presented herein. In determining the boundary, the resulting loss in local lift at the leading edge was used to determine the approximate angle of attack for leading-edge-flow separation. Figure 5 shows representative plots of C_p against α at three wing stations for the orifice closest to the leading edge for both flap undeflected and flap deflected. The angle of attack at which C_p ceased to increase with increasing angle of attack was taken to be indicative of leading-edge-flow separation. At $M \approx 0.55$ with flap undeflected, separation had already occurred at the lowest angle of attack for these tests, and at $M = 0.85$ the angle of attack reached with flap deflected in these tests was not sufficient to cause separation.

In all cases shown in figure 5, deflecting the leading-edge flap results in a higher angle of attack being reached before separation; the effects of this on the chordwise load distributions may be seen in figure 4. The delay in separation explains the larger loading at the leading edge for $\delta_f \approx 7^\circ$ than for $\delta_f = 0^\circ$ at moderate angles of attack and Mach numbers of about 0.55 and 0.71.

Figure 6 shows the resulting boundaries for leading-edge-flow separation for the root, midsemispan, and tip orifice stations determined from data typical of those shown in figure 5. Deflecting the leading-edge flap about 7° at Mach numbers between 0.7 and 0.8 delays the onset of leading-edge-flow separation to an angle of attack about 4° greater than for $\delta_f = 0^\circ$. Deflecting the flap 27° results in a still larger increase in angle of attack before separation at the midsemispan and tip stations; no separation was indicated at the root station. It may be noted that separation did not occur simultaneously at all spanwise stations across the wing for either flap undeflected or deflected. The effect of Mach number is large; for $\delta_f \approx 7^\circ$ the minimum angle of attack for separation occurs at a Mach number near 0.7. At $\delta_f = 0^\circ$ and Mach numbers below 0.7 the boundary for leading-edge separation could not be established because separation had already occurred at the lowest angle of attack of these tests.

Wing-Section and Wing-Panel Characteristics

The effect of deflecting the leading-edge flap on the normal-force coefficient, pitching-moment coefficient, and center of pressure of the wing section at root, midsemispan, and tip orifice stations is shown in figure 7. The effect of flap deflection on the wing-panel characteristics for the same conditions is presented in figure 8.

Normal-force coefficient.- Deflecting the leading-edge flap about 7° has little effect on the section and panel normal-force curves except at angles of attack near the stall. This is explained by the chordwise load distributions of figure 4 which show that when the flap is deflected 7° at low angles of attack the load decreases near the leading edge, but increases over the hinge line. Conversely, at the higher angles of attack the load increases near the leading edge as a result of the delay in leading-edge-flow separation, but decreases behind the hinge line. In either case, total load changes only slightly; however, the maximum C_N' (fig. 8(a)) is increased about 0.05 to 0.1 in the Mach number range up to 0.76 as a result of the delay in leading-edge-flow separation. At the higher Mach numbers no conclusions can be drawn from the data obtained concerning maximum C_N' in figure 8(a), since maximum C_N' was not reached with either flap undeflected or deflected.

Deflecting the leading-edge flap 27° at $M \approx 0.55$ decreases the normal-force coefficient slightly at the root and tip wing sections throughout most of the angle-of-attack range; however, a large increase in the maximum normal-force coefficient that is obtainable is realized as a result of the delay in leading-edge-flow separation. Maximum obtainable C_N' increases from about 0.67 for $\delta_f = 0^{\circ}$ to about 0.95 for $\delta_f \approx 27^{\circ}$.

Pitching-moment coefficient.- As a result of the change in chordwise load distribution when the leading-edge flap is deflected about 7°, the section and panel pitching-moment curves are shifted in the negative direction over most of the lift range as the center of pressure is moved rearward by the deflected flap (figs. 7 and 8(b)). Flap deflection also delays to a higher normal-force coefficient the strong nose-down moment that occurs near maximum lift. Increasing the flap deflection to 27° at $M \approx 0.55$ increases the effects noted for $\delta_f \approx 7^{\circ}$.

Bending-moment coefficient.- The bending-moment coefficient of the wing panel experiences no change when the leading-edge flap is deflected (fig. 8(c)).

Center of pressure.- As a result of the change in chordwise load distribution when the leading-edge flap is deflected, the chordwise position of the center of pressure is rearward of that for $\delta_f = 0^\circ$ over most of the lift range (figs. 7 and 8(d)). The effect of Mach number for $\delta_f \approx 7^\circ$ is to increase the rearward displacement. At high lift the center of pressure with the flap deflected is slightly forward of that for $\delta_f = 0^\circ$. The spanwise position of the center of pressure is unaffected by flap deflection (fig. 8(e)).

Span Load and Pitching-Moment Distributions

Reference 6 shows that the span load distribution with leading-edge flap undeflected is nearly elliptic for most of the lift range. Figure 9 shows that deflecting the leading-edge flap has little effect on the span load distribution below wing stall. This results, of course, from the previously noted fact that deflecting the flap has little effect on the wing-section normal-force coefficient or the spanwise position of the center of pressure.

Figure 10 shows that deflecting the leading-edge flap has little effect on the shape of the pitching-moment distribution, because the previously mentioned change in the pitching moment at each wing section occurs almost uniformly over the span.

Leading-Edge-Flap Characteristics

The variation of the flap normal-force coefficient and hinge-moment coefficient with angle of attack for leading-edge flap undeflected and deflected is presented for the root, midsemispan, and tip sections in figure 11 and for the total flap in figure 12. In addition, the variation of C_{h_f} with C_{N_f} is shown in figure 13. The data cover the Mach number range from 0.55 to 1.15. When the leading-edge flap is undeflected, the variation of the section and total normal-force and hinge-moment coefficients with angle of attack is approximately linear up to maximum normal-force coefficient at the lower Mach numbers. As the Mach number increases, the curves become increasingly nonlinear. As would be expected, the angle of attack for maximum flap-section normal-force coefficient correlates closely with the leading-edge-separation boundary shown in figure 6. Above $M = 0.9$ no leading-edge separation is indicated and a maximum normal-force coefficient is not reached. The magnitudes of c_{n_f} and C_{N_f} are naturally much larger than the corresponding magnitudes of c_n and C_N', since the forward portion of the wing carries the greater percentage of the load. Also, at the lower Mach numbers, the flap loading is noticeably greater inboard than at the tip.

In general, deflecting the flap decreases the load and hinge moment at a given angle of attack, but noticeably increases the maximum load and hinge moment as a result of the delay in the leading-edge-flow separation.

The direct dependence of hinge moment on normal force is shown in figure 13 in which C_{h_f} is an approximately linear function of C_{N_f} for both flap undeflected and flap deflected, indicating very little change in center of pressure for the flap.

Comparison With Wind-Tunnel Data

A comparison of the flight data with the wind-tunnel data of reference 8 for a 0.16-scale model of the X-3 is presented in figures 14 to 16 for $M = 0.55$ to 0.90 with the leading-edge flap deflected. A comparison of similar data for $\delta_f = 0^{\circ}$ was made in reference 6, where good agreement was obtained at Mach numbers below 0.90. Figure 14 presents chordwise load distributions for midsemispan stations of the wing for both flight and wind-tunnel data. In general, the chordwise load distributions from wind-tunnel and flight are similar for both $\delta_f \approx 7^{\circ}$ and $\delta_f \approx 27^{\circ}$, although at the higher angles of attack the peak pressures at the leading edge and at the flap hinge line are higher for the flight data than predicted by the wind-tunnel tests, and the pressures rearward of 40-percent chord are lower than predicted. Figures 15 and 16 present the variation of c_n, c_{n_f}, and c_{h_f} with angle of attack for the midsemispan stations of the wing for both flight and wind-tunnel data. The wind-tunnel data were obtained by integrating the pressure distributions presented in reference 8.

Other wind-tunnel results from an X-3 model (ref. 9) and from models of thin wings similar to the X-3 (refs. 2 to 4) show the same effects on the load and pitching-moment characteristics of deflecting the leading-edge flap as discussed herein, although maximum lift coefficient is about 0.1 higher for the wind-tunnel models.

CONCLUDING REMARKS

Wing loads and load distributions were obtained by pressure measurements over the wing of the Douglas X-3 research airplane with leading-edge flap deflected. The data cover the angle-of-attack range of the airplane at Mach numbers up to 0.90 with the flap deflected. In addition, the normal-force and hinge-moment characteristics of the leading-edge flap are presented for Mach numbers up to 1.15 with flap undeflected, as well as for Mach numbers up to 0.90 with flap deflected.

Deflecting the leading-edge flap affects the chordwise load distribution over about 75-percent chord, and the effects are generally similar at each wing station. The deflected flap delays leading-edge-flow separation to higher angles of attack, and, as a result, the maximum normal-force coefficient is 0.05 to 0.1 greater with flap deflected a nominal 7° at Mach numbers up to 0.76 and about 0.3 greater with the flap deflected a nominal 27° at a Mach number of about 0.55. Below maximum lift, deflecting the flap about 7° does not change the normal-force coefficient appreciably at a given angle of attack; however, the center of pressure is moved rearward over most of the lift range, the rearward displacement increasing with increasing Mach number. No change occurs in the spanwise location of the center of pressure with flap deflection.

Deflecting the flap decreases the flap normal-force and hinge-moment coefficients considerably at a particular angle of attack; however, the maximum normal-force and hinge-moment coefficients increase with flap deflection as a result of the delay in leading-edge-flow separation. The hinge-moment coefficient of the leading-edge flap is an approximately linear function of the normal-force coefficient of the flap.

Wind-tunnel results from an X-3 model and from models of similar wings show the same effects on the load and pitching-moment characteristics of deflecting the leading-edge flap as are shown by the flight results. The chordwise load distributions from wind tunnel and flight are similar, although at the higher angles of attack the peak loads at the leading edge and flap hinge line are higher for the flight data.

High-Speed Flight Station,
National Advisory Committee for Aeronautics,
Edwards, Calif., April 14, 1958.

REFERENCES

1. McCullough, George B., and Gault, Donald E.: Examples of Three Representative Types of Airfoil-Section Stall at Low Speed. NACA TN 2502, 1951.

2. Johnson, Ben H., Jr., and Reed, Verlin D.: Investigation of a Thin Wing of Aspect Ratio 4 in the Ames 12-Foot Pressure Wind Tunnel. IV - The Effect of a Constant-Chord Leading-Edge Flap at High Subsonic Speeds. NACA RM A8K19, 1949.

3. Heitmeyer, John C.: Effect of a Leading-Edge Flap Upon the Lift, Drag, and Pitching Moment of an Airplane Employing a Thin, Unswept, Wing. NACA RM A54B16, 1954.

4. Schmeer, James W.: Effect of Leading-Edge Droop on the Aerodynamic and Loading Characteristics of a 4-Percent-Thick Unswept-Wing-Fuselage Combination at Transonic Speeds. NACA RM L56C14, 1956.

5. Jordan, Gareth H., and Hutchins, C. Kenneth, Jr.: Preliminary Flight-Determined Pressure Distributions Over the Wing of the Douglas X-3 Research Airplane at Subsonic and Transonic Mach Numbers. NACA RM H55A10, 1955.

6. Keener, Earl R., and Jordan, Gareth H.: Wing Loads and Load Distributions Throughout the Lift Range of the Douglas X-3 Research Airplane at Transonic Speeds. NACA RM H56G13, 1956.

7. Huston, Wilber B.: Accuracy of Airspeed Measurements and Flight Calibration Procedures. NACA Rep. 919, 1948.

8. Cleary, Joseph W., and Mellenthin, Jack A.: Wind-Tunnel Tests of a 0.16-Scale Model of the X-3 Airplane at High Subsonic Speeds - Wing and Fuselage Pressure Distribution. NACA RM A50D07, 1950.

9. Hamilton, William T., and Cleary, Joseph W.: Wind-Tunnel Tests of a 0.16-Scale Model of the X-3 Airplane at High Subsonic Speeds - Stability and Control Characteristics. NACA RM A50A03, 1950.

TABLE I.- PHYSICAL CHARACTERISTICS OF THE DOUGLAS X-3 AIRPLANE

Wing:	
Airfoil section	Modified hexagon
Airfoil thickness ratio, percent chord	4.5
Total area, sq ft	166.50
Span, ft	22.69
Mean aerodynamic chord (wing station 4.81 ft), ft	7.84
Root chord, ft	10.58
Tip chord (extended), ft	4.11
Taper ratio	0.39
Aspect ratio	3.09
Sweep at 0.75 chord line, deg	0
Sweep at leading edge, deg	23.16
Sweep at trailing edge, deg	-8.12
Incidence, deg	0
Dihedral, deg	0
Geometric twist, deg	0
Leading-edge flap:	
Type	Plain
Area (each), sq ft	8.38
Span at hinge line (each), ft	8.916
Chord, normal to hinge line, in.	11.49
Travel, leading edge down, deg	30
Wing panel (outboard of wing station 3.415 ft):	
Area (one panel), sq ft	50.42
Span (one panel), ft	7.93
Mean aerodynamic chord (wing station 6.85 ft), ft	6.68
Average chord, ft	6.37
Horizontal tail:	
Airfoil section	Modified hexagon
Airfoil thickness ratio at root chord, percent chord	8.01
Airfoil thickness ratio outboard of station 26, percent chord	4.50
Total area, sq ft	43.24
Span, ft	13.77
Mean aerodynamic chord, ft	3.34
Root chord, ft	4.475
Tip chord, ft	1.814
Taper ratio	0.405
Aspect ratio	4.38
Sweep at leading edge, deg	21.14
Sweep at trailing edge, deg	0
Dihedral, deg	0
Travel:	
Leading edge up, deg	6
Leading edge down, deg	17
Hinge-line location, percent root chord	46.46
Vertical tail:	
Airfoil section	Modified hexagon
Airfoil thickness ratio, percent chord	4.5
Area, sq ft	23.73
Span, (from horizontal-tail hinge line), ft	5.59
Mean aerodynamic chord, ft	4.69
Root chord, ft	6.508
Tip chord, ft	1.93
Taper ratio	0.292
Aspect ratio	1.315
Sweep at leading edge, deg	45
Sweep at trailing edge, deg	9.39
Rudder:	
Area, rearward of hinge line, sq ft	5.441
Span at hinge line, ft	3.535
Root chord, ft	1.98
Tip chord, ft	1.097
Travel, deg	±20
Fuselage:	
Length including boom, ft	66.75
Maximum width, ft	6.08
Maximum height, ft	4.81
Base area, sq ft	7.94
Powerplant:	
Engines	Two Westinghouse J34-WE-17 with afterburner
Rating, each engine:	
Static sea-level maximum thrust, lb	4,850
Static sea-level military thrust, lb	3,370
Airplane weight, lb:	
Basic (without fuel, oil, water, pilot)	16,120
Total (full fuel, oil, water, no pilot)	21,900
Center-of-gravity location, percent mean aerodynamic chord:	
Basic weight - gear down	2.63
Total weight - gear down	4.59
Total weight - gear up	3.91

TABLE II

PROFILE AND ORDINATES OF THE WING SECTIONS AT THE ORIFICE STATIONS

[Modified 4.5-percent-thick hexagonal airfoil]

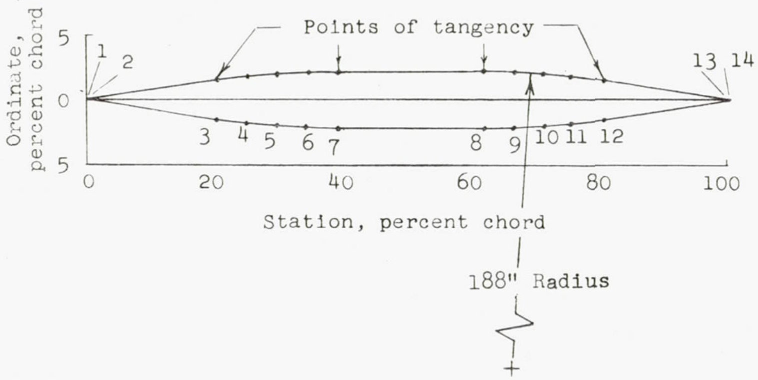

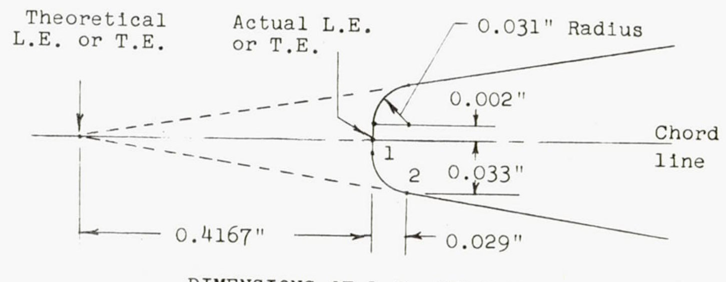

DIMENSIONS OF L.E. AND T.E.
(Same at all stations)

Stations and ordinates in percent of local chord

Station number	Row 1		Row 2		Row 3		Row 4		Row 5	
	Station	Ordinate	Station	Ordinate	Station	Ordinate	Station	Ordinate	Station	Ordinate
1	0	±0.002	0	±0.002	0	±0.003	0	±0.003	0	±0.004
2	.028	±.032	.032	±.036	.037	±.042	.043	±.049	.052	±.059
3	22.382	±1.709	21.333	±1.634	19.948	±1.536	18.238	±1.414	15.998	±1.255
4	25.990	±1.946	25.438	±1.904	24.709	±1.848	23.812	±1.781	22.643	±1.691
5	29.604	±2.115	29.549	±2.096	29.477	±2.072	29.466	±2.041	29.300	±2.002
6	33.219	±2.216	33.663	±2.212	34.248	±2.206	34.969	±2.198	35.960	±2.189
7	36.836	±2.250	37.779	±2.250	39.023	±2.250	40.554	±2.250	42.625	±2.251
8	63.602	±2.250	62.721	±2.250	61.558	±2.250	60.120	±2.250	58.264	±2.251
9	67.000	±2.218	66.587	±2.214	66.043	±2.208	65.365	±2.201	64.524	±2.192
10	70.397	±2.123	70.451	±2.105	70.526	±2.082	70.610	±2.053	70.782	±2.016
11	73.791	±1.964	74.314	±1.925	75.005	±1.872	75.850	±1.809	77.035	±1.725
12	77.183	±1.741	78.172	±1.671	79.480	±1.579	81.116	±1.465	83.282	±1.314
13	99.972	±.032	99.968	±.036	99.962	±.042	99.953	±.049	99.998	±.059
14	100.000	±.002	100.000	±.002	100.000	±.003	100.000	±.003	100.000	±.004

TABLE III

CHORDWISE LOCATIONS OF THE STATIC PRESSURE ORIFICES

[Percent local chord]

Row	1			2			3			4			5		
Orifice	Upper	Lower	Average	Upper	Lower	Average	Upper	Lower	Average	Upper	Lower	Average	Upper	Lower	Average
1	2.1	2.1	2.1	2.6	2.2	2.4	2.5	2.5	2.5	2.5	2.5	2.5	5.2	5.2	5.2
2	5.0	5.0	5.0	4.9	4.7	4.8	4.8	4.9	4.9	5.0	5.0	5.0	7.4	7.5	7.5
3	7.8	7.6	7.7	7.6	7.5	7.6	7.3	7.4	7.4	7.4	7.5	7.5	14.4	14.2	14.3
4	9.3	9.0	9.2	10.0	9.9	10.0	10.1	10.1	10.1	10.2	10.3	10.3	24.6	25.0	24.8
5	15.3	15.1	15.2	15.2	15.2	15.2	17.8	18.0	17.9	13.9	13.9	13.9	29.0	29.5	29.3
6	20.0	19.9	20.0	21.3	21.2	21.3	20.2	20.3	20.3	20.5	20.5	20.5	37.9	38.0	38.0
7	25.0	24.9	25.0	24.9	24.8	24.9	24.4	24.4	24.4	25.1	25.2	25.2	47.3	47.5	47.4
8	29.5	29.6	29.6	33.1	32.8	33.0	29.5	29.6	29.6	29.2	29.4	29.3	61.9	62.0	62.0
9	37.4	37.4	37.4	38.1	37.8	38.0	37.9	37.9	37.9	37.9	37.9	37.9	68.2	68.3	68.3
10	47.6	47.5	47.6	47.5	47.3	47.4	47.4	47.4	47.4	47.3	47.5	47.4	75.6	75.7	75.7
11	55.5	55.4	55.5	55.0	54.5	54.8	55.0	55.0	55.0	54.8	54.9	54.9	79.9	80.2	80.1
12	62.0	62.0	62.0	62.0	61.8	61.9	64.6	64.5	64.6	61.8	61.9	61.9	84.5	84.7	84.6
13	69.0	69.0	69.0	68.9	68.7	68.8	68.7	68.7	68.7	68.4	68.5	68.5	90.0	90.0	90.0
14	74.2	74.1	74.2	74.2	74.0	74.1	74.1	74.0	74.1	75.3	75.5	75.4	92.4	92.4	92.4
15	80.0	80.0	80.0	80.0	79.8	79.9	80.0	80.0	80.0	79.8	80.0	79.9	97.4	97.4	97.4
16	85.4	85.0	85.2	85.0	84.8	84.9	85.0	84.9	85.0	84.8	85.0	84.9			
17	90.0	90.0	90.0	90.0	90.0	90.0	90.0	90.0	90.0	90.0	90.0	90.0			
18	92.5	92.5	92.5	92.6	92.4	92.5	92.5	92.5	92.5	92.4	92.4	92.4			
19	98.3	98.1	98.2	97.9	97.9	97.9	97.7	97.7	97.7	97.4	97.4	97.4			

Note: Orifices above dashed line are on the leading-edge flap.

TABLE IV.- PRESSURE COEFFICIENTS AND AERODYNAMIC CHARACTERISTICS OF THE DOUGLAS X-3 WING

$\left[M \approx 0.55;\ \delta_f \approx 0^\circ\right]$

(a) $M = 0.64$ $\quad \alpha = 7.6^\circ$
$C_{N_A} = 0.40$ $\quad \delta_{a_L} = .1^\circ$ up
$\delta_f = 0^\circ$

Orifice	Row				
	1	2	3	4	5
1	2.310	2.385	1.500	1.368	1.096
2	1.800	2.265	1.385	1.271	1.054
3	1.385	1.834	1.320	1.258	.884
4	1.288	1.210	1.212	1.169	.663
5	.764	.725	1.044	1.061	.590
6	.621	.559	1.008	.861	.390
7	.501	.514	.831	.751	.263
8	.437	.383	.805	.758	.083
9	.343	.345	.524	.506	.042
10	.257	.296	.361	.372	-.056
11	.203	.218	.253	.286	.014
12	.156	.176	.070	.152	.043
13	.113	.106	.049	.042	-.027
14	.153	.113	.045	-.056	.042
15	.034	.063	.021	-.036	-.029
16	.035	.061	.028	-.021	
17	.022	.056	.042	.049	
18	-.014	.014	-.021	-.014	
19	.041	.056	.065	.014	
c_n	0.433	0.458	0.479	0.444	0.358
c_m	.0174	.0179	.0073	.0137	.0140

$C_N{}' = 0.429$ $\quad x'_{cp} = 20.9$
$C_m{}' = .0177$
$C_b{}' = .180$ $\quad y'_{cp} = 42.0$

(b) $M = 0.59$ $\quad \alpha = 8.5^\circ$
$C_{N_A} = 0.47$ $\quad \delta_{a_L} = .4^\circ$ up
$\delta_f = 0^\circ$

Orifice	Row				
	1	2	3	4	5
1	2.298	2.275	1.548	1.447	1.125
2	2.132	2.226	1.416	1.363	1.097
3	1.781	1.933	1.389	1.283	.938
4	1.628	1.620	1.251	1.296	.721
5	.959	.979	1.109	1.129	.683
6	.693	.740	1.066	.911	.486
7	.571	.620	.940	.846	.378
8	.463	.443	.900	.853	.123
9	.371	.409	.654	.599	.083
10	.296	.342	.476	.490	-.058
11	.214	.258	.316	.373	.042
12	.201	.184	.125	.213	.042
13	.126	.109	.075	.059	.033
14	.165	.117	.069	-.033	.033
15	.049	.058	.042	-.051	.026
16	.049	.073	.074	.000	
17	.034	.041	.008	.041	
18	.000	.025	.033	.025	
19	.033	.041	.086	.000	
c_n	0.500	0.522	0.541	0.506	0.419
c_m	.0198	.0186	-.0053	.0059	.0017

$C_N{}' = 0.490$ $\quad x'_{cp} = 22.1$
$C_m{}' = .0144$
$C_b{}' = .206$ $\quad y'_{cp} = 42.1$

TABLE IV.- Continued.

[$M \approx 0.55$; $\delta_f \approx 0°$]

(c) $M = 0.55$ $\quad \alpha = 9.4°$
$C_{N_A} = 0.54$ $\quad \delta_{a_L} = 0$
$\delta_f = 0°$

Orifice	Row				
	1	2	3	4	5
1	2.192	1.771	1.485	1.419	1.164
2	2.107	1.740	1.351	1.359	1.170
3	1.951	1.603	1.339	1.282	1.023
4	1.903	1.603	1.245	1.319	.797
5	1.209	1.394	1.123	1.145	.734
6	.830	1.239	1.086	.968	.612
7	.691	1.021	.951	.931	.462
8	.530	.747	.969	.900	.216
9	.494	.601	.700	.676	.142
10	.321	.420	.573	.599	.048
11	.294	.304	.438	.436	.106
12	.203	.172	.200	.281	.115
13	.153	.115	.123	.125	.037
14	.170	.086	.115	.141	.086
15	.037	.076	.067	-.010	.010
16	.066	.056	.132	.105	
17	.049	.057	.028	.047	
18	.000	.038	.056	.087	
19	.037	.038	.079	-.029	
c_n	0.555	0.596	0.584	0.571	0.485
c_m	.0176	.0091	-.0203	-.0154	-.0111

$C_N' = 0.552$ $\quad x'_{cp} = 24.4$
$C_m' = .0031$
$C_b' = .232$ $\quad y'_{cp} = 42.1$

(d) $M = 0.52$ $\quad \alpha = 10.4°$
$C_{N_A} = 0.57$ $\quad \delta_{a_L} = .3°$ up
$\delta_f = 0°$

Orifice	Row				
	1	2	3	4	5
1	2.058	1.758	1.585	1.432	1.180
2	1.917	1.797	1.409	1.350	1.160
3	1.797	1.634	1.371	1.268	.998
4	1.856	1.633	1.323	1.306	.812
5	1.540	1.445	1.203	1.188	.804
6	1.180	1.329	1.163	.925	.680
7	.946	1.173	1.028	1.006	.601
8	.730	.930	1.008	.972	.330
9	.552	.753	.820	.751	.280
10	.391	.564	.659	.708	.052
11	.312	.353	.605	.542	.180
12	.222	.210	.239	.421	.190
13	.140	.116	.208	.231	.061
14	.166	.126	.125	.134	.115
15	.031	.093	.105	.107	.032
16	.082	.071	.145	.083	
17	.075	.041	.083	.134	
18	-.020	.021	.113	.074	
19	.031	.010	.097	.064	
c_n	0.615	0.661	0.648	0.622	0.548
c_m	.0141	.0017	-.0315	-.0310	-.0323

$C_N' = 0.610$ $\quad x'_{cp} = 26.0$
$C_m' = -.0064$
$C_b' = .257$ $\quad y'_{cp} = 42.1$

TABLE IV.- Concluded.

[$M \approx 0.55$; $\delta_f \approx 0°$]

(e) $M = 0.50$ $\alpha = 11.5°$

$C_{N_A} = 0.63$ $\delta_{a_L} = .2°$ down

$\delta_f = 0°$

Orifice	Row				
	1	2	3	4	5
1	2.000	1.787	1.585	1.494	1.140
2	1.891	1.738	1.409	1.378	1.105
3	1.709	1.652	1.415	1.334	.989
4	1.807	1.591	1.306	1.286	.778
5	1.467	1.436	1.209	1.264	.766
6	1.256	1.370	1.195	.955	.680
7	1.093	1.219	1.036	.955	.673
8	.891	1.034	1.072	.976	.472
9	.691	.912	.872	.810	.375
10	.523	.723	.767	.764	.200
11	.377	.490	.677	.622	.270
12	.268	.357	.377	.525	.213
13	.139	.191	.342	.335	.163
14	.176	.168	.267	.263	.144
15	.087	.099	.211	.137	.136
16	.099	.097	.209	.244	
17	.092	.099	.099	.132	
18	.021	.067	.164	.202	
19	.000	.033	.115	.011	
c_n	0.668	0.729	0.713	0.685	0.593
c_m	.0019	-.0183	-.0557	-.0541	-.0586

$C_N' = 0.670$ $x'_{cp} = 28.9$

$C_m' = -.0261$ $y'_{cp} = 42.1$

$C_b' = .282$

TABLE V.- PRESSURE COEFFICIENTS AND AERODYNAMIC CHARACTERISTICS OF THE DOUGLAS X-3 WING

$\left[M \approx 0.55;\ \delta_f \approx 7^\circ\right]$

(a) $M = 0.65$, $C_{N_A} = 0.38$, $\alpha = 7.4^\circ$, $\delta_{a_L} = 0$, $\delta_f = 7.8^\circ$

Orifice	Row 1	Row 2	Row 3	Row 4	Row 5
1	1.131	1.874	1.958	1.632	1.233
2	1.236	1.844	1.622	1.541	1.121
3	1.033	1.211	1.202	1.391	.617
4	1.167	.772	.723	1.245	.611
5	.875	.821	.848	.908	.485
6	.710	.643	.770	.765	.312
7	.530	.580	.655	.667	.255
8	.460	.436	.607	.618	.108
9	.376	.356	.412	.362	.088
10	.276	.301	.303	.293	.027
11	.197	.224	.253	.209	.083
12	.178	.178	.136	.134	.028
13	.116	.131	.122	.076	.027
14	.176	.137	.133	.040	.034
15	.047	.047	.048	.000	.007
16	.054	.060	.081	.007	
17	.014	.054	.020	.040	
18	-.007	.014	.034	-.007	
19	.040	.054	.077	-.014	
c_n	0.395	0.417	0.425	0.427	0.340
c_m	.0009	.0055	-.0023	.0176	.0054

$C_N' = 0.396$, $C_m' = .0081$, $C_b' = .168$; $x'_{cp} = 22.9$, $y'_{cp} = 42.5$

(b) $M = 0.61$, $C_{N_A} = 0.45$, $\alpha = 8.4^\circ$, $\delta_{a_L} = 0$, $\delta_f = 7.7^\circ$

Orifice	Row 1	Row 2	Row 3	Row 4	Row 5
1	1.328	2.265	2.057	1.897	1.364
2	1.714	2.255	1.939	1.782	1.316
3	1.277	1.709	1.648	1.639	.930
4	1.425	.986	1.299	1.513	.606
5	.991	.969	.981	1.221	.513
6	.790	.639	.869	.864	.353
7	.613	.722	.653	.730	.287
8	.542	.409	.711	.641	.140
9	.426	.411	.493	.402	.117
10	.311	.332	.311	.338	.047
11	.244	.200	.292	.249	.104
12	.198	.262	.165	.171	.048
13	.162	.112	.141	.095	.046
14	.180	.191	.131	.070	.032
15	.077	.039	.055	-.008	.016
16	.062	.138	.102	.016	
17	.041	.023	.024	.031	
18	.008	.079	.047	.000	
19	.031	.016	.073	-.016	
c_n	0.470	0.492	0.521	0.499	0.410
c_m	.0035	.0048	.0017	.0200	.0054

$C_N' = 0.470$, $C_m' = .0096$, $C_b' = .200$; $x'_{cp} = 22.9$, $y'_{cp} = 42.6$

TABLE V.- Continued.

$[M \approx 0.55;\ \delta_f \approx 7^\circ]$

(c) $M = 0.57$ $\quad C_{N_A} = 0.51$ $\quad \alpha = 9.5^\circ$ $\quad \delta_{a_L} = .2^\circ$ up $\quad \delta_f = 7.7^\circ$

Orifice	Row				
	1	2	3	4	5
1	1.481	2.498	1.768	2.103	1.464
2	1.990	2.519	1.629	1.971	1.398
3	1.563	2.064	1.632	1.822	1.159
4	1.688	1.446	1.542	1.702	.730
5	1.111	1.028	1.260	1.464	.572
6	.872	.806	1.180	.967	.409
7	.695	.713	.892	.851	.307
8	.590	.535	.840	.726	.177
9	.501	.475	.549	.456	.124
10	.318	.394	.415	.357	.063
11	.276	.294	.349	.282	.127
12	.216	.269	.134	.167	.090
13	.167	.180	.178	.099	.035
14	.177	.171	.107	.062	.072
15	.079	.098	.072	-.009	.018
16	.044	.104	.071	.027	
17	.037	.071	.044	.044	
18	.009	.054	.044	.009	
19	.035	.035	.074	.000	
c_n	0.525	0.579	0.578	0.557	0.467
c_m	.0083	.0092	-.0001	.0231	.0049

$C_N' = 0.536$ $\quad x'_{cp} = 22.5$

$C_m' = .0133$ $\quad y'_{cp} = 42.2$

$C_b' = .227$

(d) $M = 0.53$ $\quad C_{N_A} = 0.57$ $\quad \alpha = 10.7^\circ$ $\quad \delta_{a_L} = 0$ $\quad \delta_f = 7.7^\circ$

Orifice	Row				
	1	2	3	4	5
1	1.783	2.441	1.695	1.569	1.655
2	2.235	2.418	1.607	1.490	1.525
3	1.837	2.229	1.550	1.447	1.193
4	1.954	1.838	1.542	1.502	.836
5	1.314	1.244	1.366	1.430	.663
6	.969	.975	1.366	1.174	.524
7	.777	.825	1.074	1.120	.408
8	.670	.675	1.093	1.006	.235
9	.569	.601	.740	.693	.175
10	.358	.436	.552	.558	.114
11	.320	.350	.435	.390	.126
12	.260	.239	.155	.265	.178
13	.166	.199	.165	.156	.051
14	.205	.136	.105	.072	.093
15	.081	.123	.093	.042	.011
16	.082	.080	.123	.041	
17	.075	.082	.041	.082	
18	.010	.042	.112	.031	
19	.020	.041	.096	.021	
c_n	0.602	0.642	0.660	0.615	0.537
c_m	.0093	.0121	-.0143	-.0038	-.0034

$C_N' = 0.601$ $\quad x'_{cp} = 23.8$

$C_m' = .0070$ $\quad y'_{cp} = 42.2$

$C_b' = .254$

TABLE V.- Continued.

$\left[M \approx 0.55;\ \delta_f \approx 7^\circ\right]$

(e) $M = 0.50$, $C_{N_A} = 0.65$, $\alpha = 11.5^\circ$, $\delta_{a_L} = .2^\circ$ up, $\delta_f = 7.7^\circ$

Orifice	Row 1	Row 2	Row 3	Row 4	Row 5
1	2.604	2.035	1.663	1.538	1.514
2	2.343	1.991	1.557	1.538	1.476
3	2.037	1.931	1.515	1.476	1.267
4	2.056	1.915	1.477	1.598	.873
5	1.448	1.675	1.373	1.431	.769
6	1.060	1.391	1.343	1.169	.544
7	.875	1.096	1.117	1.109	.459
8	.739	.837	1.125	.962	.276
9	.641	.700	.798	.734	.197
10	.403	.502	.678	.604	.151
11	.348	.383	.478	.534	.224
12	.248	.234	.267	.367	.247
13	.208	.212	.232	.199	.057
14	.196	.153	.162	.115	.186
15	.126	.139	.117	.060	.000
16	.081	.102	.150	.105	
17	.072	.116	.046	.127	
18	.011	.047	.103	.130	
19	.023	.046	.096	.047	
c_n	0.669	0.706	0.695	0.657	0.574
c_m	.0143	.0028	-.0286	-.0201	-.0157

$C_N' = 0.650$, $C_m' = -.0013$, $C_b' = .272$, $x'_{cp} = 25.2$, $y'_{cp} = 41.8$

(f) $M = 0.48$, $C_{N_A} = 0.69$, $\alpha = 12.4^\circ$, $\delta_{a_L} = 0$, $\delta_f = 7.7^\circ$

Orifice	Row 1	Row 2	Row 3	Row 4	Row 5
1	2.874	1.917	1.718	1.436	1.396
2	2.445	1.956	1.501	1.402	1.405
3	2.102	1.793	1.493	1.322	1.260
4	2.170	1.872	1.502	1.397	.923
5	1.520	1.616	1.392	1.342	.825
6	1.251	1.425	1.328	1.172	.607
7	1.019	1.289	1.132	1.156	.606
8	.890	.914	1.206	1.098	.296
9	.700	.826	.906	.824	.310
10	.480	.626	.727	.735	.175
11	.360	.446	.599	.598	.291
12	.290	.289	.262	.406	.215
13	.178	.189	.298	.251	.147
14	.235	.164	.196	.148	.175
15	.073	.173	.200	.103	.089
16	.123	.097	.185	.087	
17	.077	.149	.087	.173	
18	.024	.100	.123	.063	
19	.037	.000	.090	.038	
c_n	0.742	0.742	0.734	0.677	0.626
c_m	.0119	-.0082	-.0386	-.0307	-.0382

$C_N' = 0.687$, $C_m' = -.0107$, $C_b' = .286$, $x'_{cp} = 26.6$, $y'_{cp} = 41.6$

TABLE V.- Concluded.

[$M \approx 0.55$; $\delta_f \approx 7°$]

(g) $M = 0.45$ $\alpha = 13.4°$
$C_{N_A} = 0.71$ $\delta_{a_L} = .4°$ up
$\delta_f = 7.5°$

Orifice	Row				
	1	2	3	4	5
1	3.035	1.853	1.697	1.464	1.333
2	2.425	1.656	1.586	1.390	1.361
3	2.043	1.744	1.560	1.305	1.185
4	2.197	1.597	1.482	1.402	.985
5	1.573	1.517	1.435	1.330	.945
6	1.316	1.451	1.349	1.108	.788
7	1.224	1.288	1.206	1.179	.696
8	1.049	1.095	1.147	1.150	.493
9	.897	.974	.979	.931	.469
10	.597	.798	.839	.821	.284
11	.500	.609	.702	.756	.328
12	.378	.475	.431	.598	.368
13	.253	.259	.389	.421	.198
14	.241	.258	.325	.293	.270
15	.119	.254	.244	.222	.124
16	.160	.197	.294	.324	
17	.125	.174	.188	.187	
18	.052	.149	.226	.328	
19	-.013	.027	.153	.069	
c_n	0.824	0.801	0.803	0.774	0.699
c_m	-.0008	-.0415	-.0676	-.0748	-.0675

$C_N' = 0.759$ $x'_{cp} = 30.5$
$C_m' = -.0420$
$C_b' = .319$ $y'_{cp} = 42.0$

TABLE VI.- PRESSURE COEFFICIENTS AND AERODYNAMIC CHARACTERISTICS OF THE DOUGLAS X-3 WING

$\left[M \approx 0.55;\ \delta_f \approx 27^\circ\right]$

(a) $M = 0.71$; $C_{N_A} = 0.28$; $\alpha = 6.7^\circ$; $\delta_{a_L} = .2^\circ$ up; $\delta_f = 29.0^\circ$

Orifice	Row 1	Row 2	Row 3	Row 4	Row 5
1	-1.344	-1.134	-1.890	-0.742	-1.520
2	-.806	-.724	-1.110	-.574	-1.417
3	-.366	-.174	-.298	-.445	-.411
4	-.165	.062	-.087	-.356	1.046
5	1.367	1.694	1.413	-.214	1.003
6	.930	1.436	1.353	.601	.871
7	.813	1.144	1.167	.575	.689
8	.684	.684	1.127	.712	.383
9	.520	.529	.841	.702	.292
10	.411	.415	.659	.700	.114
11	.289	.308	.501	.585	.162
12	.232	.262	.240	.441	.135
13	.149	.169	.186	.302	.124
14	.212	.175	.148	.165	.120
15	.105	.073	.094	.137	.062
16	.046	.104	.099	.127	
17	.028	.080	.066	.145	
18	.013	.047	.059	.095	
19	.052	.066	.083	.075	
c_n	0.587	0.653	0.649	0.637	0.522
c_m	-.0324	-.0378	-.0564	-.0508	-.0650

$C_N' = 0.605$; $C_m' = -.0397$; $C_b' = .256$; $x'_{cp} = 31.6$; $y'_{cp} = 42.3$

(b) $M = 0.65$; $C_{N_A} = 0.50$; $\alpha = 10.0^\circ$; $\delta_{a_L} = .5^\circ$ down; $\delta_f = 28.0^\circ$

Orifice	Row 1	Row 2	Row 3	Row 4	Row 5
1	-0.198	-0.049	-0.186	-0.413	-0.884
2	.180	.289	.043	-.261	-.603
3	.629	.536	.280	-.010	.435
4	.811	.769	.506	.284	1.307
5	1.966	2.469	1.702	.637	1.155
6	1.398	1.846	1.601	1.484	1.007
7	1.259	1.405	1.433	1.371	.775
8	1.106	.862	1.303	1.263	.445
9	.714	.713	1.067	.957	.330
10	.449	.539	.811	.844	.214
11	.309	.416	.656	.628	.232
12	.267	.326	.308	.467	.240
13	.190	.215	.267	.294	.139
14	.243	.183	.197	.195	.182
15	.093	.141	.166	.154	.073
16	.094	.092	.164	.119	
17	.057	.118	.079	.125	
18	.030	.095	.140	.080	
19	.046	.039	.106	.072	
c_n	0.520	0.593	0.615	0.541	0.436
c_m	-.0371	-.0408	-.0733	-.0815	-.1003

$C_N' = 0.539$; $C_m' = -.0521$; $C_b' = .225$; $x'_{cp} = 34.7$; $y'_{cp} = 41.7$

TABLE VI.- Continued.

[$M \approx 0.55$; $\delta_f \approx 27°$]

(c) $M = 0.56$; $C_{N_A} = 0.64$; $\alpha = 12.0°$; $\delta_{a_L} = .4°$ down; $\delta_f = 27.4°$

Orifice	Row 1	Row 2	Row 3	Row 4	Row 5
1	0.297	0.577	0.578	0.379	0.168
2	.735	.758	.581	.483	.292
3	1.151	.968	.721	.646	.676
4	1.398	1.216	.899	.830	1.914
5	2.061	2.712	2.356	1.087	1.506
6	1.734	1.926	2.205	1.766	.962
7	1.351	1.209	1.837	1.682	.576
8	1.198	.873	1.510	1.503	.351
9	.726	.733	.975	1.097	.224
10	.476	.636	.605	.826	.204
11	.343	.455	.495	.526	.207
12	.291	.389	.279	.339	.163
13	.221	.239	.225	.270	.116
14	.256	.206	.189	.181	.129
15	.137	.171	.108	.088	.044
16	.096	.105	.160	.086	
17	.100	.160	.032	.127	
18	.041	.119	.138	.022	
19	.053	.011	.144	.066	
c_n	0.635	0.687	0.701	0.660	0.541
c_m	-.0280	-.0371	-.0522	-.0560	-.0627

$C_N' = 0.638$ $x'_{cp} = 31.0$

$C_m' = -.0383$ $y'_{cp} = 42.1$

$C_b' = .268$

(d) $M = 0.55$; $C_{N_A} = 0.71$; $\alpha = 13.4°$; $\delta_{a_L} = .2°$ up; $\delta_f = 27.2°$

Orifice	Row 1	Row 2	Row 3	Row 4	Row 5
1	0.512	1.389	1.341	0.814	0.347
2	.985	.857	.721	.676	.403
3	1.379	1.089	.906	.771	.758
4	1.675	1.317	1.003	.948	1.537
5	2.219	2.777	2.338	1.224	1.313
6	1.838	1.905	2.167	1.842	1.093
7	1.455	1.381	1.783	1.654	.832
8	1.196	.903	1.490	1.452	.440
9	.785	.769	1.087	1.090	.309
10	.524	.635	.703	.877	.189
11	.355	.502	.612	.646	.237
12	.333	.391	.311	.471	.259
13	.218	.270	.255	.302	.120
14	.287	.213	.196	.209	.211
15	.142	.199	.123	.126	.046
16	.132	.108	.187	.134	
17	.103	.199	.066	.132	
18	.064	.145	.153	.056	
19	.044	-.011	.149	.057	
c_n	0.701	0.736	0.762	0.722	0.597
c_m	-.0276	-.0343	-.0561	-.0628	-.0803

$C_N' = 0.693$ $x'_{cp} = 30.8$

$C_m' = -.0403$ $y'_{cp} = 42.2$

$C_b' = .292$

TABLE VI.- Continued.

[$M \approx 0.55$; $\delta_f \approx 27°$]

(e) $M = 0.51$ $\quad \alpha = 14.6°$
$C_{N_A} = 0.77$ $\quad \delta_{a_L} = .7°$ up
$\delta_f = 27.0°$

Orifice	Row				
	1	2	3	4	5
1	0.756	2.020	1.980	1.643	0.556
2	1.184	1.554	1.481	1.290	.640
3	1.606	1.239	1.160	.979	.946
4	1.885	1.513	1.206	1.140	1.835
5	2.339	2.780	2.708	1.420	1.632
6	1.826	1.651	2.160	2.545	1.197
7	1.421	1.346	1.564	1.883	.730
8	1.213	.943	1.327	1.460	.344
9	.833	.791	.957	.976	.279
10	.579	.684	.647	.734	.187
11	.399	.490	.602	.545	.244
12	.349	.390	.334	.382	.203
13	.227	.270	.306	.256	.144
14	.265	.216	.198	.185	.147
15	.131	.212	.134	.082	.068
16	.119	.117	.172	.067	
17	.083	.186	.080	.119	
18	.051	.161	.105	.014	
19	.052	-.027	.124	.082	
c_n	0.740	0.779	0.791	0.790	0.657
c_m	-.0232	-.0276	-.0405	-.0337	-.0688

$C_N' = 0.740$ $\quad x'_{cp} = 28.9$
$C_m' = -.0286$
$C_b' = .315$ $\quad y'_{cp} = 42.6$

(f) $M = 0.50$ $\quad \alpha = 15.2°$
$C_{N_A} = 0.80$ $\quad \delta_{a_L} = 1.4°$ up
$\delta_f = 27.0°$

Orifice	Row				
	1	2	3	4	5
1	0.778	2.165	2.149	1.810	0.612
2	1.263	1.843	1.780	1.563	.661
3	1.650	1.334	1.290	1.230	1.004
4	1.987	1.574	1.283	1.200	1.936
5	2.299	2.689	2.671	1.428	1.695
6	1.889	1.624	2.120	2.524	1.178
7	1.428	1.336	1.573	1.823	.707
8	1.254	.966	1.299	1.433	.372
9	.852	.836	.962	.955	.307
10	.556	.674	.690	.751	.161
11	.416	.505	.578	.534	.191
12	.351	.432	.309	.384	.177
13	.240	.285	.268	.216	.171
14	.254	.217	.211	.106	.135
15	.145	.213	.148	.041	.069
16	.106	.118	.173	.081	
17	.097	.173	.067	.120	
18	.078	.135	.133	.068	
19	-.013	.000	.125	.055	
c_n	0.755	0.796	0.809	0.799	0.672
c_m	-.0208	-.0268	-.0384	-.0276	-.0669

$C_N' = 0.754$ $\quad x'_{cp} = 28.5$
$C_m' = -.0260$
$C_b' = .321$ $\quad y'_{cp} = 42.5$

TABLE VI.- Continued.

[$M \approx 0.55$; $\delta_f \approx 27°$]

(g) $M = 0.50$ $\alpha = 16.0°$
$C_{N_A} = 0.87$ $\delta_{a_L} = .2°$ down
$\delta_f = 27.0°$

Orifice	Row				
	1	2	3	4	5
1	1.091	2.641	2.735	2.133	1.384
2	1.521	2.635	2.316	2.027	.965
3	2.075	1.769	1.762	1.952	1.069
4	2.422	1.546	1.500	1.657	2.233
5	2.436	2.657	2.605	1.610	1.688
6	1.942	1.652	2.020	2.343	1.022
7	1.451	1.356	1.599	1.695	.699
8	1.308	.993	1.282	1.399	.519
9	.904	.887	.989	.940	.384
10	.598	.734	.737	.814	.360
11	.442	.559	.636	.591	.308
12	.388	.458	.373	.422	.293
13	.259	.321	.358	.348	.216
14	.288	.251	.243	.260	.249
15	.163	.233	.208	.184	.042
16	.137	.188	.178	.125	
17	.100	.192	.096	.178	
18	.066	.167	.136	.056	
19	.014	-.014	.128	.099	
c_n	0.830	0.865	0.873	0.877	0.760
c_m	-.0186	-.0281	-.0397	-.0363	-.0761

$C_N' = 0.825$ $x'_{cp} = 28.5$
$C_m' = -.0289$
$C_b' = .352$ $y'_{cp} = 42.7$

(h) $M = 0.48$ $\alpha = 17.5°$
$C_{N_A} = 0.95$ $\delta_{a_L} = .5°$ up
$\delta_f = 26.8°$

Orifice	Row				
	1	2	3	4	5
1	1.349	3.080	3.136	2.585	1.972
2	1.814	3.163	2.751	2.494	1.807
3	2.503	2.658	2.442	2.487	1.208
4	2.930	1.936	1.924	2.356	2.445
5	2.580	2.254	2.210	2.093	1.502
6	2.050	1.677	1.867	2.112	1.041
7	1.579	1.516	1.582	1.667	.751
8	1.406	1.266	1.398	1.386	.544
9	1.034	1.132	1.168	1.011	.384
10	.758	.834	.895	.816	.342
11	.521	.601	.743	.591	.361
12	.446	.478	.445	.469	.316
13	.292	.315	.399	.314	.218
14	.310	.300	.303	.279	.268
15	.219	.251	.268	.153	.107
16	.147	.231	.265	.193	
17	.138	.221	.178	.176	
18	.114	.194	.220	.136	
19	-.015	-.015	.138	.076	
c_n	0.946	0.971	0.983	0.953	0.852
c_m	-.0224	-.0317	-.0561	-.0321	-.0678

$C_N' = 0.920$ $x'_{cp} = 28.3$
$C_m' = -.0307$
$C_b' = .390$ $y'_{cp} = 42.4$

TABLE VI.- Concluded.

[$M \approx 0.55$; $\delta_f \approx 27°$]

(i) $M = 0.48$ $\alpha = 18.3°$

$C_{N_A} = 1.04$ $\delta_{a_L} = .4°$ up

$\delta_f = 26.6°$

Orifice	Row 1	Row 2	Row 3	Row 4	Row 5
1	1.570	2.813	3.167	2.614	1.979
2	2.042	2.863	2.802	2.503	1.910
3	2.649	2.630	2.588	2.574	1.271
4	3.186	2.395	1.990	2.405	1.946
5	2.687	1.951	1.893	1.967	1.269
6	2.154	1.683	1.683	1.809	.857
7	1.546	1.561	1.490	1.459	.679
8	1.450	1.290	1.403	1.332	.560
9	1.100	1.152	1.203	.940	.415
10	.761	.912	.869	.819	.388
11	.615	.715	.776	.608	.393
12	.447	.645	.521	.544	.407
13	.346	.407	.475	.435	.277
14	.341	.406	.400	.383	.328
15	.322	.370	.329	.276	.183
16	.177	.319	.384	.284	
17	.170	.266	.208	.295	
18	.129	.285	.294	.166	
19	.000	.000	.154	.137	
c_n	1.012	1.030	1.004	0.956	0.820
c_m	-.0247	-.0585	-.0737	-.0511	-.0738

$C_N' = 0.949$ $x'_{cp} = 29.9$

$C_m' = -.0461$ $y'_{cp} = 41.6$

$C_b' = .394$

TABLE VII.- PRESSURE COEFFICIENTS AND AERODYNAMIC CHARACTERISTICS OF THE DOUGLAS X-3 WING

$\left[M \approx 0.85;\ \delta_f \approx 7^\circ\right]$

(a) $M = 0.85$; $C_{N_A} = 0.10$; $\alpha = 2.7^\circ$; $\delta_{a_L} = .2^\circ$ up; $\delta_f = 9.4^\circ$

Orifice	Row				
	1	2	3	4	5
1	-0.278	-0.431	-0.360	-0.553	-0.367
2	-.189	-.074	-.210	-.205	-.201
3	-.092	.074	-.157	-.055	.037
4	.048	.213	.055	.066	.967
5	.374	.931	.994	.153	.924
6	.266	.346	.876	.983	.261
7	.274	.212	.306	.818	-.071
8	.237	.403	.536	.761	-.056
9	.256	.417	.462	.444	-.112
10	.136	.141	.104	.014	-.205
11	.102	.099	.092	.000	-.064
12	.082	.085	.021	.007	-.014
13	.038	.078	.042	-.064	-.048
14	.140	.078	.059	-.042	.000
15	-.028	-.028	-.028	-.080	-.007
16	.007	.000	.021	-.035	
17	-.029	.035	.035	.007	
18	-.027	.007	.000	-.007	
19	.014	.049	.051	.000	
c_n	0.103	0.162	0.176	0.160	0.080
c_m	-.0158	-.0156	-.0147	-.0033	.0079

$C_N' = 0.143$
$C_m' = -.0099$
$C_b' = .060$

$x'_{cp} = 31.9$
$y'_{cp} = 42.1$

(b) $M = 0.85$; $C_{N_A} = 0.12$; $\alpha = 2.9^\circ$; $\delta_{a_L} = .2^\circ$ up; $\delta_f = 9.3^\circ$

Orifice	Row				
	1	2	3	4	5
1	-0.305	-0.334	-0.276	-0.349	-0.302
2	-.057	.046	-.199	-.130	-.164
3	-.119	.064	-.102	-.028	.037
4	.192	.315	.046	.103	.972
5	.410	1.030	1.037	.198	.908
6	.338	.308	.892	.972	.308
7	.210	.285	.388	.844	-.043
8	.310	.356	.489	.843	-.056
9	.292	.458	.496	.450	-.119
10	.162	.134	.090	.021	-.232
11	.094	.099	.091	.000	-.050
12	.088	.092	.028	-.014	.007
13	.044	.078	.035	-.071	-.055
14	.147	.085	.065	-.069	.007
15	-.041	-.028	-.035	-.087	-.022
16	.028	.000	.035	-.042	
17	-.036	.035	.021	.007	
18	-.014	.014	.007	-.007	
19	-.007	.035	.044	.000	
c_n	0.138	0.177	0.179	0.177	0.089
c_m	-.0154	-.0133	-.0144	.0008	.0085

$C_N' = 0.158$
$C_m' = -.0076$
$C_b' = .065$

$x'_{cp} = 29.8$
$y'_{cp} = 41.4$

TABLE VII.- Continued.

[$M \approx 0.85$; $\delta_f \approx 7°$]

(c) $M = 0.85$ $\alpha = 4.2°$
$C_{N_A} = 0.23$ $\delta_{a_L} = .2°$ up
$\delta_f = 8.6°$

Orifice	Row				
	1	2	3	4	5
1	0.194	0.131	0.165	0.147	0.027
2	.169	.284	.095	.185	.073
3	.192	.330	.184	.266	.147
4	.346	.415	.238	.299	.956
5	.700	1.082	1.106	.332	.912
6	.538	.521	.953	.978	.799
7	.382	.431	.876	.933	.206
8	.445	.448	.614	.944	-.139
9	.459	.576	.608	.772	-.125
10	.358	.309	.436	.231	-.309
11	.123	.138	.098	.000	-.050
12	.115	.085	-.028	-.083	.007
13	.044	.064	.000	-.106	-.055
14	.174	.057	.039	-.139	.007
15	-.034	-.028	-.049	-.122	-.022
16	.048	-.007	.014	-.070	
17	-.043	.042	.021	.000	
18	-.027	.021	.014	-.021	
19	.000	.007	.043	.007	
c_n	0.250	0.260	0.285	0.262	0.185
c_m	-.0171	-.0101	-.0127	.0089	.0071

$C_N' = 0.246$ $x'_{cp} = 26.7$
$C_m' = -.0042$ $y'_{cp} = 41.8$
$C_b' = .103$

(d) $M = 0.85$ $\alpha = 5.2°$
$C_{N_A} = 0.30$ $\delta_{a_L} = .2°$ up
$\delta_f = 8.4°$

Orifice	Row				
	1	2	3	4	5
1	0.461	0.376	0.532	0.485	0.237
2	.441	.512	.274	.416	.235
3	.384	.420	.350	.384	.248
4	.575	.562	.348	.476	.967
5	.771	1.126	1.140	.475	.911
6	.665	.753	1.014	1.013	.845
7	.526	.586	.948	.959	.283
8	.544	.587	.911	1.035	-.118
9	.531	.639	.691	.875	-.132
10	.498	.540	.615	.468	-.329
11	.188	.171	.133	.100	-.035
12	.115	.084	-.042	-.090	.014
13	.044	.042	-.049	-.106	-.055
14	.125	.063	.013	-.194	.021
15	-.034	-.028	-.049	-.144	-.036
16	.007	-.020	.014	-.084	
17	-.036	.035	.014	-.042	
18	-.013	.070	.000	-.035	
19	.000	.014	.029	.007	
c_n	0.326	0.353	0.369	0.337	0.230
c_m	-.0129	-.0132	-.0123	.0108	.0085

$C_N' = 0.324$ $x'_{cp} = 26.0$
$C_m' = -.0033$ $y'_{cp} = 41.3$
$C_b' = .134$

TABLE VII.- Continued.

[$M \approx 0.85$; $\delta_f \approx 7°$]

(e) $M = 0.85$ $\quad C_{N_A} = 0.33$ $\quad \alpha = 5.9°$ $\quad \delta_{a_L} = .1°$ down $\quad \delta_f = 8.2°$

Orifice	Row				
	1	2	3	4	5
1	0.697	0.548	0.868	0.756	0.308
2	.636	.564	.386	.507	.307
3	.564	.573	.431	.501	.292
4	.725	.614	.465	.622	.950
5	.849	1.094	1.171	.535	.935
6	.716	.888	1.028	1.082	.821
7	.605	.647	.990	.991	.634
8	.596	.686	.997	1.096	-.131
9	.594	.706	.794	.907	-.104
10	.570	.615	.688	.870	-.335
11	.244	.249	.237	.234	.035
12	.135	.091	-.049	-.021	.021
13	.025	.021	-.076	-.133	-.061
14	.118	.042	-.006	-.214	.014
15	-.041	-.041	-.056	-.179	-.029
16	.000	-.014	-.007	-.070	
17	-.036	.014	-.611	-.048	
18	-.027	-.007	-.021	.000	
19	.007	.028	.043	-.014	
c_n	0.376	0.392	0.411	0.334	0.307
c_m	-.0106	-.0107	-.0038	.0076	-.0074

$C_N' = 0.357$ $\quad x'_{cp} = 25.5$
$C_m' = -.0019$
$C_b' = .147$ $\quad y'_{cp} = 41.1$

(f) $M = 0.86$ $\quad C_{N_A} = 0.44$ $\quad \alpha = 7.0°$ $\quad \delta_{a_L} = .2°$ up $\quad \delta_f = 8.1°$

Orifice	Row				
	1	2	3	4	5
1	0.956	1.558	1.609	1.659	1.222
2	1.113	1.370	1.260	1.350	1.064
3	.842	.770	1.082	1.210	.773
4	.995	.785	.825	1.078	.801
5	.969	1.148	1.134	.843	.824
6	.928	1.020	1.081	1.046	.741
7	.720	.906	.983	1.082	.631
8	.738	.767	1.052	1.069	-.020
9	.741	.832	.974	.906	-.102
10	.653	.715	.819	.835	-.295
11	.325	.445	.357	.300	.007
12	.133	.097	-.062	.041	.021
13	.012	-.035	-.096	-.124	-.013
14	.082	.028	-.044	-.285	.048
15	-.020	-.054	-.076	-.197	-.028
16	-.007	-.013	-.014	-.096	
17	-.035	.014	-.007	-.020	
18	-.026	-.007	-.027	-.042	
19	.007	.020	.042	.021	
c_n	0.472	0.513	0.535	0.523	0.429
c_m	-.0053	-.0002	-.0002	.0223	.0100

$C_N' = 0.488$ $\quad x'_{cp} = 23.6$
$C_m' = .0066$
$C_b' = .209$ $\quad y'_{cp} = 42.8$

TABLE VII.- Continued.

[$M \approx 0.85$; $\delta_f \approx 7°$]

(g) $M = 0.86$ $\quad C_{N_A} = 0.53$ $\quad \alpha = 8.0°$ $\quad \delta_{a_L} = 0$ $\quad \delta_f = 7.4°$

Orifice	Row				
	1	2	3	4	5
1	1.145	1.833	1.853	1.866	1.432
2	1.486	1.677	1.515	1.625	1.336
3	1.109	1.349	1.376	1.439	1.096
4	1.312	1.171	1.200	1.403	1.012
5	1.154	1.226	1.411	1.166	.952
6	1.052	1.092	1.403	1.312	.886
7	.916	.969	1.152	1.268	.618
8	.872	.904	1.165	1.331	.114
9	.882	.940	1.041	1.074	.020
10	.759	.899	.933	.583	-.258
11	.476	.581	.435	.519	.041
12	.223	.143	.068	.301	.082
13	.012	-.034	-.027	.116	.013
14	.081	.014	.000	-.107	.068
15	-.007	-.054	-.082	-.056	-.014
16	.000	-.007	-.007	-.020	
17	-.028	.000	-.020	.040	
18	-.052	.007	-.020	-.014	
19	-.007	.013	.042	.021	
c_n	0.580	0.618	0.663	0.669	0.545
c_m	-.0055	-.0008	-.0046	.0035	.0046

$C_N' = 0.604$ $\quad x'_{cp} = 24.8$

$C_m' = .0010$ $\quad y'_{cp} = 43.3$

$C_b' = .262$

(h) $M = 0.86$ $\quad C_{N_A} = 0.59$ $\quad \alpha = 9.0°$ $\quad \delta_{a_L} = .2°$ down $\quad \delta_f = 7.2°$

Orifice	Row				
	1	2	3	4	5
1	1.249	2.022	2.023	2.046	1.617
2	1.833	1.829	1.662	1.769	1.449
3	1.222	1.650	1.527	1.599	1.191
4	1.552	1.474	1.358	1.565	1.057
5	1.319	1.385	1.568	1.382	.896
6	1.173	1.197	1.471	1.381	.612
7	1.045	1.099	1.410	1.185	.511
8	1.009	1.073	1.435	.946	.223
9	.986	1.041	.799	.684	.176
10	.841	.959	.648	.627	-.096
11	.380	.353	.574	.543	.187
12	.225	.206	.286	.404	.193
13	.037	.062	.163	.241	.114
14	.109	.069	.177	.095	.157
15	.007	.007	.089	.098	.035
16	.020	.027	.149	.144	
17	-.035	.034	.068	.196	
18	-.026	.021	.094	.132	
19	.000	.027	.085	.090	
c_n	0.662	0.705	0.750	0.705	0.586
c_m	-.0049	-.0041	-.0280	-.0192	-.0120

$C_N' = 0.671$ $\quad x'_{cp} = 26.1$

$C_m' = -.0076$ $\quad y'_{cp} = 42.5$

$C_b' = .285$

TABLE VII.- Continued.

[$M \approx 0.85$; $\delta_f \approx 7^\circ$]

(i) $M = 0.86$ $\alpha = 9.5^\circ$
$C_{N_A} = 0.63$ $\delta_{a_L} = 0$
$\delta_f = 7.2^\circ$

Orifice	Row				
	1	2	3	4	5
1	1.420	2.090	2.050	2.099	1.679
2	1.879	1.900	1.735	1.805	1.529
3	1.338	1.713	1.589	1.670	1.227
4	1.571	1.555	1.438	1.611	1.084
5	1.354	1.456	1.612	1.434	.827
6	1.253	1.270	1.524	1.310	.618
7	1.115	1.143	1.428	.998	.532
8	1.071	1.091	1.435	.919	.250
9	1.050	1.089	.847	.684	.197
10	.868	.911	.681	.634	-.082
11	.359	.385	.636	.564	.138
12	.251	.254	.334	.431	.228
13	.061	.117	.245	.275	.134
14	.136	.103	.215	.122	.171
15	.007	.034	.151	.063	.070
16	.047	.033	.183	.171	
17	-.028	.075	.122	.236	
18	.000	.014	.135	.187	
19	.013	.034	.113	.111	
c_n	0.698	0.735	0.793	0.717	0.601
c_m	-.0090	-.0065	-.0381	-.0250	-.0138

$C_N' = 0.696$ $x'_{cp} = 26.6$
$C_m' = -.0111$
$C_b' = .294$ $y'_{cp} = 42.2$

(j) $M = 0.85$ $\alpha = 9.9^\circ$
$C_{N_A} = 0.67$ $\delta_{a_L} = .5^\circ$ up
$\delta_f = 7.2^\circ$

Orifice	Row				
	1	2	3	4	5
1	1.601	2.125	2.132	2.145	1.770
2	1.990	1.990	1.801	1.906	1.601
3	1.357	1.785	1.689	1.734	1.326
4	1.694	1.574	1.529	1.694	.898
5	1.391	1.538	1.665	1.514	.821
6	1.307	1.352	1.578	1.471	.612
7	1.169	1.198	1.483	1.275	.567
8	1.160	1.128	1.480	1.166	.257
9	1.108	1.151	.916	.787	.224
10	.901	.822	.790	.710	-.178
11	.458	.508	.663	.634	-.104
12	.311	.275	.348	.485	.256
13	.006	.097	.191	.261	.174
14	.183	.076	.158	.020	.212
15	-.047	.020	.055	-.126	.133
16	.095	.060	.122	.082	
17	-.035	.041	.061	.162	
18	-.020	.034	.040	.125	
19	.007	.014	.106	.063	
c_n	0.749	0.754	0.816	0.766	0.609
c_m	-.0109	-.0051	-.0291	-.0140	-.0097

$C_N' = 0.724$ $x'_{cp} = 25.9$
$C_m' = -.0068$
$C_b' = .306$ $y'_{cp} = 42.3$

TABLE VII.- Concluded.

[$M \approx 0.85$; $\delta_f \approx 7°$]

(k) $M = 0.85$ $\quad$ $\alpha = 10.5°$
$C_{N_A} = 0.70$ $\quad$ $\delta_{a_L} = .2°$ up
$\delta_f = 7.2°$

Orifice	Row				
	1	2	3	4	5
1	1.835	2.219	2.213	2.217	1.796
2	2.045	2.053	1.866	1.915	1.609
3	1.535	1.848	1.743	1.734	1.299
4	1.722	1.709	1.600	1.667	.785
5	1.453	1.573	1.700	1.409	.636
6	1.343	1.461	1.639	1.221	.572
7	1.267	1.260	1.519	.972	.518
8	1.231	1.210	1.348	.947	.338
9	1.186	1.192	.882	.711	.272
10	.750	.610	.695	.689	-.062
11	.458	.450	.616	.613	-.035
12	.271	.295	.362	.512	.325
13	.079	.138	.265	.365	.234
14	.136	.110	.247	.162	.301
15	.040	.088	.185	-.014	.168
16	.047	.093	.237	.246	
17	.007	.102	.191	.291	
18	-.020	.062	.202	.249	
19	.033	.020	.141	.118	
c_n	0.755	0.775	0.838	0.755	0.603
c_m	-.0044	-.0044	-.0431	-.0370	-.0214

$C_N' = 0.733$ $\quad$ $x'_{cp} = 26.7$
$C_m' = -.0123$ $\quad$ $y'_{cp} = 41.9$
$C_b' = .307$

(l) $M = 0.85$ $\quad$ $\alpha = 10.9°$
$C_{N_A} = 0.73$ $\quad$ $\delta_{a_L} = .2°$ up
$\delta_f = 7.0°$

Orifice	Row				
	1	2	3	4	5
1	1.912	2.259	2.236	2.169	1.836
2	2.106	2.112	1.954	1.947	1.622
3	1.566	1.897	1.784	1.693	1.303
4	1.745	1.785	1.658	1.671	.854
5	1.465	1.622	1.704	1.377	.679
6	1.364	1.501	1.678	1.108	.620
7	1.323	1.299	1.522	.939	.506
8	1.234	1.268	1.351	.949	.373
9	1.196	1.127	.870	.734	.299
10	.692	.653	.724	.718	.000
11	.473	.457	.645	.691	.014
12	.278	.324	.438	.561	.333
13	.080	.138	.328	.407	.268
14	.170	.124	.304	.203	.309
15	.013	.095	.227	.042	.218
16	.054	.120	.292	.247	
17	-.014	.102	.218	.325	
18	-.007	.069	.196	.229	
19	.020	.020	.127	.133	
c_n	0.762	0.803	0.870	0.764	0.629
c_m	-.0031	-.0067	-.0512	-.0447	-.0290

$C_N' = 0.754$ $\quad$ $x'_{cp} = 27.2$
$C_m' = -.0162$ $\quad$ $y'_{cp} = 41.9$
$C_b' = .316$

TABLE VIII.- PRESSURE COEFFICIENTS AND AERODYNAMIC CHARACTERISTICS OF THE DOUGLAS X-3 WING

$\left[M \approx 0.90;\ \delta_f \approx 7^\circ\right]$

(a) $M = 0.90$ $C_{N_A} = 0.07$ $\alpha = 2.4^\circ$ $\delta_{a_L} = 0.2^\circ$ up $\delta_f = 10.5^\circ$

Orifice	Row 1	Row 2	Row 3	Row 4	Row 5
1	-0.585	-0.913	-1.158	-1.235	-1.253
2	-.572	-.414	-.725	-.765	-.599
3	-.223	-.088	-.377	-.462	.008
4	-.150	.048	-.231	-.171	.973
5	.300	.980	.961	-.008	.866
6	.206	.210	.789	.866	.694
7	.182	.223	.553	.739	.536
8	.166	.235	.338	.804	-.133
9	.177	.336	.387	.366	-.248
10	.287	.275	.385	.450	-.342
11	.100	.275	.354	.410	-.148
12	.195	.129	.164	.300	-.037
13	.098	.117	.091	-.172	-.060
14	.411	.319	.107	-.319	-.012
15	-.114	-.163	-.232	-.213	-.019
16	-.042	-.071	.000	-.079	
17	-.057	.000	.012	-.030	
18	-.029	-.006	-.024	-.037	
19	.006	.012	.031	.019	
c_n	0.090	0.132	0.140	0.145	0.106
c_m	-.0367	-.0312	-.0381	-.0246	-.0177

$C_N' = 0.125$ $C_m' = -.0299$ $C_b' = .055$ $x'_{cp} = 49.0$ $y'_{cp} = 44.3$

(b) $M = 0.90$ $C_{N_A} = 0.15$ $\alpha = 2.9^\circ$ $\delta_{a_L} = 0.4^\circ$ up $\delta_f = 10.6^\circ$

Orifice	Row 1	Row 2	Row 3	Row 4	Row 5
1	-0.434	-0.488	-0.921	-0.990	-0.667
2	-.369	-.191	-.446	-.468	-.308
3	-.167	-.048	-.241	-.192	.000
4	-.067	.121	-.120	-.057	.969
5	.364	.959	1.018	.047	.880
6	.318	.373	.846	.900	.713
7	.230	.216	.707	.781	.556
8	.261	.341	.425	.822	-.097
9	.247	.386	.382	.617	-.243
10	.323	.343	.477	.457	-.452
11	.176	.344	.410	.448	-.229
12	.225	.160	.226	.319	-.037
13	.147	.136	.152	-.104	-.084
14	.418	.283	.068	-.368	.000
15	-.102	-.097	-.270	-.301	-.044
16	-.060	-.131	-.024	-.110	
17	-.050	.067	-.006	-.048	
18	-.035	-.031	-.012	-.037	
19	.012	.042	.032	.006	
c_n	0.143	0.190	0.198	0.194	0.142
c_m	-.0373	-.0284	-.0370	-.0188	-.0039

$C_N' = 0.176$ $C_m' = -.0258$ $C_b' = .076$ $x'_{cp} = 39.7$ $y'_{cp} = 43.1$

TABLE VIII.- Continued.

[$M \approx 0.90$; $\delta_f \approx 7°$]

(c) $M = 0.90$ $\alpha = 3.9°$
$C_{N_A} = 0.24$ $\delta_{a_L} = 0.4°$ up
$\delta_f = 10.1°$

Orifice	Row				
	1	2	3	4	5
1	-0.128	-0.190	-0.183	-0.239	-0.285
2	-.041	.016	-.206	-.113	-.173
3	.000	.127	-.048	.016	.088
4	.142	.248	.016	.097	.965
5	.560	1.082	1.092	.148	.889
6	.435	.614	.913	.992	.746
7	.378	.406	.832	.833	.609
8	.355	.389	.745	.883	.283
9	.385	.470	.503	.694	.097
10	.410	.451	.523	.723	-.469
11	.288	.406	.493	.484	-.506
12	.265	.257	.298	.378	-.178
13	.234	.154	.248	.226	-.107
14	.429	.392	.394	-.307	.006
15	-.101	-.272	-.385	-.537	-.025
16	-.024	-.041	-.060	-.170	
17	-.044	-.018	.012	-.102	
18	-.018	-.031	-.042	-.062	
19	.006	.030	.044	-.019	
c_n	0.240	0.283	0.323	0.308	0.222
c_m	-.0402	-.0331	-.0449	-.0193	-.0109

$C_N' = 0.274$ $x'_{cp} = 35.9$
$C_m' = -.0298$ $y'_{cp} = 43.3$
$C_b' = .119$

(d) $M = 0.90$ $\alpha = 5.1°$
$C_{N_A} = 0.31$ $\delta_{a_L} = 0.1°$ down
$\delta_f = 9.2°$

Orifice	Row				
	1	2	3	4	5
1	0.247	0.182	0.143	0.158	0.032
2	.203	.269	.139	.208	.071
3	.237	.356	.159	.238	.151
4	.365	.415	.230	.291	.902
5	.722	1.078	1.080	.295	.892
6	.615	.837	.940	.980	.749
7	.503	.531	.844	.885	.643
8	.495	.500	.851	.944	.305
9	.491	.583	.745	.776	.265
10	.496	.535	.592	.792	-.152
11	.393	.478	.582	.747	-.209
12	.311	.408	.357	.460	-.325
13	.287	.196	.308	.305	-.083
14	.439	.421	.443	-.090	.036
15	-.089	-.216	-.334	-.417	.006
16	.048	.000	-.066	-.200	
17	-.013	-.006	-.024	-.042	
18	.012	.000	-.042	-.031	
19	.012	.012	.019	.006	
c_n	0.345	0.387	0.413	0.413	0.305
c_m	-.0452	-.0413	-.0486	-.0341	-.0289

$C_N' = 0.371$ $x'_{cp} = 35.3$
$C_m' = -.0380$ $y'_{cp} = 43.0$
$C_b' = .159$

TABLE VIII.- Continued.

[$M \approx 0.90$; $\delta_f \approx 7°$]

(e) $M = 0.90$, $C_{N_A} = 0.36$, $\alpha = 6.0°$, $\delta_{a_L} = 0.5°$ up, $\delta_f = 8.9°$

Orifice	Row 1	Row 2	Row 3	Row 4	Row 5
1	0.452	0.391	0.363	0.426	0.180
2	.412	.441	.293	.398	.203
3	.409	.449	.309	.378	.237
4	.536	.500	.355	.442	.898
5	.805	1.072	1.090	.432	.863
6	.682	.888	.974	.967	.774
7	.547	.638	.895	.920	.664
8	.594	.610	.924	1.004	.381
9	.570	.653	.850	.820	.299
10	.534	.604	.673	.812	-.151
11	.472	.544	.663	.774	-.183
12	.338	.479	.433	.612	-.274
13	.350	.231	.366	.376	-.419
14	.431	.443	.318	-.125	-.133
15	-.053	-.245	-.302	-.384	.025
16	.006	-.129	-.227	-.459	
17	.012	.012	-.048	-.107	
18	.006	-.006	.012	-.037	
19	.024	.018	.062	.006	
c_n	0.404	0.436	0.460	0.450	0.320
c_m	-.0442	-.0396	-.0456	-.0250	-.0171

$C_N' = 0.412$, $C_m' = -.0330$, $C_b' = .174$; $x'_{cp} = 33.0$, $y'_{cp} = 42.3$

(f) $M = 0.90$, $C_{N_A} = 0.46$, $\alpha = 7.0°$, $\delta_{a_L} = 0.4°$ up, $\delta_f = 8.4°$

Orifice	Row 1	Row 2	Row 3	Row 4	Row 5
1	0.810	1.318	1.336	1.389	0.965
2	.915	.827	1.060	1.116	.827
3	.693	.646	.809	.978	.348
4	.826	.675	.521	.780	.822
5	.946	1.097	1.083	.533	.791
6	.809	.954	1.037	1.015	.716
7	.696	.813	.888	.968	.653
8	.672	.707	1.018	1.021	.406
9	.658	.750	.906	.815	.359
10	.633	.714	.792	.837	-.030
11	.560	.629	.749	.744	-.098
12	.373	.546	.500	.636	-.165
13	.334	.335	.396	.498	-.295
14	.228	.474	.168	-.042	-.193
15	-.024	-.211	-.315	-.328	.037
16	.113	-.106	-.131	-.362	
17	.106	.024	-.078	-.137	
18	.075	.006	.048	-.037	
19	.041	.018	.087	.012	
c_n	0.499	0.547	0.567	0.563	0.414
c_m	-.0415	-.0407	-.0405	-.0196	-.0156

$C_N' = 0.516$, $C_m' = -.0307$, $C_b' = .219$; $x'_{cp} = 30.9$, $y'_{cp} = 42.4$

TABLE VIII.- Continued.

[$M \approx 0.90$; $\delta_f \approx 7°$]

(g) $M = 0.90$, $C_{N_A} = 0.53$, $\alpha = 8.0°$, $\delta_{a_L} = 0.4°$ up, $\delta_f = 8.1°$

Orifice	Row 1	Row 2	Row 3	Row 4	Row 5
1	1.004	1.581	1.580	1.624	1.198
2	1.227	1.416	1.285	1.345	1.097
3	.941	1.194	1.139	1.235	.850
4	1.128	.941	1.006	1.114	.937
5	1.068	1.141	1.289	1.008	.855
6	.946	1.021	1.266	1.185	.808
7	.840	.895	.987	1.122	.729
8	.777	.846	1.101	1.194	.503
9	.780	.856	.940	1.012	.457
10	.711	.820	.911	.974	.049
11	.655	.717	.818	.765	-.025
12	.469	.621	.635	.609	-.141
13	.270	.453	.133	.481	-.225
14	.216	.153	.022	-.048	-.176
15	.036	-.216	-.194	-.305	.000
16	.120	-.059	-.090	-.315	
17	.125	.048	.036	-.168	
18	.064	.018	.060	-.025	
19	.059	.054	.119	.019	
c_n	0.592	0.632	0.684	0.676	0.549
c_m	-.0421	-.0328	-.0412	-.0181	-.0217

$C_N' = 0.615$, $C_m' = -.0287$, $C_b' = .266$, $x'_{cp} = 29.7$, $y'_{cp} = 43.2$

(h) $M = 0.90$, $C_{N_A} = 0.60$, $\alpha = 9.0°$, $\delta_{a_L} = 0.4°$ up, $\delta_f = 7.9°$

Orifice	Row 1	Row 2	Row 3	Row 4	Row 5
1	1.156	1.807	1.800	1.812	1.398
2	1.614	1.626	1.444	1.565	1.263
3	1.124	1.451	1.348	1.429	1.032
4	1.329	1.341	1.205	1.358	1.064
5	1.274	1.293	1.432	1.188	.953
6	1.088	1.118	1.362	1.321	.790
7	1.005	1.078	1.276	1.242	.611
8	.933	.975	1.282	1.277	.290
9	.894	.942	1.052	.812	.224
10	.805	.930	.735	.646	-.018
11	.736	.832	.617	.578	.006
12	.549	.558	.311	.415	-.074
13	.256	.228	.195	.258	-.137
14	.224	.080	.158	.060	-.073
15	-.024	-.151	-.024	-.132	-.138
16	.054	-.065	.042	-.165	
17	-.019	.061	.061	-.103	
18	-.041	.031	.072	-.105	
19	.030	.055	.069	.019	
c_n	0.672	0.707	0.713	0.662	0.544
c_m	-.0326	-.0238	-.0299	.0011	.0031

$C_N' = 0.652$, $C_m' = -.0129$, $C_b' = .272$, $x'_{cp} = 27.0$, $y'_{cp} = 41.6$

TABLE VIII.- Concluded.

[$M \approx 0.90$; $\delta_f \approx 7°$]

(i) $M = 0.90$ $\alpha = 9.6°$
$C_{N_A} = 0.65$ $\delta_{a_L} = 0.4°$ down
$\delta_f = 7.9°$

Orifice	Row				
	1	2	3	4	5
1	1.157	1.827	1.821	1.857	1.455
2	1.641	1.637	1.495	1.592	1.304
3	1.108	1.469	1.366	1.455	1.056
4	1.363	1.359	1.238	1.392	1.041
5	1.282	1.294	1.442	1.204	.929
6	1.104	1.102	1.411	1.323	.664
7	.996	1.069	1.285	1.155	.485
8	.940	.957	1.347	1.032	.286
9	.926	.961	.750	.621	.226
10	.798	.937	.625	.583	.098
11	.741	.589	.603	.501	.081
12	.499	.389	.325	.376	.025
13	.126	.124	.226	.229	-.030
14	.110	.130	.182	.182	.006
15	-.090	-.098	-.006	-.057	-.076
16	-.067	-.054	.091	-.062	
17	-.051	.098	.086	-.012	
18	-.071	.062	.109	.000	
19	.000	.049	.076	.031	
c_n	0.647	0.685	0.705	0.642	0.544
c_m	-.0154	-.0175	-.0298	-.0056	-.0044

$C_N' = 0.635$ $x'_{cp} = 26.6$
$C_m' = -.0104$ $y'_{cp} = 41.8$
$C_b' = .266$

TABLE IX.- NORMAL-FORCE AND HINGE-MOMENT COEFFICIENTS FOR LEADING-EDGE FLAP OF X-3 WING.

(a) $M \approx 0.55$; $\delta_f = 0°$

α, deg	c_{n_f}					C_{N_f}	c_{h_f}					C_{h_f}
Row	1	2	3	4	5		1	2	3	4	5	
7.6	1.726	1.770	1.279	1.179	0.956	1.301	1.005	1.055	0.676	0.632	0.519	0.736
8.5	1.945	1.909	1.319	1.257	.998	1.394	1.072	1.057	.696	.673	.536	.759
9.4	2.025	1.663	1.292	1.261	1.064	1.336	1.061	.857	.674	.669	.560	.698
10.4	1.921	1.682	1.373	1.273	1.061	1.345	.990	.859	.714	.673	.566	.699
11.5	1.877	1.667	1.362	1.320	1.034	1.344	.967	.861	.714	.694	.550	.701

TABLE IX.- NORMAL-FORCE AND HINGE-MOMENT COEFFICIENTS FOR LEADING-EDGE FLAP OF X-3 WING.- Continued.

(b) $M \approx 0.71$; $\delta_f = 0°$

α, deg / Row	c_{n_f}					C_{N_f}	c_{h_f}					C_{h_f}
	1	2	3	4	5		1	2	3	4	5	
3.2	0.424	0.534	0.542	0.568	0.390	0.473	0.245	0.356	0.390	0.396	0.287	0.324
3.7	.586	.723	.662	.756	.523	.628	.350	.496	.488	.502	.351	.426
4.2	.806	.932	.836	.944	.662	.803	.487	.614	.598	.583	.411	.518
4.6	.949	1.035	.981	1.037	.758	.904	.578	.661	.658	.628	.462	.568
5.4	1.256	1.314	1.204	1.301	.924	1.138	.737	.838	.655	.758	.550	.680
6.2	1.405	1.522	1.260	1.438	1.055	1.274	.828	.935	.676	.831	.603	.746
6.8	1.579	1.705	1.289	1.523	1.018	1.365	.911	.983	.695	.849	.565	.770
7.7	1.822	1.821	1.420	1.308	1.027	1.388	1.043	.978	.749	.699	.560	.750
8.3	1.935	1.706	1.400	1.326	1.013	1.365	1.072	.881	.740	.712	.542	.724
9.6	1.865	1.620	1.472	1.319	1.023	1.342	.962	.831	.777	.709	.539	.703
10.8	1.673	1.473	1.404	1.226	.957	1.238	.861	.749	.741	.652	.510	.645
12.2	1.604	1.402	1.278	1.218	.972	1.193	.830	.716	.672	.648	.530	.624
15.5	1.323	1.212	1.064	1.086	.968	1.045	.691	.624	.570	.578	.535	.552

TABLE IX.- NORMAL-FORCE AND HINGE-MOMENT COEFFICIENTS FOR LEADING-EDGE FLAP OF X-3 WING.- Continued.

(c) $M \approx 0.77$; $\delta_f = 0°$

α, deg	c_{n_f}					C_{N_f}	c_{h_f}					C_{h_f}
Row	1	2	3	4	5		1	2	3	4	5	
2.2	0.198	0.231	0.233	0.319	0.132	0.220	0.115	0.126	0.173	0.220	0.082	0.140
2.4	.302	.386	.392	.454	.260	.350	.177	.237	.285	.321	.182	.234
3.5	.531	.703	.647	.742	.522	.611	.311	.461	.455	.487	.364	.405
3.8	.660	.858	.788	.892	.646	.744	.390	.561	.544	.558	.433	.482
4.9	.950	1.142	1.036	1.176	.876	.995	.568	.711	.699	.692	.532	.613
5.5	1.126	1.343	1.276	1.301	1.012	1.156	.673	.816	.791	.762	.622	.697
6.2	1.381	1.610	1.519	1.498	1.148	1.362	.814	.916	.866	.854	.674	.781
6.6	1.516	1.717	1.598	1.540	1.214	1.438	.891	.980	.887	.869	.704	.819
7.6	1.812	1.849	1.563	1.644	1.230	1.529	1.034	.996	.826	.907	.675	.834
8.2	1.865	1.818	1.557	1.453	1.149	1.464	1.062	.945	.818	.781	.624	.781
8.9	1.912	1.685	1.456	1.400	1.091	1.394	1.051	.859	.763	.747	.593	.734
10.4	1.786	1.590	1.460	1.349	1.110	1.343	.934	.815	.760	.719	.601	.704
11.9	1.654	1.436	1.342	1.290	1.054	1.246	.857	.743	.707	.683	.570	.654

TABLE IX.- NORMAL-FORCE AND HINGE-MOMENT COEFFICIENTS FOR LEADING-EDGE FLAP OF X-3 WING.- Continued.

(d) $M \approx 0.83$; $\delta_f = 0°$

α, deg	c_{n_f}					C_{N_f}	c_{h_f}					C_{h_f}
Row	1	2	3	4	5		1	2	3	4	5	
2.3	0.234	0.274	0.308	0.369	0.192	0.267	0.141	0.156	0.216	0.260	0.130	0.175
2.4	.274	.324	.363	.442	.243	.320	.168	.196	.270	.306	.182	.216
3.1	.437	.547	.568	.597	.360	.486	.261	.354	.395	.414	.258	.327
3.8	.676	.796	.780	.859	.606	.712	.416	.528	.548	.594	.479	.491
4.5	.906	1.073	1.054	1.174	.874	.972	.549	.694	.710	.764	.621	.638
5.2	1.094	1.301	1.407	1.474	1.130	1.219	.649	.796	.820	.854	.704	.728
5.7	1.238	1.563	1.542	1.597	1.342	1.390	.726	.871	.862	.898	.785	.786
6.2	1.348	1.632	1.616	1.661	1.391	1.454	.780	.904	.892	.931	.790	.814
6.9	1.472	1.738	1.711	1.743	1.492	1.545	.842	.950	.934	.973	.832	.856
7.4	1.551	1.806	1.764	1.802	1.561	1.605	.889	.984	.963	1.001	.868	.887
8.2	1.661	1.928	1.878	1.813	1.572	1.672	.952	1.038	1.017	1.020	.892	.924
10.1	1.802	1.520	1.620	1.048	.852	1.235	.965	.778	.860	.562	.482	.654
11.1	1.806	1.579	1.580	1.341	1.007	1.343	.949	.812	.822	.722	.548	.707

TABLE IX.- NORMAL-FORCE AND HINGE-MOMENT COEFFICIENTS FOR LEADING-EDGE FLAP OF X-3 WING.- Continued.

(e) $M \approx 0.88$; $\delta_f = 0°$

α, deg	c_{n_f}					C_{N_f}	c_{h_f}					C_{h_f}
Row	1	2	3	4	5		1	2	3	4	5	
1.6	0.123	0.155	0.131	0.207	0.077	0.140	0.071	0.080	0.104	0.140	0.055	0.089
2.3	.266	.285	.226	.325	.099	.238	.157	.160	.146	.209	.061	.145
2.6	.352	.337	.426	.540	.211	.361	.213	.186	.318	.390	.174	.244
3.4	.591	.688	.684	.793	.541	.633	.365	.465	.482	.540	.416	.435
4.2	.775	.948	1.070	1.157	.922	.927	.457	.606	.636	.676	.560	.562
4.6	.904	1.117	1.177	1.271	1.042	1.050	.526	.669	.685	.729	.612	.615
5.1	.997	1.317	1.251	1.329	1.075	1.148	.582	.734	.716	.758	.622	.653
5.4	1.100	1.372	1.339	1.374	1.126	1.205	.642	.760	.751	.776	.646	.679
6.2	1.261	1.485	1.434	1.470	1.216	1.304	.720	.819	.796	.824	.688	.728
6.8	1.369	1.587	1.524	1.564	1.298	1.392	.783	.869	.840	.871	.727	.772
8.4	1.602	1.768	1.682	1.733	1.467	1.557	.894	.955	.922	.953	.817	.853
9.5	1.741	1.910	1.812	1.732	1.432	1.625	.958	1.020	.986	.964	.805	.889
10.8	1.876	2.054	1.888	1.528	1.004	1.581	1.025	1.088	1.029	.853	.564	.860
11.8	1.955	2.108	1.827	1.477	.914	1.571	1.058	1.113	1.019	.823	.513	.855
12.5	2.047	2.183	1.910	1.548	1.030	1.647	1.096	1.146	1.046	.858	.547	.885
14.4	1.705	1.603	1.594	1.474	1.129	1.393	.898	.809	.826	.772	.612	.723
15.2	1.480	1.328	1.242	1.260	1.069	1.178	.768	.684	.652	.667	.577	.617

TABLE IX.- NORMAL-FORCE AND HINGE-MOMENT COEFFICIENTS FOR LEADING-EDGE FLAP OF X-3 WING.- Continued.

(f) $M \approx 0.90$; $\delta_f = 0°$

α, deg	c_{n_f}					C_{N_f}	c_{h_f}					C_{h_f}
Row	1	2	3	4	5		1	2	3	4	5	
2.6	0.386	0.368	0.468	0.566	0.315	0.400	0.226	0.203	0.351	0.400	0.274	0.271
3.1	.518	.622	.587	.688	.464	.556	.323	.412	.430	.401	.378	.386
3.7	.672	.836	.803	.973	.807	.784	.406	.532	.546	.607	.505	.497
4.2	.767	.953	1.047	1.136	.932	.921	.446	.604	.627	.662	.553	.555
4.8	.924	1.197	1.179	1.247	1.022	1.067	.540	.692	.679	.710	.604	.616
5.3	1.026	1.303	1.268	1.317	1.085	1.147	.599	.722	.720	.747	.632	.650
5.7	1.146	1.386	1.312	1.370	1.136	1.210	.661	.766	.742	.774	.653	.681
6.2	1.246	1.453	1.378	1.450	1.201	1.278	.717	.798	.770	.812	.687	.715
6.9	1.353	1.555	1.470	1.530	1.284	1.363	.776	.846	.815	.853	.723	.756
7.6	1.456	1.643	1.567	1.610	1.370	1.445	.827	.891	.862	.893	.761	.797
8.5	1.570	1.751	1.659	1.709	1.460	1.538	.883	.942	.907	.944	.812	.843
9.4	1.674	1.885	1.762	1.822	1.556	1.644	.930	1.010	.961	1.000	.861	.896
10.9	1.833	1.992	1.874	1.818	1.480	1.696	1.001	1.062	1.012	1.000	.825	.921
12.3	1.999	2.134	1.958	1.650	1.192	1.683	1.083	1.127	1.051	.907	.691	.911
13.3	2.116	2.213	1.961	1.649	1.076	1.702	1.129	1.163	1.049	.898	.591	.910

TABLE IX.- NORMAL-FORCE AND HINGE-MOMENT COEFFICIENTS FOR LEADING-EDGE FLAP OF X-3 WING.- Continued.

(g) $M \approx 0.92$; $\delta_f = 0°$

α, deg	c_{n_f}					C_{N_f}	c_{h_f}					C_{h_f}
Row	1	2	3	4	5		1	2	3	4	5	
1.7	0.148	0.177	0.155	0.220	0.070	0.155	0.080	0.100	0.113	0.143	0.050	0.097
2.2	.216	.250	.175	.284	.089	.204	.133	.137	.117	.186	.055	.125
2.6	.323	.329	.422	.510	.290	.358	.195	.176	.306	.365	.250	.242
3.4	.554	.667	.653	.790	.694	.639	.343	.435	.459	.529	.437	.421
3.9	.654	.843	.951	1.039	.841	.827	.389	.535	.565	.609	.499	.499
4.3	.734	.942	1.010	1.097	.909	.896	.427	.574	.590	.637	.538	.530
4.9	.870	1.128	1.124	1.180	.974	1.010	.505	.649	.642	.677	.568	.582
5.4	1.003	1.286	1.234	1.276	1.051	1.120	.581	.716	.693	.725	.606	.633
6.0	1.102	1.356	1.308	1.342	1.125	1.187	.638	.745	.728	.759	.639	.666
6.7	1.201	1.430	1.385	1.416	1.197	1.258	.692	.783	.766	.799	.677	.703
7.1	1.311	1.508	1.441	1.483	1.240	1.323	.754	.825	.798	.831	.700	.737
7.7	1.395	1.587	1.516	1.554	1.311	1.393	.794	.866	.831	.866	.734	.771
8.2	1.473	1.675	1.578	1.622	1.386	1.463	.834	.901	.862	.898	.773	.803
9.1	1.605	1.808	1.703	1.743	1.517	1.581	.899	.967	.925	.959	.839	.862
9.9	1.685	1.887	1.780	1.813	1.572	1.648	.929	1.005	.955	.997	.859	.893
10.9	1.829	1.995	1.870	1.904	1.672	1.744	.994	1.059	1.004	1.040	.911	.940
12.0	1.918	2.070	1.944	1.973	1.732	1.811	1.040	1.088	1.036	1.072	.941	.970
16.7	1.759	1.644	1.812	1.394	1.152	1.424	.903	.837	.921	.734	.618	.736
17.6	1.718	1.628	1.582	1.394	1.173	1.386	.887	.820	.818	.732	.634	.717

TABLE IX.- NORMAL-FORCE AND HINGE-MOMENT COEFFICIENTS FOR LEADING-EDGE FLAP OF X-3 WING.- Continued.

(h) $M \approx 0.96$; $\delta_f = 0°$

α, deg	c_{n_f}					C_{N_f}	c_{h_f}					C_{h_f}
Row	1	2	3	4	5		1	2	3	4	5	
1.8	0.126	0.162	0.100	0.212	0.058	0.136	0.072	0.090	0.075	0.133	0.040	0.084
2.2	.216	.231	.171	.285	.075	.196	.129	.125	.118	.182	.052	.120
2.7	.327	.331	.422	.506	.343	.365	.193	.178	.316	.361	.290	.248
3.3	.506	.604	.590	.731	.628	.583	.307	.399	.424	.489	.397	.387
3.9	.603	.762	.841	.925	.740	.739	.360	.483	.512	.553	.449	.453
4.4	.701	.897	.953	1.036	.832	.845	.408	.548	.567	.599	.488	.501
4.9	.821	1.070	1.047	1.117	.918	.954	.474	.607	.603	.642	.532	.547
5.2	.923	1.197	1.134	1.178	.977	1.037	.537	.666	.641	.671	.559	.587
5.6	1.004	1.264	1.199	1.238	1.030	1.096	.576	.697	.673	.701	.586	.616
6.2	1.119	1.333	1.273	1.312	1.086	1.164	.647	.734	.710	.737	.616	.652
6.8	1.222	1.420	1.347	1.381	1.153	1.237	.698	.780	.746	.774	.653	.690
7.5	1.343	1.526	1.439	1.474	1.251	1.330	.761	.824	.790	.824	.705	.735
8.1	1.429	1.609	1.523	1.563	1.337	1.409	.810	.870	.832	.861	.743	.774
8.6	1.498	1.675	1.586	1.616	1.394	1.466	.844	.900	.863	.894	.765	.802
9.3	1.562	1.773	1.649	1.693	1.473	1.540	.872	.946	.895	.930	.808	.838
10.3	1.648	1.826	1.699	1.750	1.501	1.590	.908	.970	.917	.958	.827	.861
10.8	1.726	1.882	1.763	1.811	1.564	1.647	.939	.999	.945	.988	.863	.889
11.2	1.812	1.964	1.837	1.880	1.639	1.718	.983	1.040	.988	1.025	.893	.925
12.0	1.911	2.037	1.907	1.956	1.709	1.788	1.028	1.072	1.022	1.059	.937	.958
11.9	1.952	2.075	1.947	1.972	1.736	1.816	1.053	1.088	1.033	1.061	.945	.969
13.6	2.036	2.141	2.020	2.051	1.811	1.884	1.086	1.115	1.064	1.095	.974	.997

890
849

TABLE IX.- NORMAL-FORCE AND HINGE-MOMENT COEFFICIENTS FOR LEADING-EDGE FLAP OF X-3 WING.- Continued.

(i) $M \approx 0.99$; $\delta_f = 0°$

α, deg / Row	c_{n_f}					C_{N_f}	c_{h_f}					C_{h_f}
	1	2	3	4	5		1	2	3	4	5	
3.0	0.210	0.244	0.325	0.419	0.268	0.282	0.129	0.132	0.257	0.304	0.266	0.202
3.5	.361	.469	.488	.569	.395	.442	.221	.303	.354	.399	.305	.305
4.4	.533	.699	.796	.875	.679	.687	.327	.442	.483	.520	.419	.420
5.0	.646	.836	.887	.965	.778	.787	.376	.509	.529	.558	.464	.467
5.3	.797	1.074	1.014	1.073	.870	.930	.464	.596	.583	.614	.508	.529
5.9	.907	1.150	1.089	1.143	.940	1.001	.525	.636	.618	.650	.544	.566
6.5	1.029	1.247	1.187	1.238	1.021	1.090	.596	.690	.665	.698	.590	.614
6.8	1.137	1.320	1.263	1.316	1.092	1.163	.658	.725	.700	.737	.627	.650
7.4	1.259	1.441	1.352	1.403	1.182	1.257	.722	.783	.745	.782	.665	.697
8.1	1.352	1.516	1.431	1.475	1.246	1.327	.769	.819	.779	.816	.695	.729
8.6	1.433	1.588	1.493	1.531	1.308	1.387	.811	.855	.812	.846	.733	.761
9.1	1.524	1.695	1.592	1.624	1.386	1.476	.851	.901	.859	.893	.767	.802
9.4	1.498	1.666	1.550	1.597	1.362	1.449	.837	.888	.843	.875	.760	.789
10.0	1.585	1.755	1.636	1.679	1.439	1.527	.878	.933	.884	.917	.799	.828
10.4	1.658	1.811	1.683	1.721	1.483	1.574	.910	.959	.908	.937	.813	.849
11.0	1.733	1.863	1.732	1.787	1.539	1.628	.943	.986	.933	.970	.852	.878
11.4	1.803	1.920	1.786	1.822	1.579	1.673	.976	1.013	.958	.990	.861	.899
12.3	1.899	2.002	1.861	1.900	1.664	1.749	1.017	1.052	.995	1.021	.905	.934

TABLE IX.- NORMAL-FORCE AND HINGE-MOMENT COEFFICIENTS FOR LEADING-EDGE FLAP OF X-3 WING.- Continued.

(j) $M \approx 1.01;\ \delta_f = 0°$

α, deg / Row	c_{n_f}					C_{N_f}	c_{h_f}					C_{h_f}
	1	2	3	4	5		1	2	3	4	5	
2.5	0.044	0.099	0.040	0.153	0.011	0.080	0.027	0.054	0.041	0.103	0.019	0.054
2.4	.140	.178	.108	.209	.024	.138	.089	.101	.077	.129	.021	.085
3.1	.328	.357	.414	.521	.348	.376	.204	.221	.305	.365	.282	.260
3.7	.453	.574	.567	.712	.596	.557	.282	.376	.400	.467	.371	.365
4.1	.545	.700	.786	.868	.688	.686	.328	.449	.477	.517	.414	.420
4.7	.618	.821	.869	.955	.762	.773	.362	.504	.515	.553	.448	.459
5.1	.765	1.038	.981	1.046	.854	.903	.452	.578	.562	.599	.499	.515
5.5	.842	1.087	1.034	1.096	.891	.950	.495	.606	.589	.627	.518	.541
6.0	.969	1.189	1.142	1.183	.986	1.043	.570	.662	.638	.674	.566	.590
6.6	1.129	1.370	1.281	1.314	1.108	1.181	.656	.762	.712	.740	.626	.663
7.2	1.261	1.441	1.374	1.416	1.196	1.266	.724	.785	.755	.791	.674	.702
7.5	1.332	1.502	1.432	1.464	1.247	1.318	.763	.818	.781	.815	.700	.729
8.1	1.417	1.580	1.497	1.534	1.308	1.385	.808	.854	.814	.850	.732	.762
9.3	1.574	1.758	1.642	1.675	1.448	1.528	.882	.939	.889	.922	.797	.832
9.7	1.593	1.774	1.667	1.703	1.470	1.548	.891	.951	.897	.934	.807	.842

TABLE IX.- NORMAL-FORCE AND HINGE-MOMENT COEFFICIENTS FOR LEADING-EDGE FLAP OF X-3 WING.- Continued.

(k) $M \approx 1.10$; $\delta_f = 0°$

α, deg / Row	c_{n_f}					C_{N_f}	c_{h_f}					C_{h_f}
	1	2	3	4	5		1	2	3	4	5	
2.7	0.136	0.158	0.199	0.288	0.019	0.164	0.093	0.079	0.173	0.207	0.039	0.115
2.7	.178	.187	.264	.353	.163	.223	.121	.099	.215	.255	.176	.161
2.8	.260	.352	.368	.461	.293	.339	.162	.230	.273	.322	.231	.236
3.3	.385	.499	.575	.675	.492	.505	.231	.313	.361	.412	.307	.313
4.1	.494	.616	.665	.761	.580	.597	.295	.375	.401	.452	.351	.359
4.5	.576	.742	.742	.831	.639	.679	.340	.429	.436	.486	.388	.398
5.2	.732	.926	.871	.945	.769	.813	.433	.509	.502	.542	.443	.462
5.5	.797	.993	.931	1.001	.819	.869	.469	.542	.530	.573	.473	.491
6.2	.909	1.109	1.043	1.103	.917	.969	.530	.605	.585	.625	.526	.544
6.6	.973	1.160	1.093	1.151	.966	1.017	.566	.633	.610	.650	.550	.569
7.6	1.121	1.263	1.200	1.254	1.050	1.114	.637	.686	.661	.699	.599	.618
8.4	1.214	1.346	1.285	1.329	1.129	1.189	.685	.729	.702	.737	.638	.656
9.1	1.270	1.427	1.356	1.402	1.197	1.257	.720	.769	.737	.772	.674	.690
9.7	1.361	1.532	1.436	1.474	1.268	1.336	.765	.818	.779	.809	.706	.728
10.1	1.433	1.599	1.498	1.531	1.325	1.394	.800	.850	.809	.837	.737	.757
10.6	1.512	1.669	1.557	1.597	1.386	1.455	.837	.883	.836	.873	.768	.787
11.4	1.603	1.744	1.635	1.661	1.447	1.522	.877	.920	.875	.905	.794	.819
12.2	1.697	1.823	1.697	1.735	1.515	1.591	.921	.961	.908	.938	.830	.854
13.0	1.786	1.891	1.760	1.797	1.581	1.654	.963	.991	.938	.967	.861	.882
13.8	1.872	1.954	1.843	1.863	1.639	1.717	.998	1.019	.972	.995	.888	.910
14.6	1.966	2.019	1.908	1.934	1.712	1.782	1.036	1.047	1.000	1.028	.927	.939
15.6	2.048	2.087	1.978	2.000	1.794	1.849	1.082	1.083	1.035	1.059	.963	.972
17.4	2.105	2.141	2.036	2.064	1.875	1.905	1.106	1.103	1.062	1.090	1.005	.998

TABLE IX.- NORMAL-FORCE AND HINGE-MOMENT COEFFICIENTS FOR LEADING-EDGE FLAP OF X-3 WING.- Concluded.

(l) $M \approx 1.15$; $\delta_f = 0°$

α, deg / Row	c_{n_f}					C_{N_f}	c_{h_f}					C_{h_f}
	1	2	3	4	5		1	2	3	4	5	
1.9	0.030	0.063	-0.007	0.131	-0.044	0.048	0.040	0.024	0.020	0.086	-0.009	0.035
1.8	.078	.096	.057	.151	-.023	.080	.065	.045	.060	.091	.008	.053
2.0	.156	.172	.230	.330	.158	.205	.105	.095	.194	.236	.154	.147
2.9	.305	.420	.467	.578	.402	.422	.185	.255	.301	.353	.267	.263
3.6	.426	.551	.581	.682	.498	.528	.257	.321	.355	.405	.312	.316
4.0	.511	.653	.648	.739	.560	.599	.308	.363	.389	.434	.343	.350
4.4	.613	.755	.726	.815	.638	.680	.361	.419	.426	.473	.381	.392
5.4	.746	.905	.848	.935	.755	.801	.431	.493	.487	.534	.440	.453
5.8	.811	.970	.908	.983	.803	.854	.464	.526	.512	.558	.466	.479
6.3	.885	1.035	.983	1.047	.855	.914	.504	.562	.548	.591	.490	.510
6.9	.965	1.102	1.047	1.109	.915	.974	.549	.598	.580	.622	.524	.542
7.8	1.087	1.219	1.156	1.210	1.022	1.077	.615	.661	.632	.674	.576	.595
8.2	1.133	1.274	1.211	1.260	1.071	1.124	.647	.688	.661	.699	.604	.620
8.9	1.232	1.348	1.279	1.328	1.129	1.190	.695	.725	.695	.734	.633	.653
9.4	1.318	1.429	1.351	1.389	1.190	1.257	.737	.765	.730	.765	.663	.686
10.2	1.397	1.533	1.429	1.474	1.268	1.338	.776	.812	.769	.804	.700	.724
11.2	1.489	1.623	1.519	1.567	1.354	1.422	.815	.856	.812	.849	.747	.765
12.2	1.566	1.704	1.595	1.632	1.418	1.490	.847	.896	.848	.881	.773	.797
13.2	1.649	1.778	1.660	1.705	1.487	1.557	.886	.931	.873	.913	.810	.827
13.9	1.736	1.843	1.728	1.761	1.548	1.616	.925	.962	.913	.939	.837	.856
14.7	1.819	1.894	1.783	1.805	1.594	1.665	.963	.983	.937	.961	.857	.878
17.0	1.942	1.968	1.863	1.913	1.684	1.750	1.028	1.014	.973	1.014	.906	.918
17.8	2.006	2.031	1.946	1.985	1.768	1.816	1.057	1.046	1.011	1.049	.956	.952

TABLE X.- NORMAL-FORCE AND HINGE-MOMENT COEFFICIENTS FOR LEADING-EDGE FLAP OF X-3 WING

(a) $M \approx 0.55$; $\delta_f = 7^\circ$

α, deg	c_{n_f}					C_{N_f}	c_{h_f}					C_{h_f}
Row	1	2	3	4	5		1	2	3	4	5	
7.4	1.160	1.330	1.162	1.245	0.896	1.109	0.577	0.808	0.739	0.717	0.545	0.656
8.4	1.448	1.646	1.530	1.512	1.098	1.378	.714	.996	.873	.848	.627	.788
9.5	1.678	1.970	1.566	1.718	1.253	1.574	.819	1.137	.812	.950	.692	.866
10.7	1.948	2.112	1.553	1.466	1.367	1.591	.959	1.153	.790	.755	.772	.843
11.5	2.282	1.947	1.504	1.481	1.339	1.568	1.220	.994	.770	.761	.723	.812
12.4	2.444	1.874	1.529	1.366	1.289	1.529	1.319	.945	.782	.698	.675	.787
13.4	2.499	1.687	1.525	1.365	1.232	1.471	1.362	.880	.783	.703	.643	.769

TABLE X.- NORMAL-FORCE AND HINGE-MOMENT COEFFICIENTS FOR LEADING-EDGE FLAP OF X-3 WING.- Continued.

(b) $M \approx 0.71$; $\delta_f = 7°$

α, deg	c_{n_f}					C_{N_f}	c_{h_f}					C_{h_f}
Row	1	2	3	4	5		1	2	3	4	5	
1.4	-0.259	-0.223	-0.207	-0.221	-0.194	-0.203	-0.191	-0.248	-0.190	-0.218	-0.227	-0.205
1.9	-.084	.022	.009	.014	-.023	.000	-.106	-.055	-.042	-.048	-.083	-.056
2.6	.111	.190	.157	.178	.074	.145	.015	.049	.059	.056	-.024	.036
3.7	.306	.390	.324	.365	.199	.311	.122	.169	.156	.168	.063	.136
4.4	.578	.611	.624	.628	.339	.531	.277	.325	.350	.345	.153	.281
4.8	.703	.742	.730	.758	.431	.642	.330	.429	.450	.441	.214	.364
5.9	.974	1.107	1.025	1.080	.757	.945	.488	.665	.646	.632	.470	.561
6.9	1.253	1.382	1.242	1.331	.949	1.174	.628	.826	.802	.761	.548	.687
7.4	1.379	1.543	1.439	1.464	1.078	1.313	.698	.905	.882	.813	.623	.752
8.3	1.648	1.811	1.714	1.612	1.253	1.518	.856	1.002	.995	.895	.700	.843
8.7	1.763	1.902	1.772	1.699	1.294	1.592	.934	1.030	.997	.934	.726	.872
9.7	2.126	1.999	1.727	1.842	1.447	1.707	1.164	1.047	.918	.999	.803	.916
10.2	2.210	1.896	1.635	1.684	1.430	1.629	1.210	.966	.860	.900	.793	.861
10.3	2.155	1.655	1.576	1.469	1.397	1.491	1.195	.838	.834	.788	.757	.785
11.4	2.197	1.695	1.515	1.549	1.402	1.513	1.231	.868	.780	.826	.741	.797
13.0	1.995	1.396	1.358	1.264	1.206	1.284	1.102	.710	.710	.657	.646	.672
14.7	2.004	1.552	1.413	1.355	.983	1.331	1.087	.786	.737	.702	.512	.690
16.4	1.574	1.176	1.015	1.118	1.305	1.106	.849	.599	.548	.585	.690	.580

TABLE X.- NORMAL-FORCE AND HINGE-MOMENT COEFFICIENTS FOR LEADING-EDGE FLAP OF X-3 WING.- Continued.

(c) $M \approx 0.76$; $\delta_f = 7°$

α, deg / Row	c_{n_f} 1	c_{n_f} 2	c_{n_f} 3	c_{n_f} 4	c_{n_f} 5	C_{N_f}	c_{h_f} 1	c_{h_f} 2	c_{h_f} 3	c_{h_f} 4	c_{h_f} 5	C_{h_f}
2.8	0.006	0.146	0.105	0.140	0.063	0.103	-0.033	0.013	0.019	0.020	-0.032	0.004
3.0	.091	.227	.182	.200	.110	.168	.016	.062	.062	.060	-.004	.043
3.7	.256	.332	.277	.312	.201	.269	.101	.130	.125	.130	.060	.107
4.4	.427	.482	.437	.494	.300	.413	.192	.217	.221	.243	.126	.193
4.9	.546	.619	.610	.649	.375	.539	.255	.318	.350	.355	.166	.281
5.6	.764	.900	.849	.863	.580	.759	.377	.530	.513	.511	.340	.442
6.4	1.030	1.183	1.097	1.159	.825	1.012	.525	.705	.687	.686	.514	.601
7.0	1.295	1.437	1.351	1.285	1.043	1.210	.644	.856	.821	.801	.618	.720
7.6	1.477	1.638	1.704	1.620	1.177	1.441	.742	.983	.992	.998	.729	.856
8.2	1.614	1.814	1.845	1.839	1.346	1.605	.809	1.058	1.046	1.061	.850	.925
8.7	1.747	1.965	1.920	1.891	1.451	1.701	.879	1.111	1.081	1.078	.891	.962
9.4	1.933	2.122	2.036	1.928	1.499	1.797	.988	1.167	1.134	1.092	.842	.994
9.9	2.061	2.223	2.026	1.923	1.566	1.846	1.068	1.222	1.147	1.074	.881	1.021
10.6	2.158	1.831	1.590	1.428	1.456	1.536	1.147	.945	.840	.750	.810	.810
11.7	2.096	1.565	1.546	1.372	1.485	1.435	1.143	.791	.827	.709	.819	.753
13.5	1.980	1.407	1.336	1.372	1.200	1.309	1.090	.712	.692	.730	.648	.688

TABLE X.- NORMAL-FORCE AND HINGE-MOMENT COEFFICIENTS FOR LEADING-EDGE FLAP OF X-3 WING.- Continued.

(d) $M \approx 0.80$; $\delta_f = 7°$

α, deg / Row	c_{n_f}					C_{N_f}	c_{h_f}					C_{h_f}
	1	2	3	4	5		1	2	3	4	5	
2.6	-0.094	0.030	-0.004	0.010	0.019	0.004	-0.094	-0.067	-0.058	-0.080	-0.095	-0.071
3.1	.057	.175	.157	.171	.093	.136	-.014	.025	.033	.020	-.036	.011
3.5	.123	.266	.224	.249	.150	.206	.034	.073	.072	.073	.005	.055
4.2	.310	.403	.357	.377	.251	.330	.127	.149	.148	.160	.073	.128
4.9	.507	.578	.535	.553	.360	.486	.231	.263	.274	.277	.141	.229
5.6	.708	.788	.776	.779	.510	.679	.345	.429	.439	.437	.250	.368
5.9	.816	.916	.852	.829	.601	.763	.392	.519	.492	.462	.330	.424
6.4	.985	1.057	1.000	.996	.574	.881	.482	.620	.605	.603	.289	.508
7.0	1.139	1.222	1.193	1.267	.898	1.085	.572	.723	.737	.765	.583	.648
7.6	1.299	1.448	1.531	1.541	1.291	1.339	.631	.847	.843	.869	.728	.752
8.3	1.457	1.658	1.671	1.688	1.428	1.492	.706	.937	.912	.944	.788	.822
8.6	1.504	1.724	1.713	1.743	1.489	1.544	.726	.955	.940	.970	.816	.844
8.6	1.538	1.786	1.716	1.764	1.490	1.572	.741	.981	.943	.978	.824	.857
9.4	1.703	1.916	1.820	1.857	1.559	1.674	.836	1.041	1.000	1.025	.874	.910
10.2	1.921	2.055	1.942	1.874	1.620	1.766	.972	1.109	1.063	1.051	.922	.965
11.6	2.177	2.230	1.910	1.257	1.435	1.654	1.123	1.205	1.074	.654	.808	.893
13.0	2.225	1.760	1.707	1.325	1.252	1.484	1.172	.899	.909	.695	.683	.778
15.0	2.076	1.532	1.530	1.239	1.035	1.326	1.130	.776	.800	.649	.543	.691
15.8	1.936	1.378	1.396	1.199	1.011	1.235	1.077	.707	.728	.625	.537	.648

.12

TABLE X.- NORMAL-FORCE AND HINGE-MOMENT COEFFICIENTS FOR LEADING-EDGE FLAP OF X-3 WING.- Continued.

(e) $M \approx 0.85$; $\delta_f = 7°$

α, deg	c_{n_f}					C_{N_f}	c_{h_f}					C_{h_f}
Row	1	2	3	4	5		1	2	3	4	5	
2.7	-0.108	-0.006	-0.011	-0.044	-0.059	-0.033	-0.103	-0.107	-0.096	-0.124	-0.133	-0.105
2.9	-.025	.088	.011	.037	-.029	.031	-.087	-.062	-.073	-.065	-.107	-.069
4.2	.261	.336	.270	.298	.168	.262	.103	.112	.093	.111	.034	.089
5.2	.509	.517	.450	.496	.310	.434	.233	.217	.217	.234	.127	.194
5.9	.696	.609	.619	.632	.361	.545	.339	.282	.326	.325	.159	.267
7.0	1.010	1.145	1.105	1.186	.980	1.028	.497	.659	.640	.685	.564	.585
8.0	1.296	1.479	1.417	1.464	1.242	1.305	.625	.823	.777	.812	.679	.713
9.0	1.516	1.713	1.575	1.640	1.372	1.480	.715	.930	.856	.898	.764	.798
9.5	1.592	1.786	1.636	1.683	1.420	1.535	.775	.964	.881	.923	.790	.827
9.9	1.728	1.829	1.717	1.761	1.488	1.602	.848	.987	.921	.956	.835	.862
10.5	1.830	1.928	1.786	1.727	1.477	1.640	.930	1.033	.957	.964	.842	.891
10.9	1.879	1.986	1.834	1.699	1.503	1.665	.962	1.057	.977	.951	.859	.903

TABLE X.- NORMAL-FORCE AND HINGE-MOMENT COEFFICIENTS FOR LEADING-EDGE FLAP OF X-3 WING.- Concluded.

(f) $M \approx 0.90$; $\delta_f = 7°$

α, deg	c_{n_f}					C_{N_f}	c_{h_f}					C_{h_f}
Row	1	2	3	4	5		1	2	3	4	5	
2.4	-0.383	-0.288	-0.443	-0.410	-0.469	-0.353	-0.255	-0.293	-0.374	-0.370	-0.496	-0.326
2.9	-.249	-.087	-.283	-.253	-.209	-.183	-.179	-.146	-.277	-.266	-.260	-.203
3.9	.020	.111	.024	.054	-.001	.052	-.033	-.025	-.051	-.040	-.094	-.041
5.1	.295	.351	.264	.287	.167	.266	.125	.127	.088	.110	.036	.095
6.0	.484	.485	.407	.456	.273	.401	.225	.212	.174	.213	.102	.178
7.0	.845	.924	.847	.920	.676	.801	.416	.532	.509	.550	.419	.467
8.0	1.110	1.251	1.206	1.246	1.017	1.104	.536	.705	.660	.691	.562	.606
9.0	1.341	1.540	1.399	1.443	1.201	1.314	.645	.831	.759	.792	.661	.707
9.6	1.362	1.556	1.429	1.470	1.236	1.337	.651	.840	.773	.809	.686	.720

TABLE XI.- NORMAL-FORCE AND HINGE-MOMENT COEFFICIENTS FOR LEADING-EDGE FLAP OF X-3 WING

(a) $M \approx 0.55$; $\delta_f = 27°$

α, deg	c_{n_f}					C_{N_f}	c_{h_f}					C_{h_f}
Row	1	2	3	4	5		1	2	3	4	5	
6.7	-0.664	-0.368	-0.580	-0.380	-0.790	-0.460	-0.506	-0.382	-0.558	-0.274	-0.615	-0.394
10.0	.360	.512	.355	.212	-.091	.278	.034	.103	.042	-.045	-.286	-.011
12.0	.897	1.006	.883	.803	.558	.790	.295	.377	.340	.297	.152	.285
13.4	1.144	1.329	1.160	1.012	.641	1.012	.411	.632	.561	.435	.229	.448
14.6	1.360	1.731	1.562	1.441	.850	1.347	.525	.891	.808	.708	.330	.654
15.2	1.427	1.850	1.681	1.546	.909	1.440	.548	.965	.885	.784	.361	.712
16.0	1.772	2.151	2.008	1.867	1.311	1.745	.708	1.186	1.112	.979	.686	.919
17.5	2.137	2.572	2.350	2.340	1.675	2.123	.861	1.431	1.319	1.232	.913	1.131
18.3	2.371	2.595	2.370	2.306	1.663	2.145	.972	1.363	1.342	1.241	.913	1.127

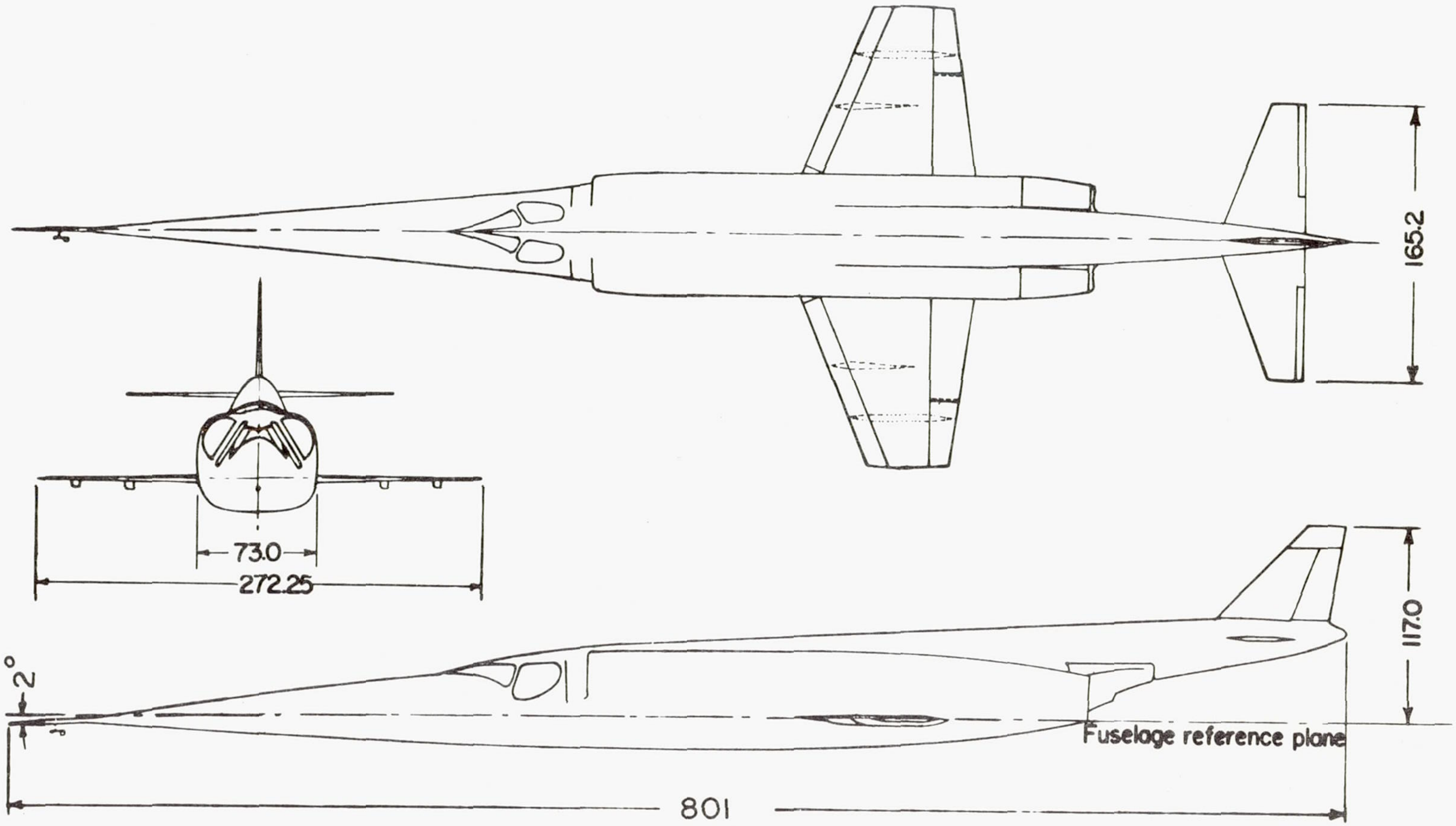

Figure 1.- Three-view drawing of the X-3 airplane. All dimensions in inches.

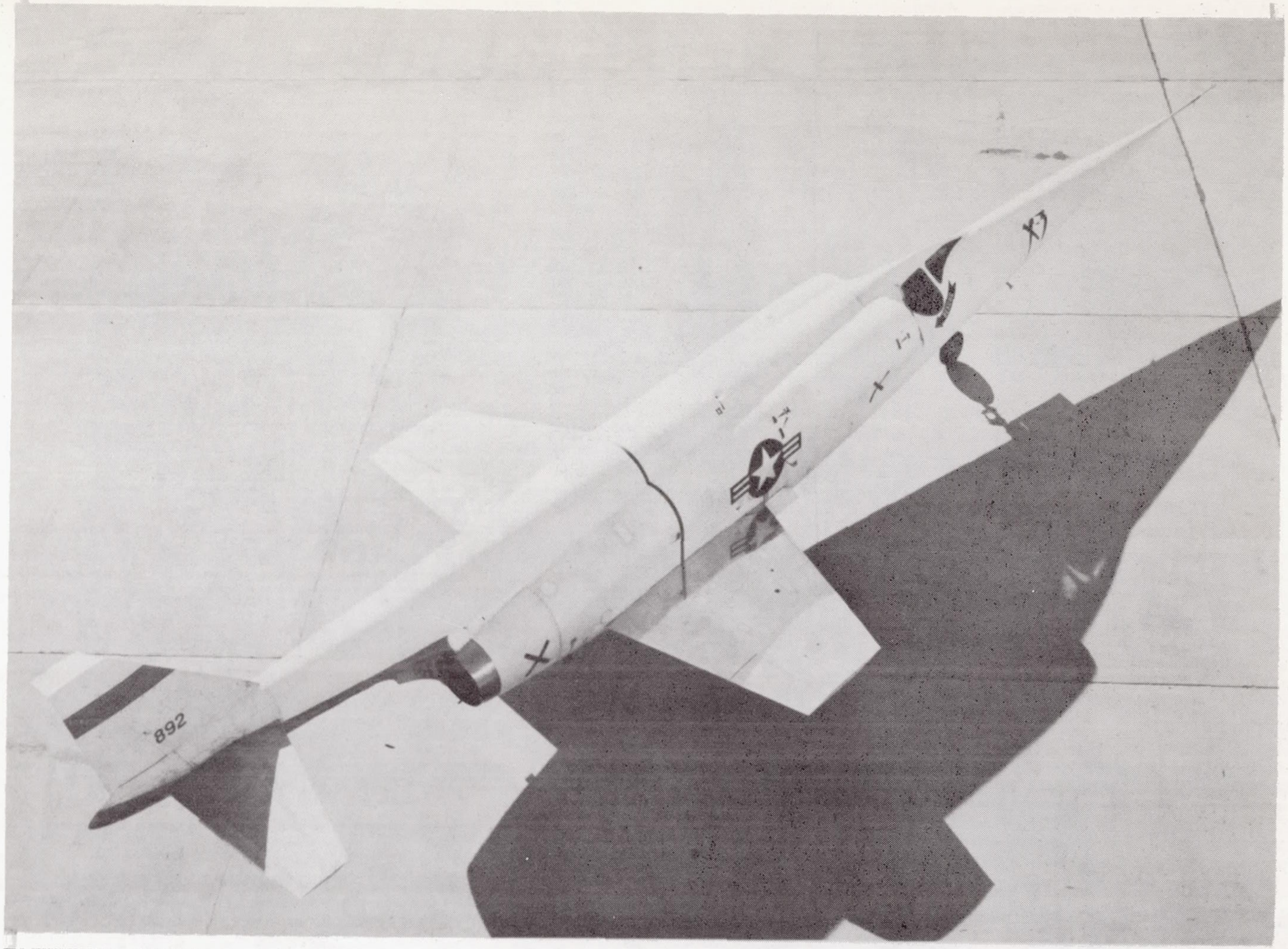

(a) Photograph of complete airplane. E-1994

Figure 2.- Photographs of the Douglas X-3 research airplane.

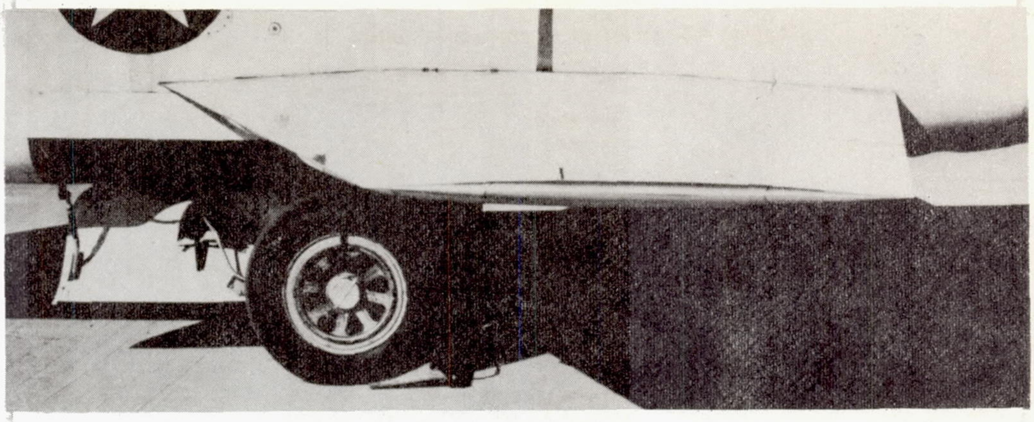

Leading-edge flap undeflected. E-2161

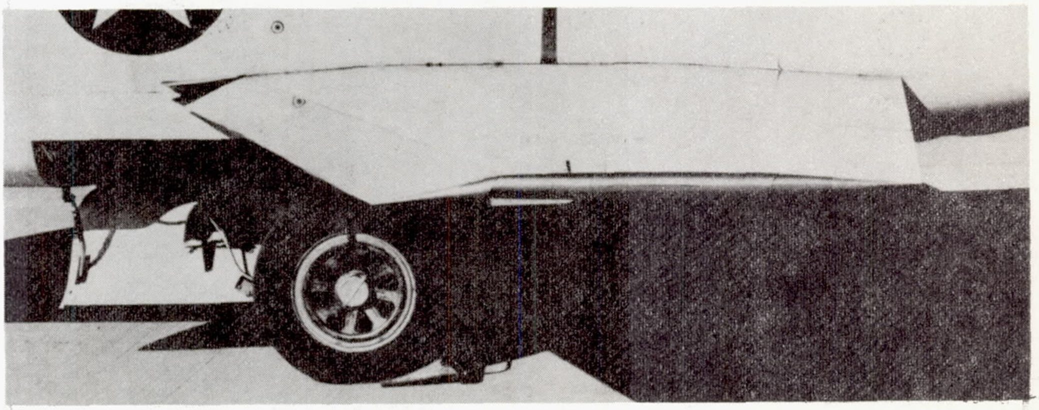

Leading-edge flap deflected 10°. E-2162

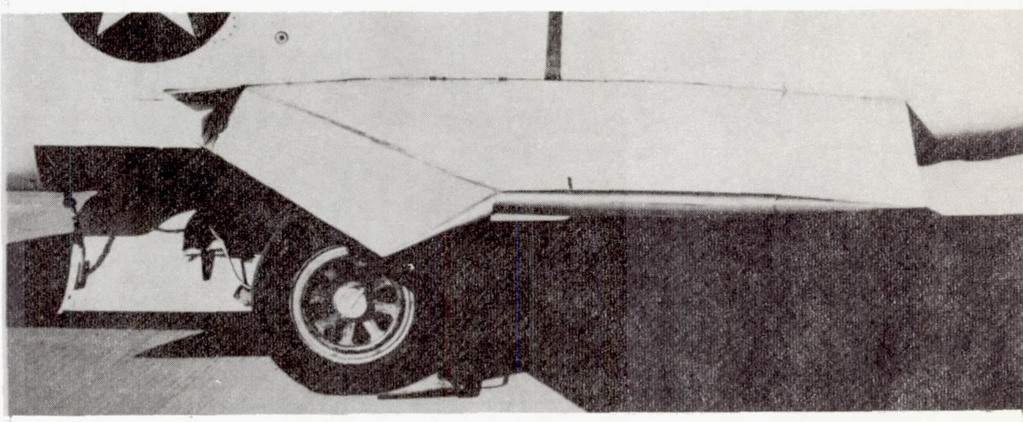

Leading-edge flap deflected 30°. E-2163

(b) Close-up views of wing with leading-edge flap.

Figure 2.- Concluded.

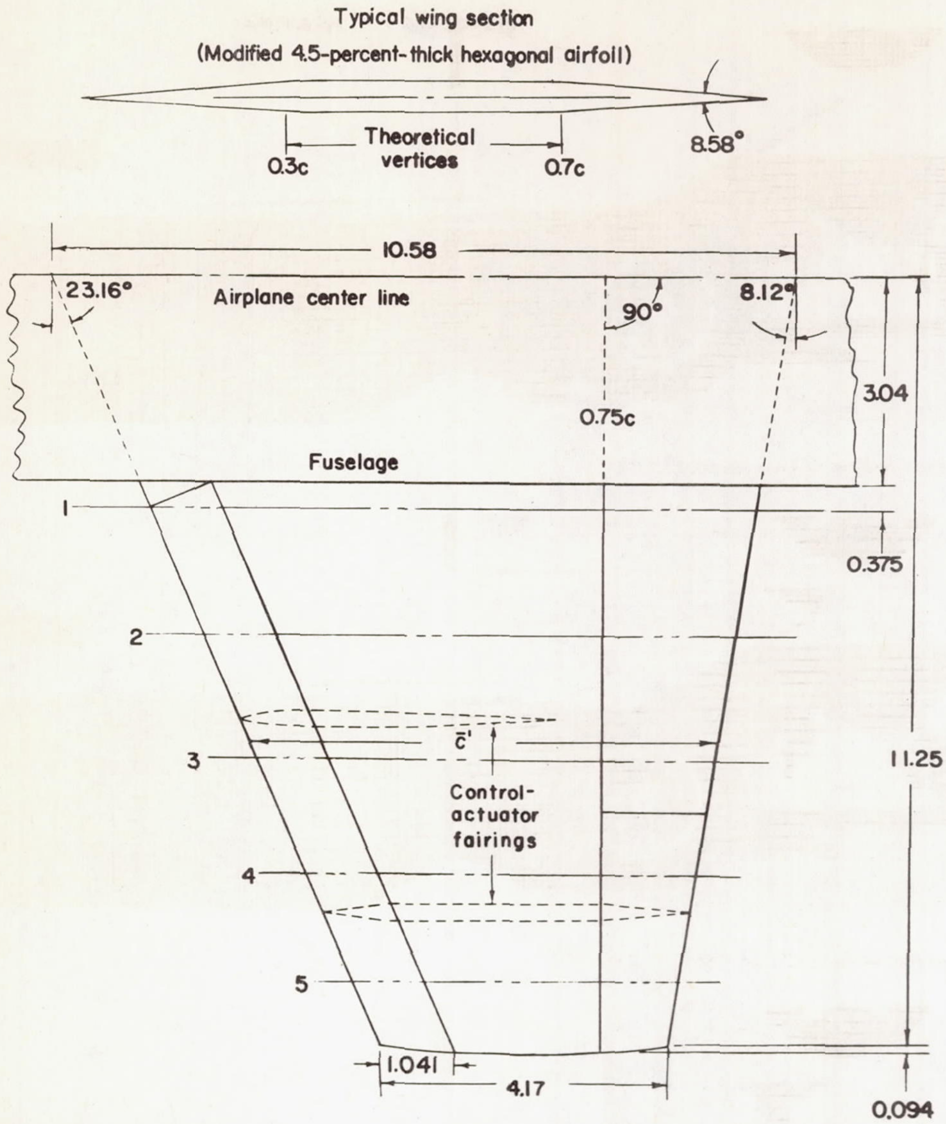

Orifice row	1	2	3	4	5
Chord length, ft	8.63	7.59	6.54	5.59	4.69
Spanwise location, percent b'/2	0	0.231	0.462	0.673	0.872
Leading-edge-flap hinge line, percent c	12.1	13.7	15.9	18.6	22.2

Figure 3.- Drawing of the left wing of the Douglas X-3 airplane showing the spanwise location of the orifice rows. All dimensions in feet unless otherwise stated.

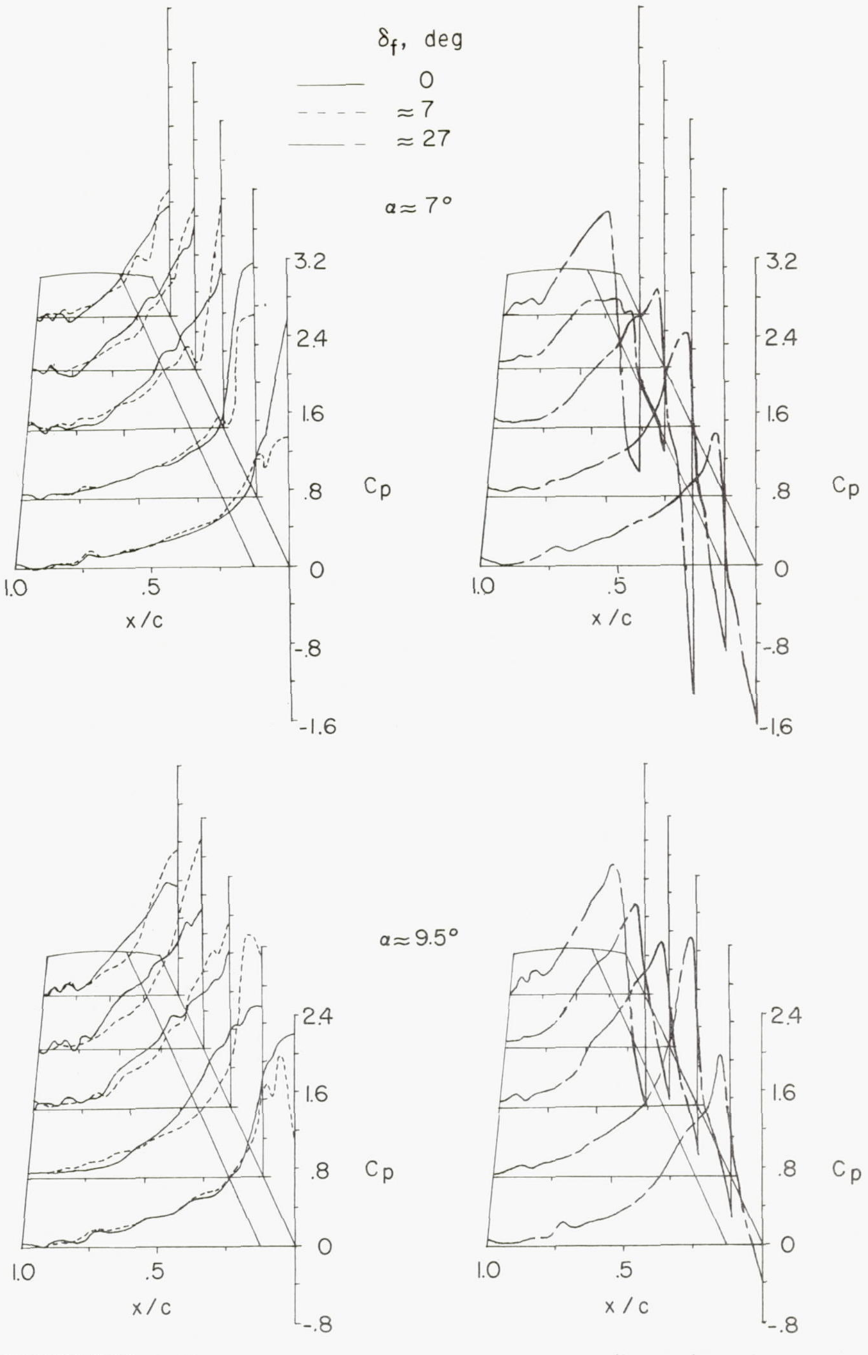

(a) $M \approx 0.55$.

Figure 4.- Effect of deflecting the leading-edge flap on the chordwise load distributions over the X-3 wing.

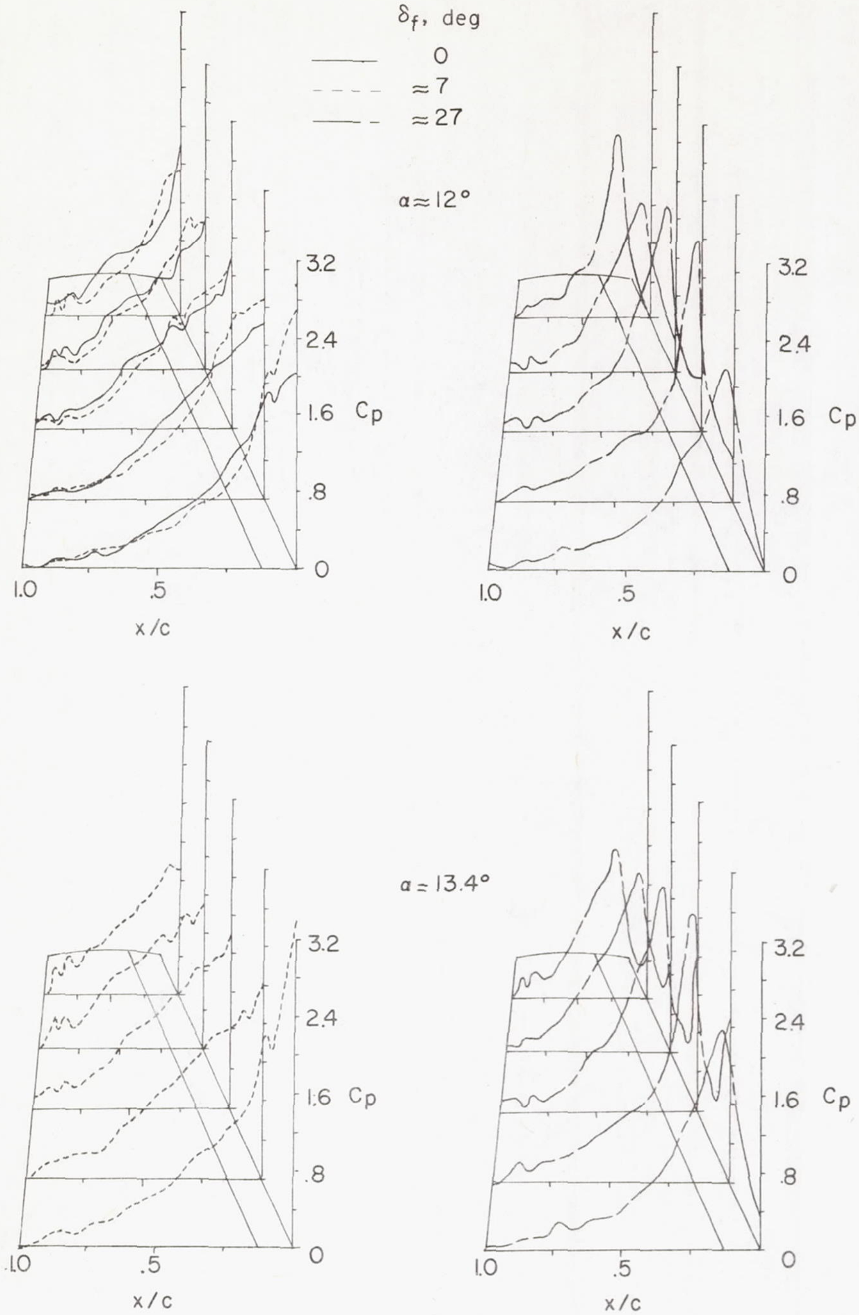

(a) M ≈ 0.55 - continued.

Figure 4.- Continued.

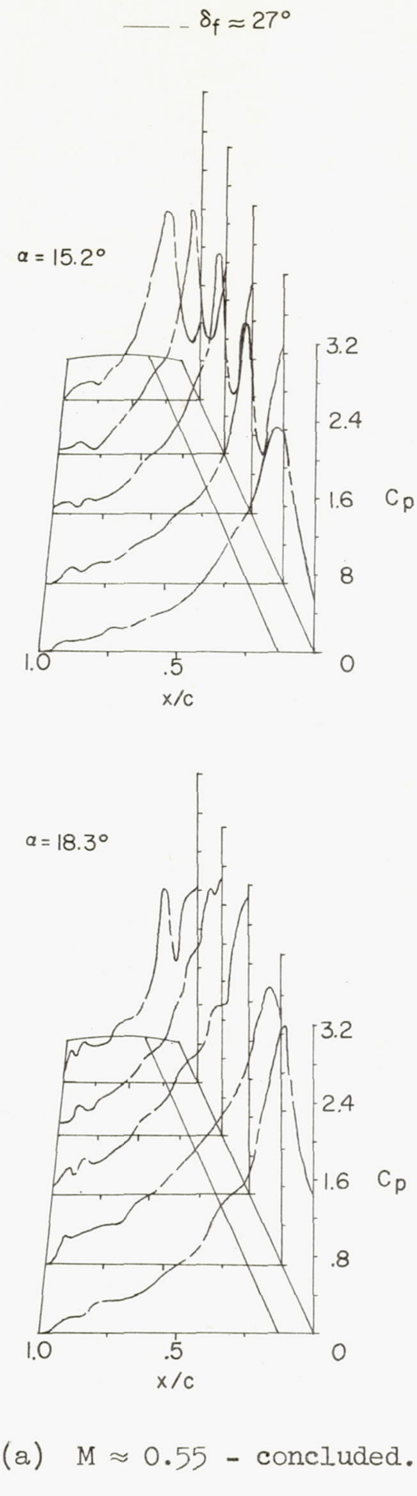

(a) M ≈ 0.55 - concluded.

Figure 4.- Continued.

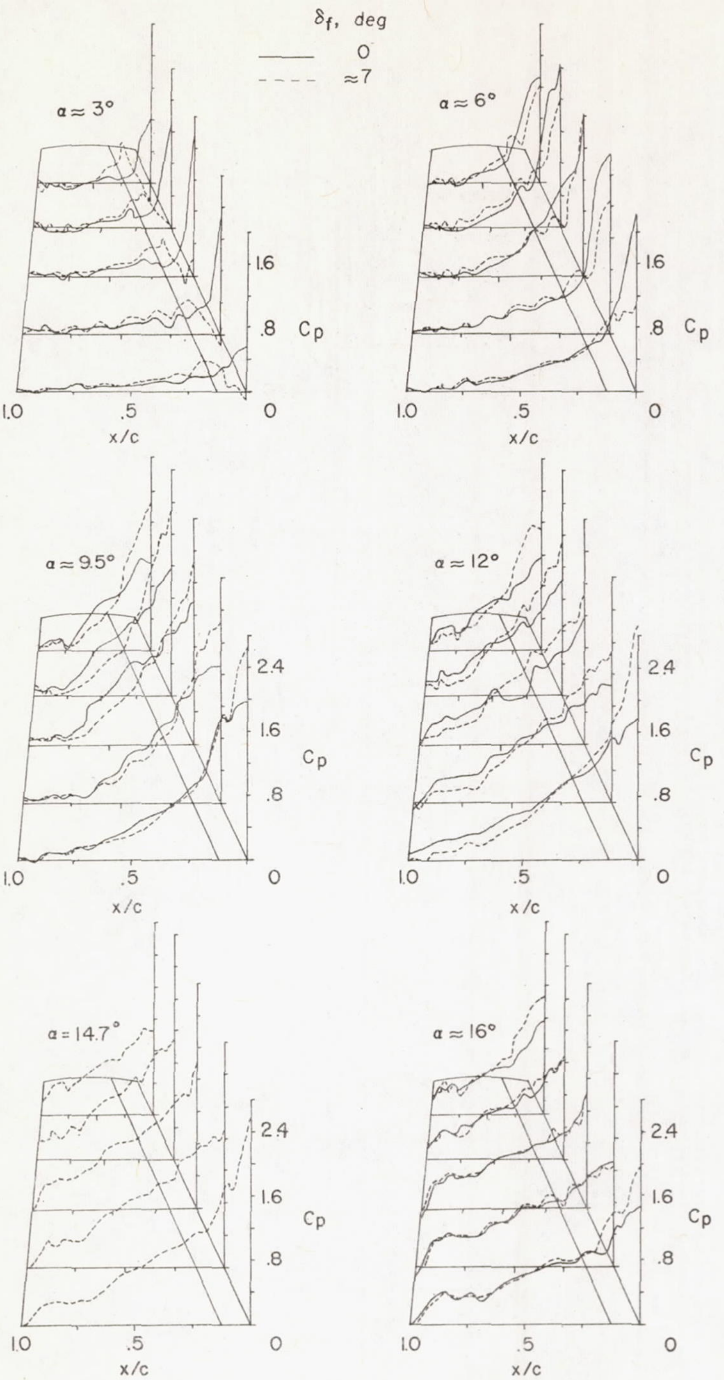

(b) M ≈ 0.71.

Figure 4.- Continued.

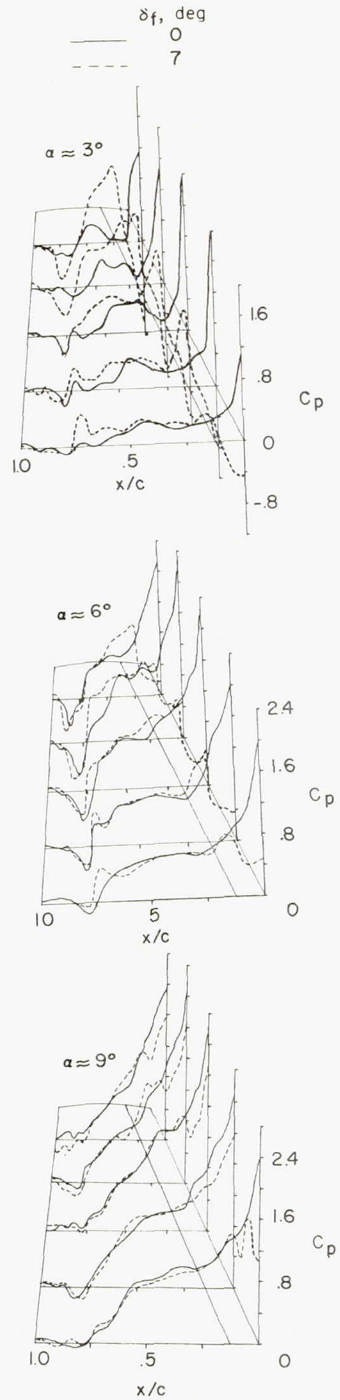

(c) $M \approx 0.90$.

Figure 4.- Concluded.

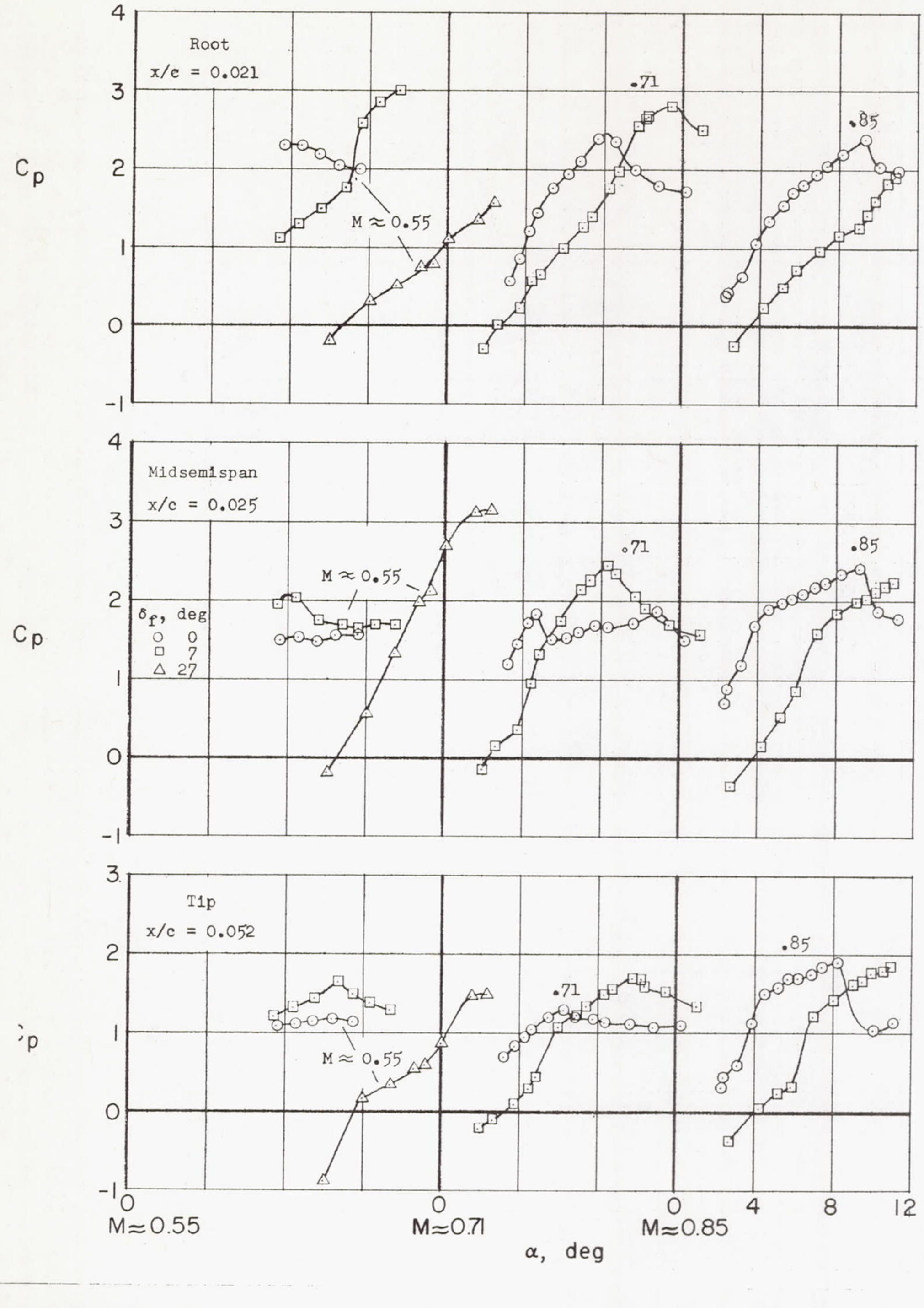

Figure 5.- Effect of deflecting the leading-edge flap on the variation with angle of attack of the differential-pressure coefficient at the leading edge of the X-3 wing.

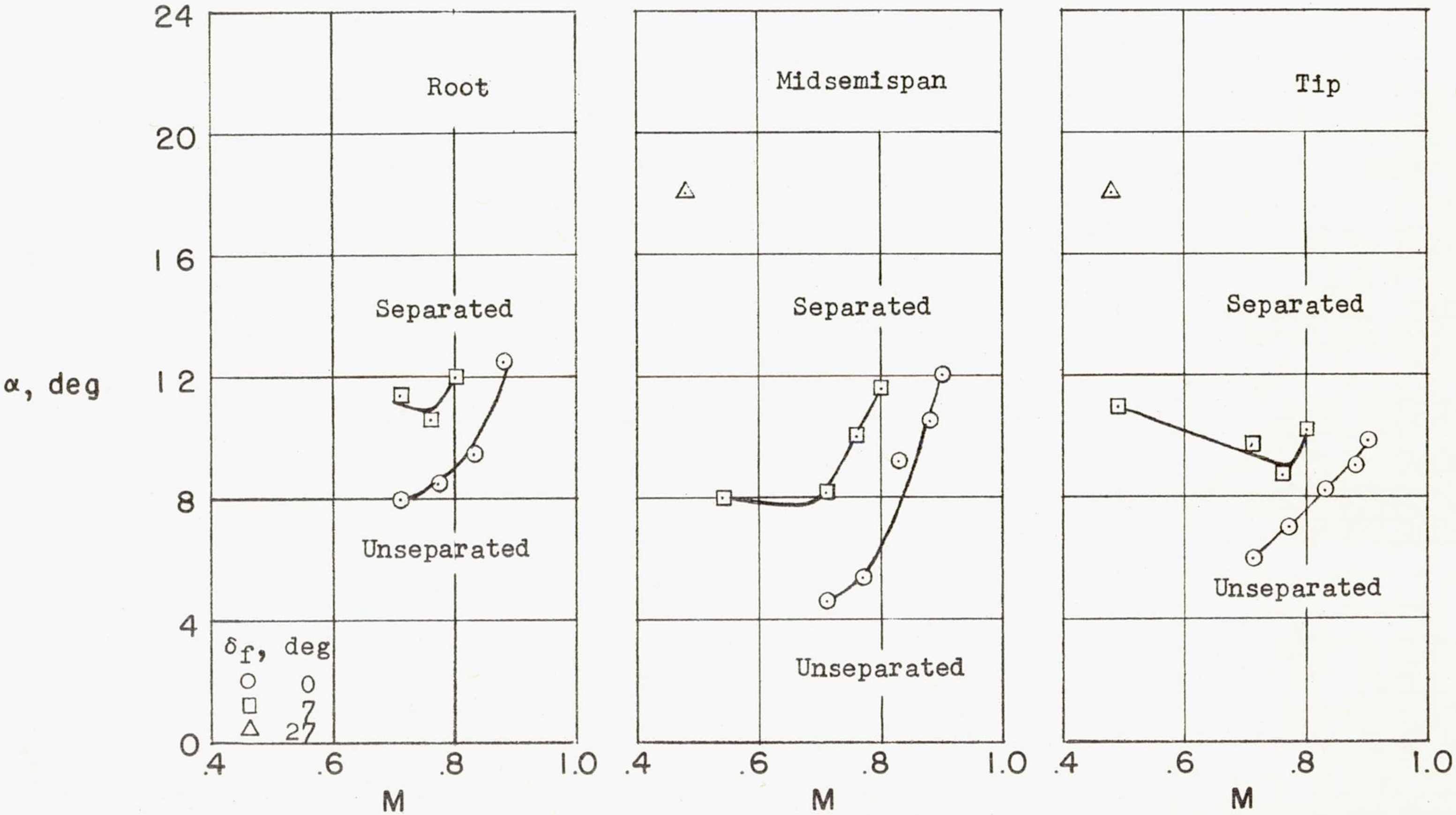

Figure 6.- Effect of deflecting the leading-edge flap on the approximate boundary for leading-edge-flow separation for the X-3 wing.

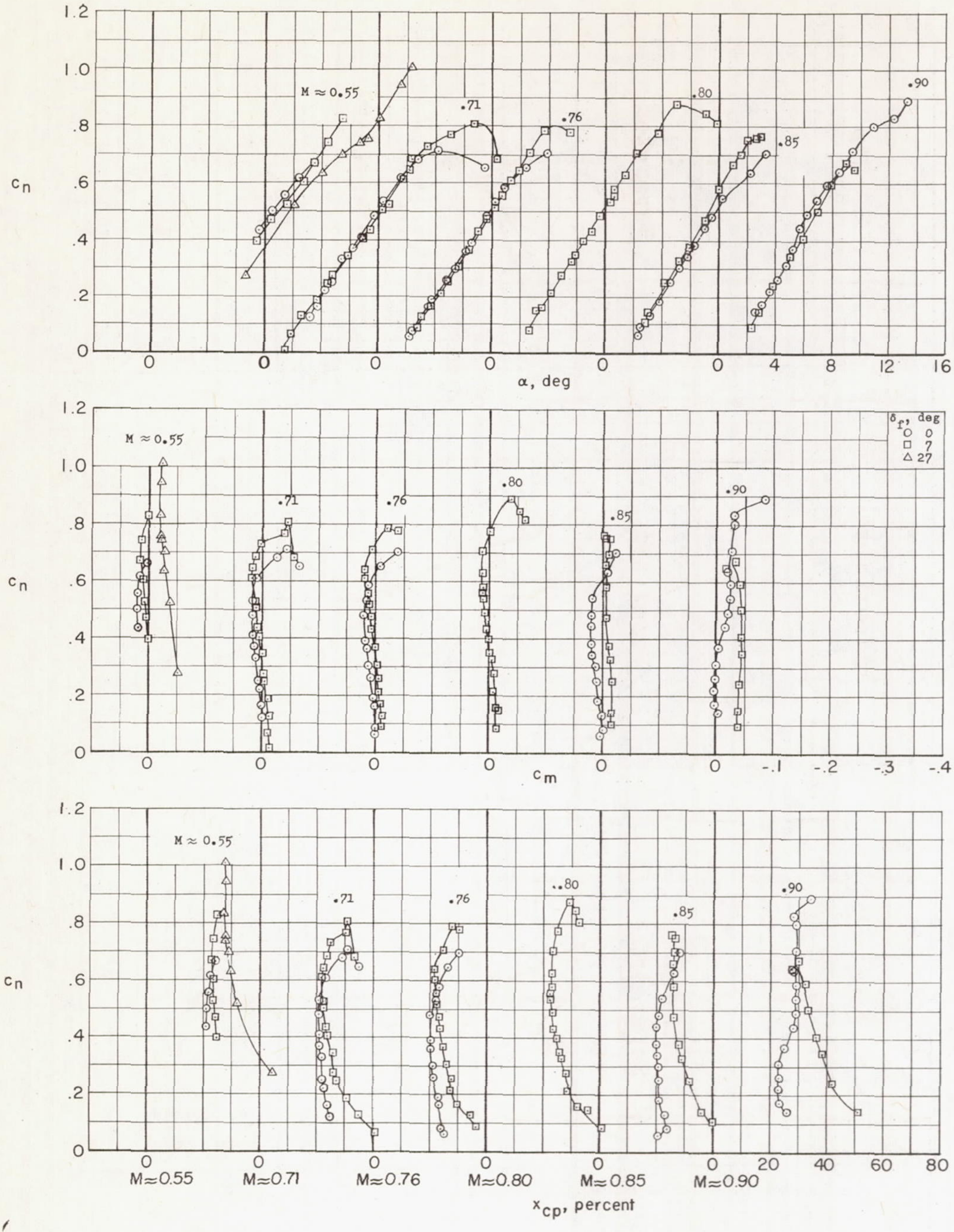

(a) Root.

Figure 7.- Effect of deflecting the leading-edge flap on the wing-section aerodynamic characteristics of the X-3 wing.

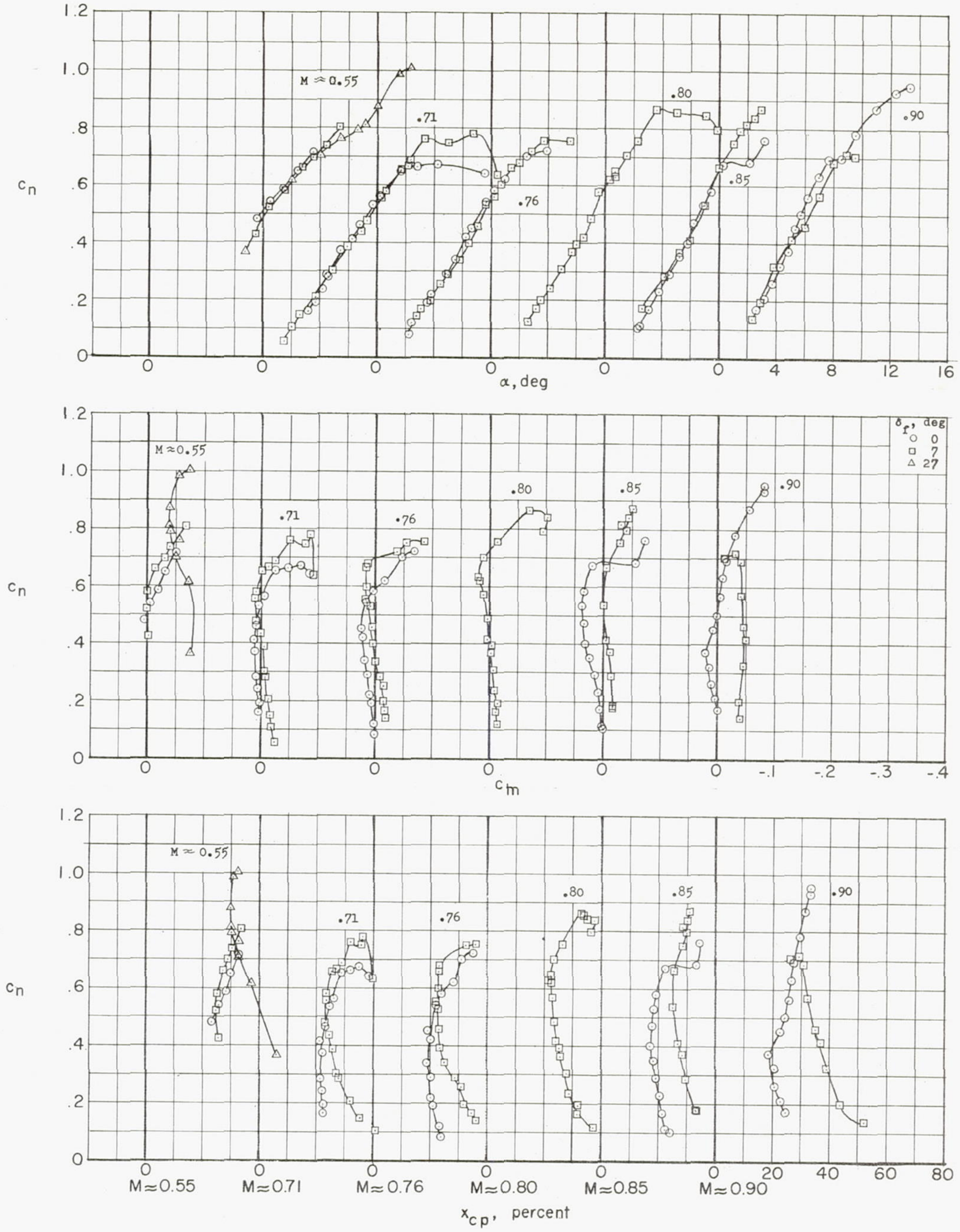

(b) Midsemispan.

Figure 7.- Continued.

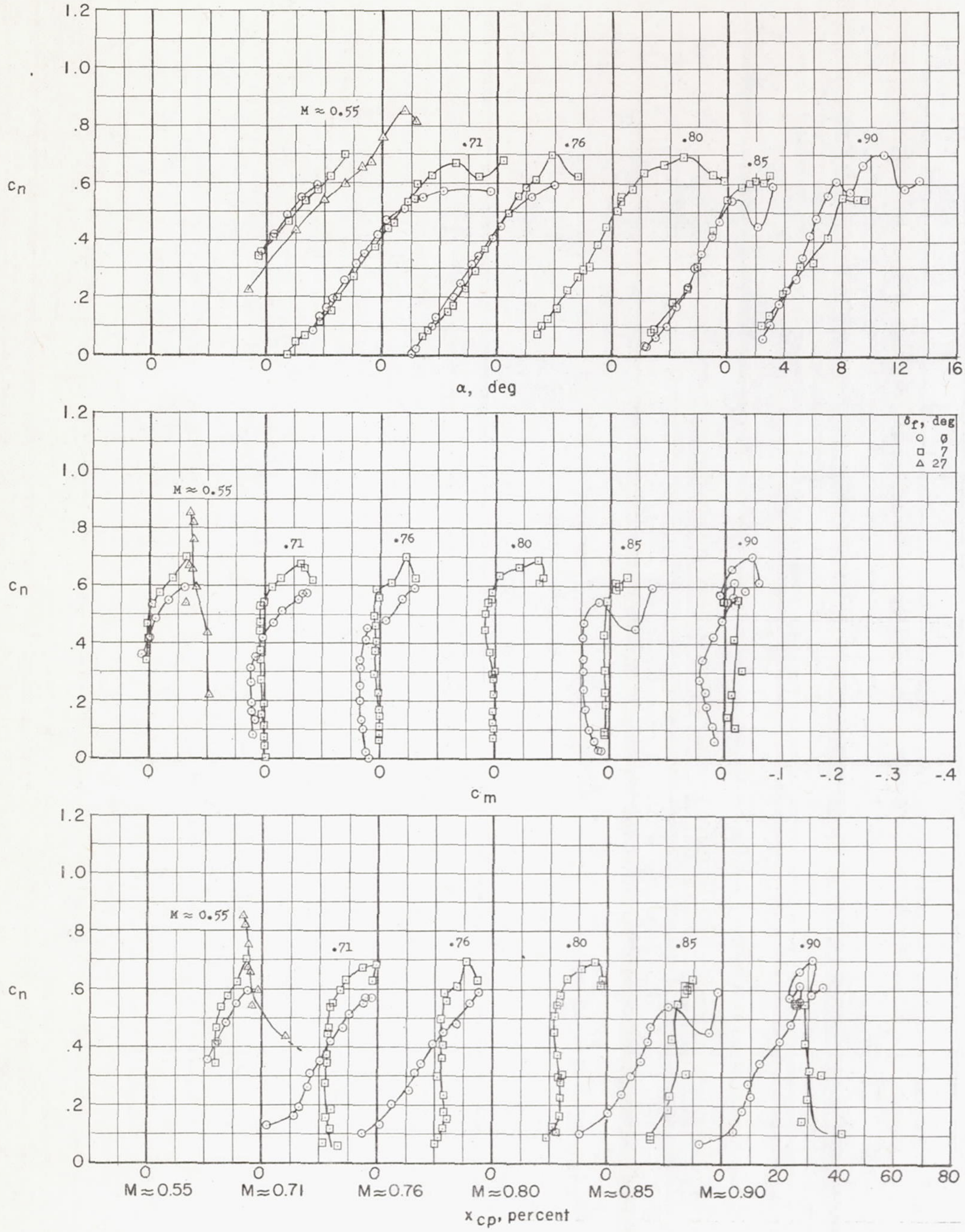

(c) Tip.

Figure 7.- Concluded.

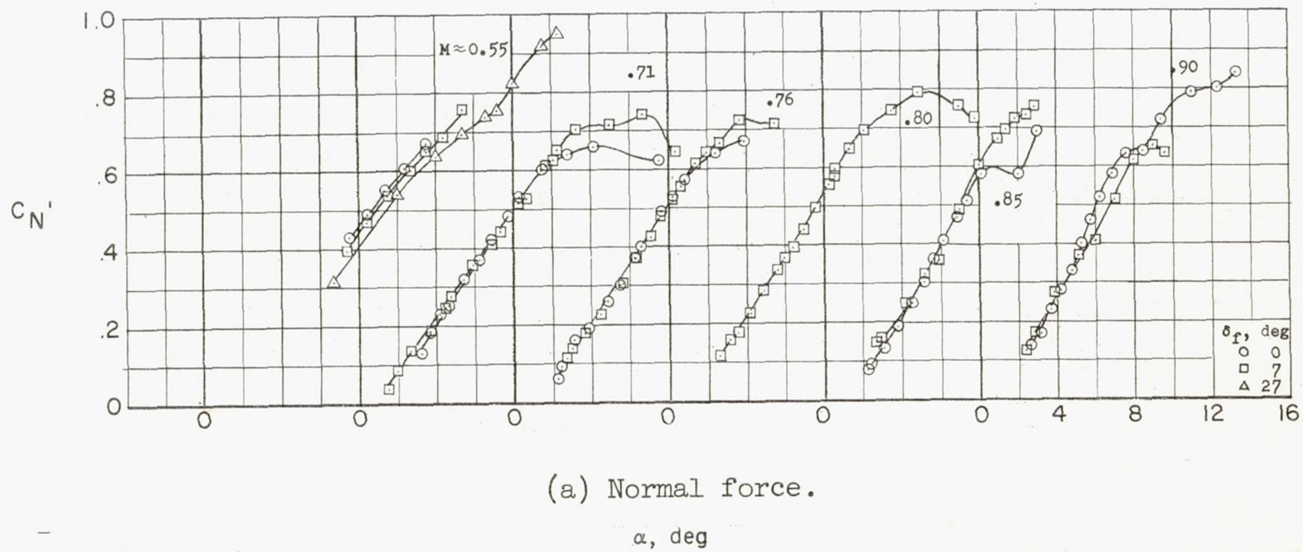

(a) Normal force.

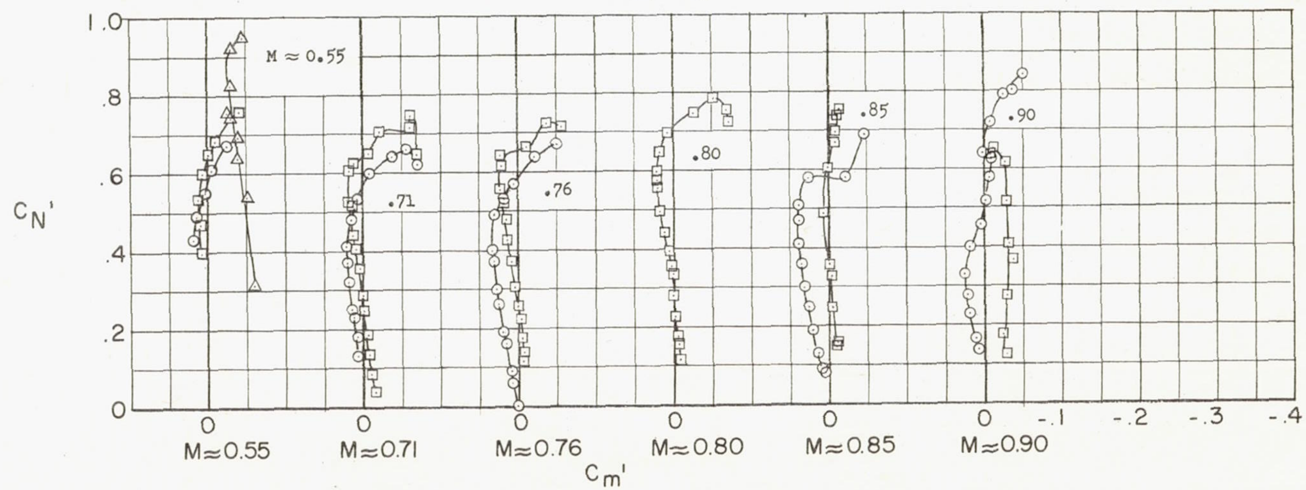

(b) Pitching moment.

Figure 8.- Effect of deflecting the leading-edge flap on the aerodynamic characteristics of the X-3 wing.

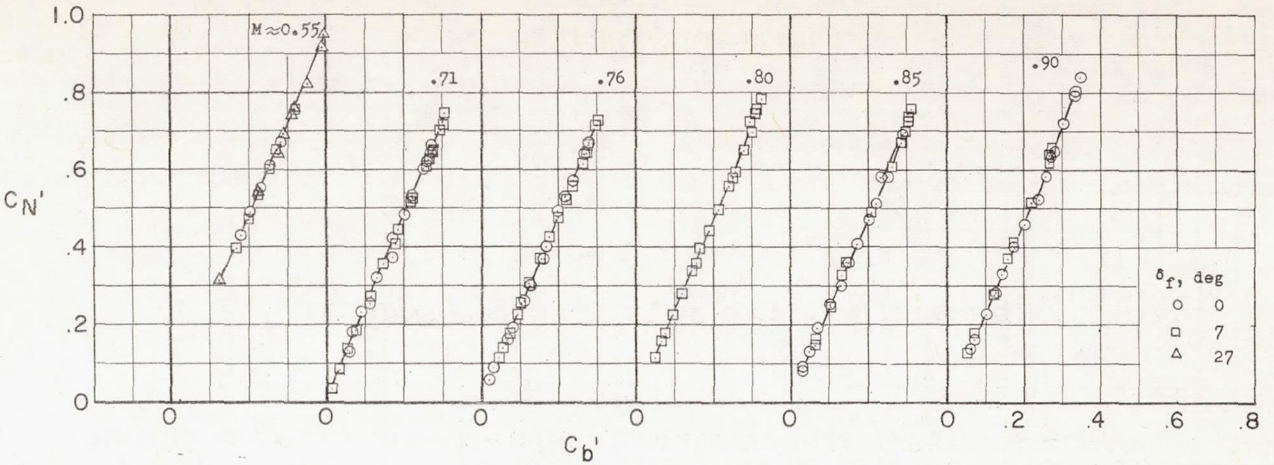

(c) Bending moment.

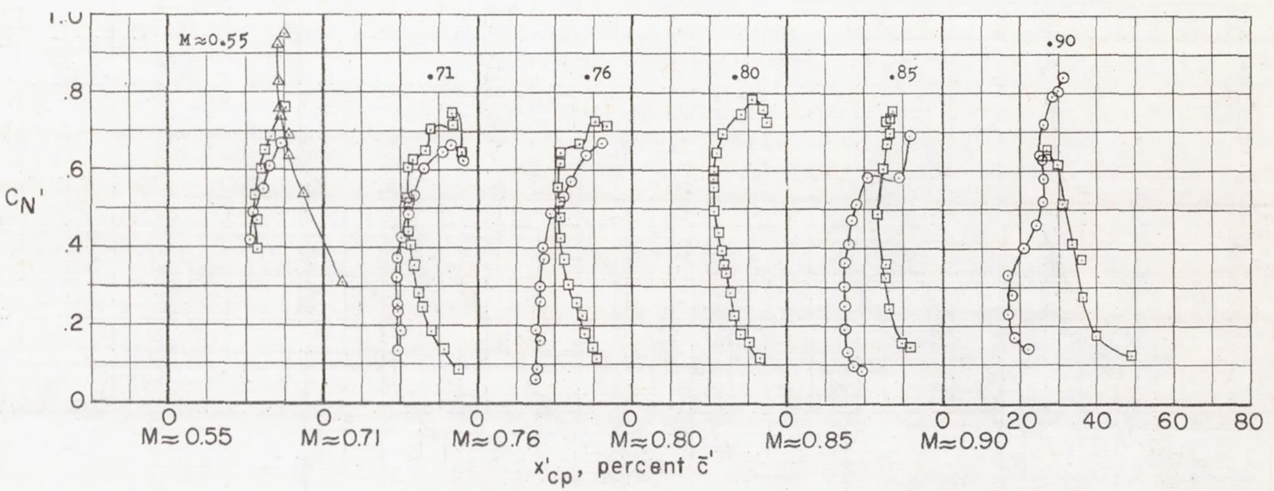

(d) Chordwise location of center of pressure.

Figure 8.- Continued.

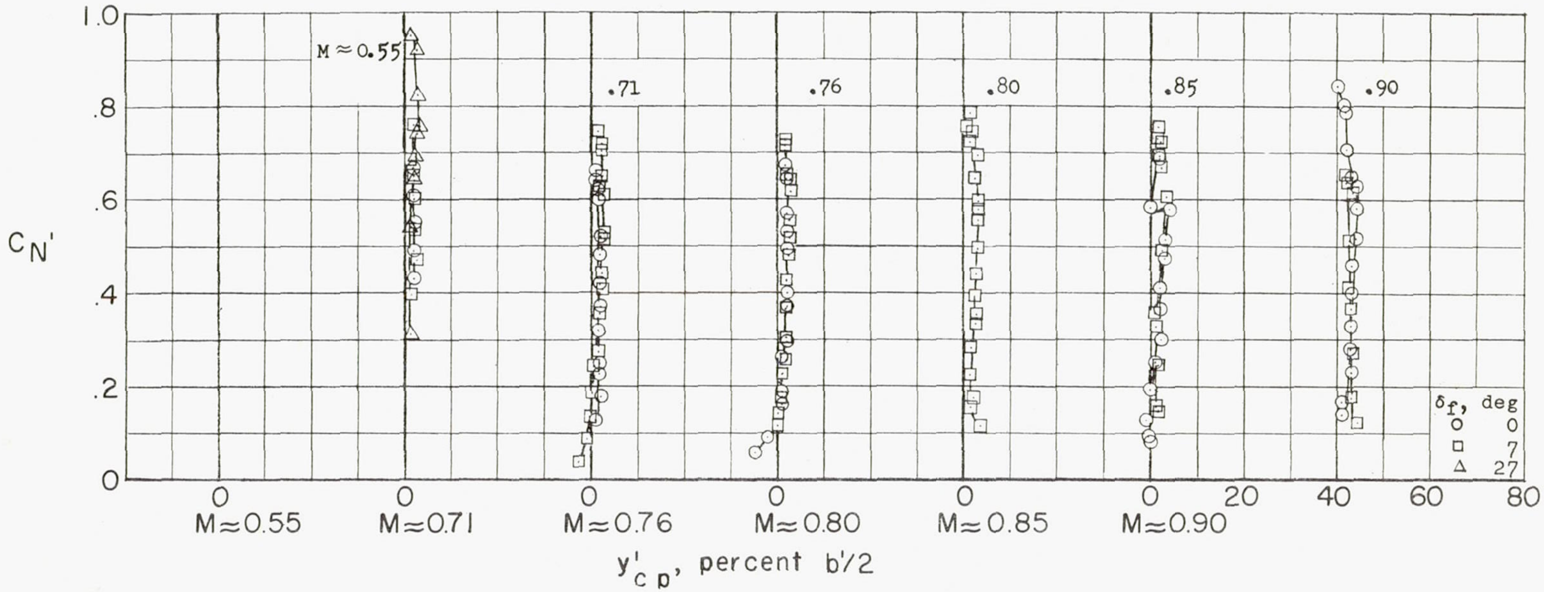

(e) Spanwise location of center of pressure.

Figure 8.- Concluded.

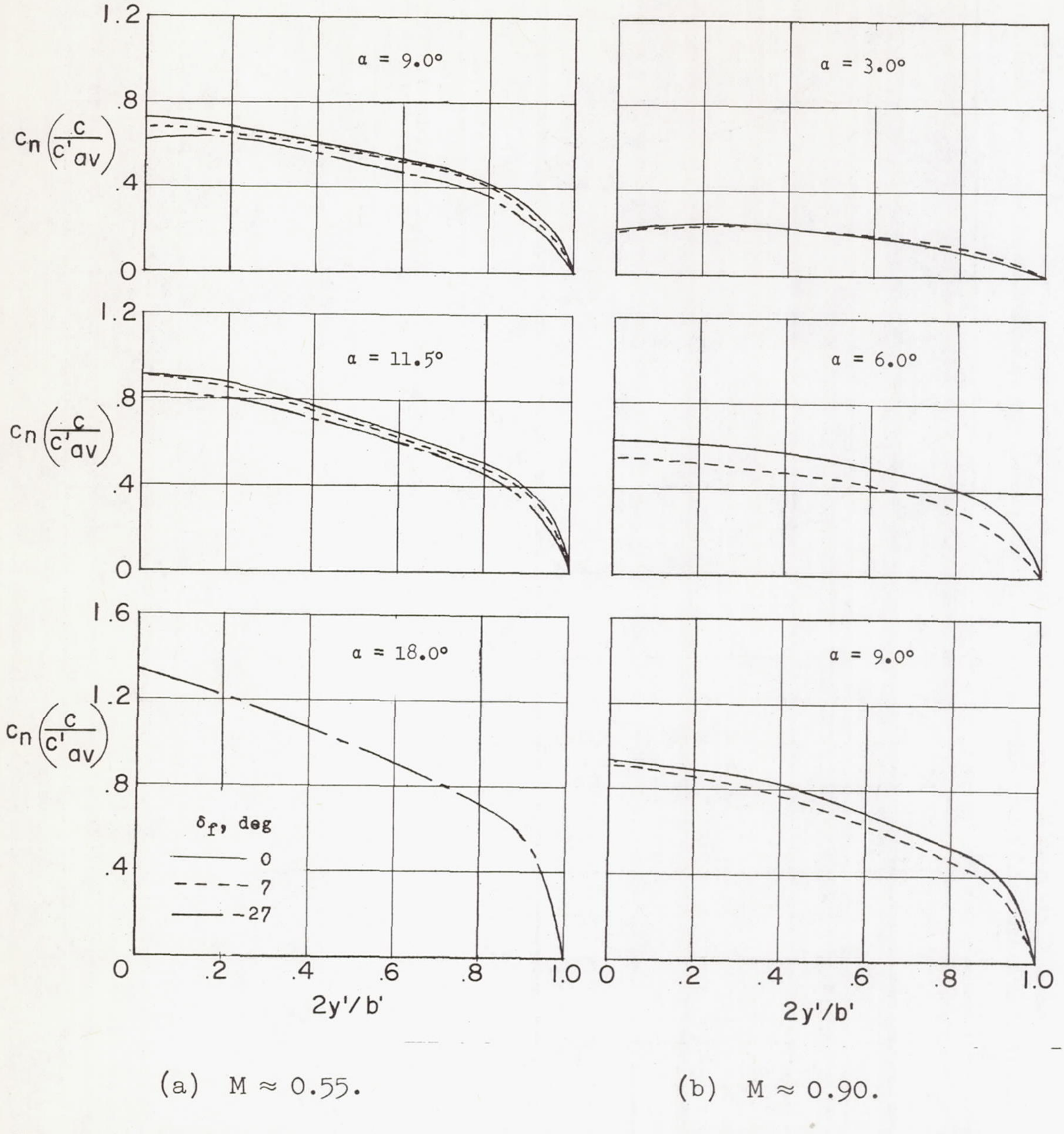

(a) $M \approx 0.55$.

(b) $M \approx 0.90$.

Figure 9.- Effect of deflecting the leading-edge flap on the span load distribution over the X-3 wing.

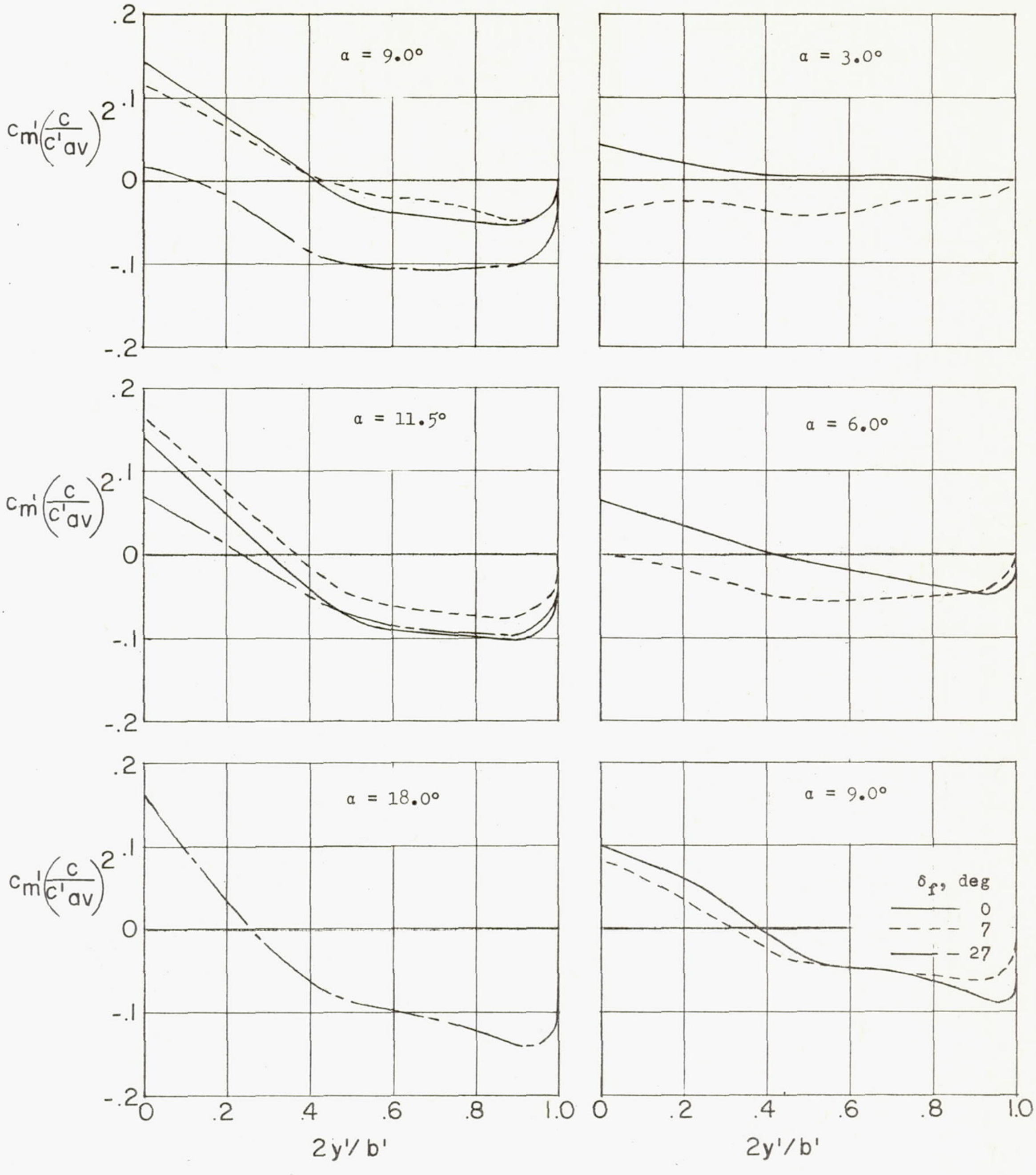

(a) M ≈ 0.55.

(b) M ≈ 0.90.

Figure 10.- Effect of deflecting the leading-edge flap on the spanwise pitching-moment distribution over the X-3 wing.

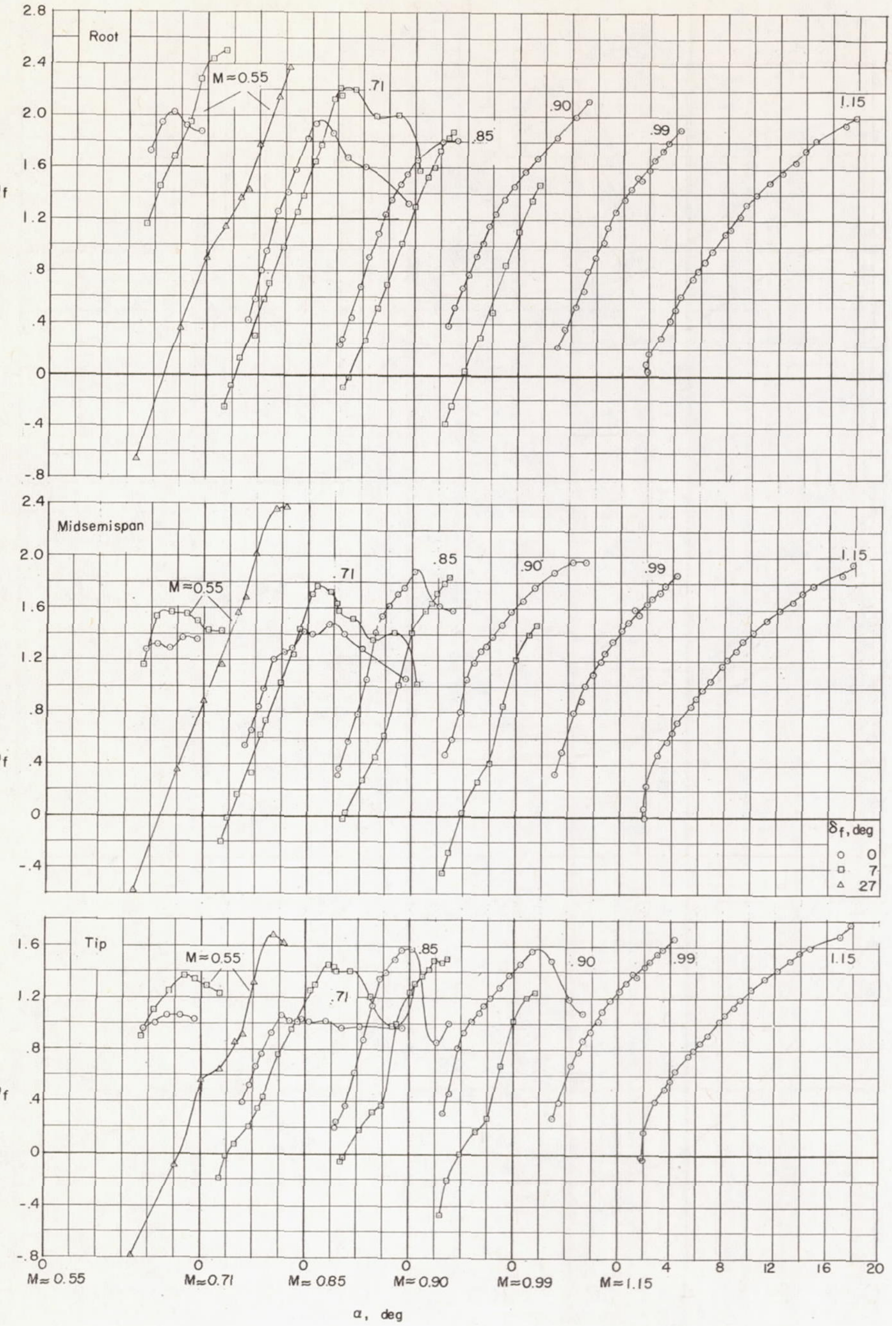

(a) Section normal force.

Figure 11.- Effect of deflecting the leading-edge flap on the section normal-force and hinge-moment characteristics of the leading-edge flap of the X-3 wing.

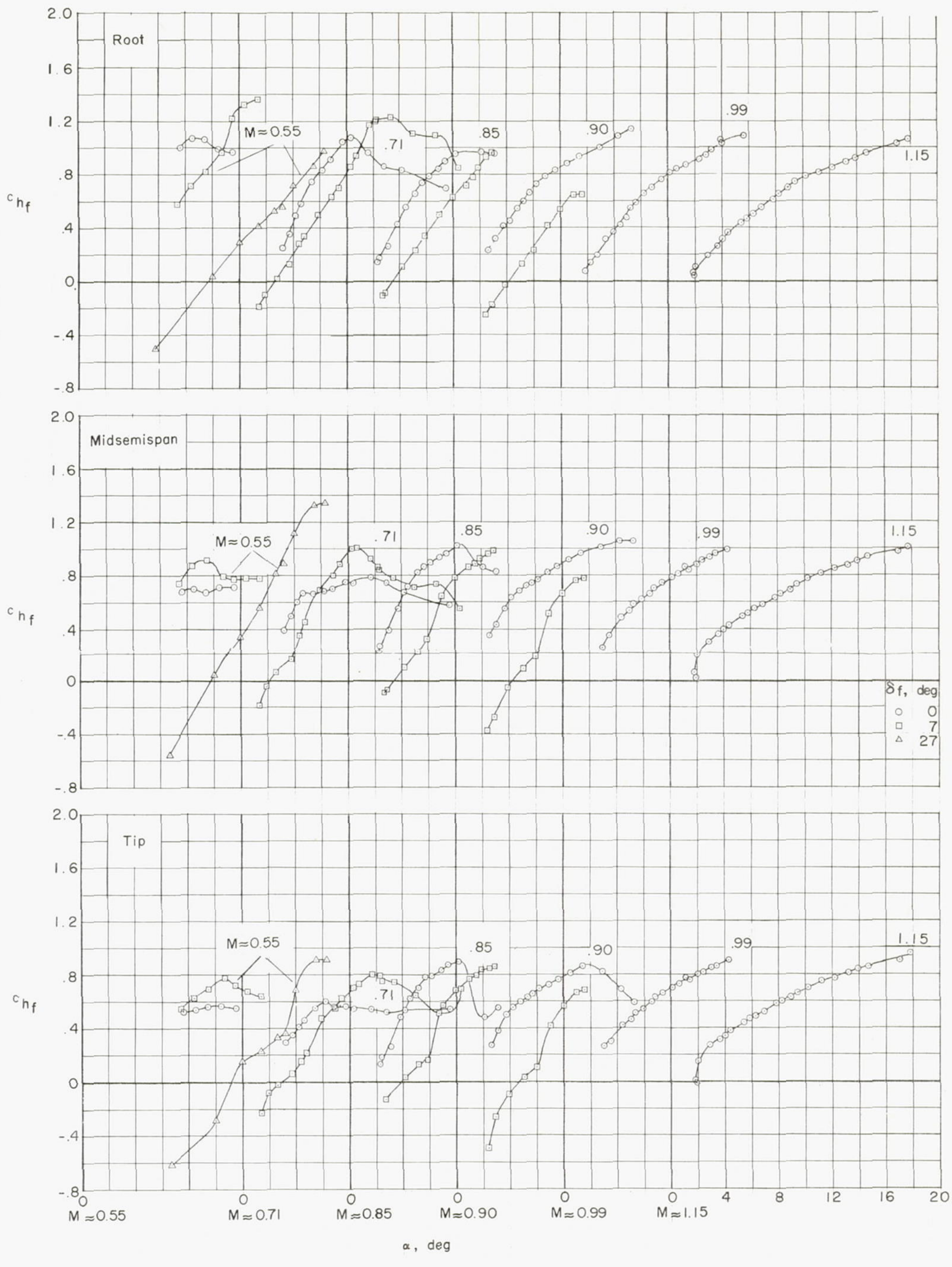

(b) Section hinge moment.

Figure 11.- Concluded.

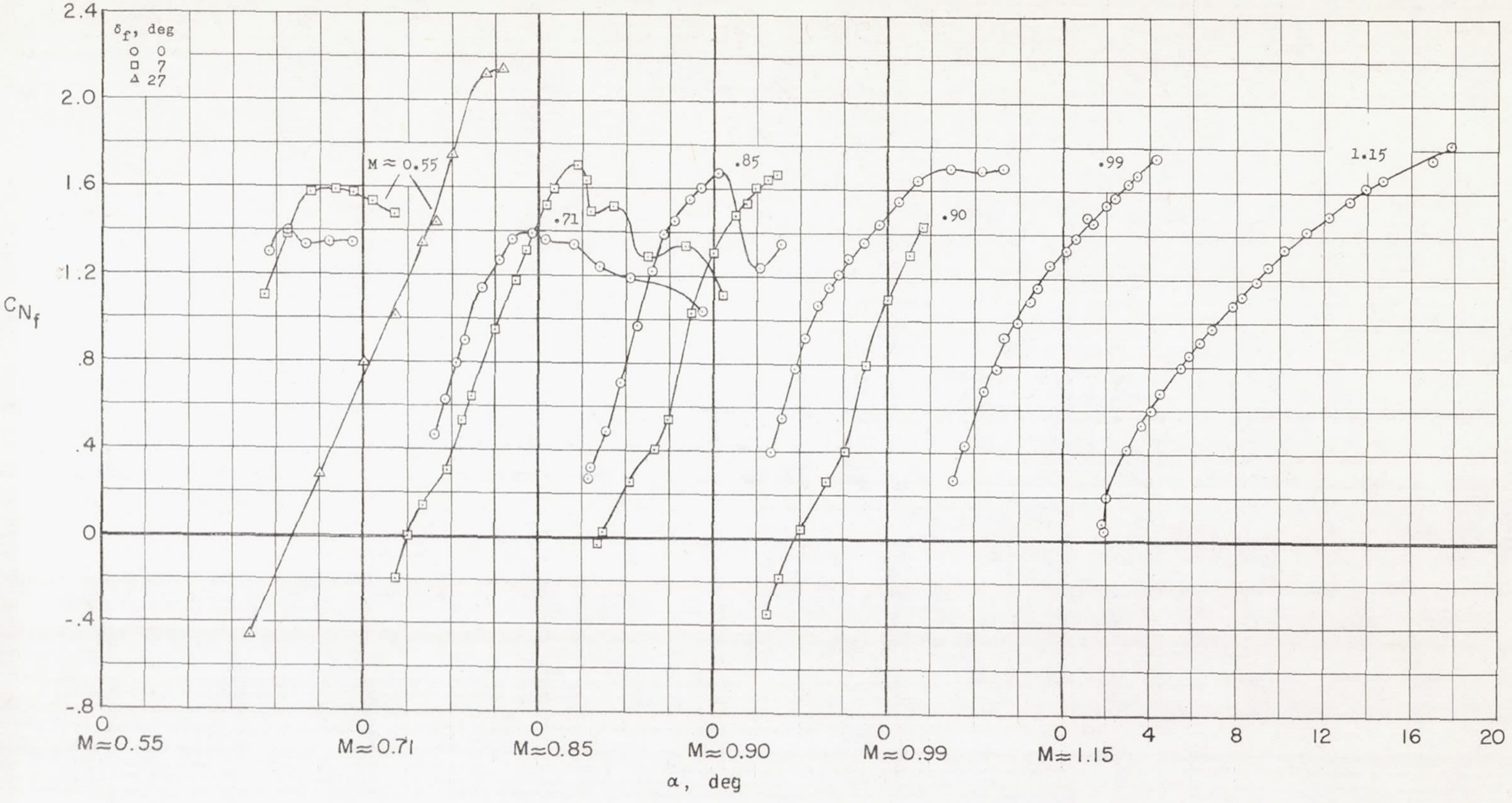

(a) Normal force.

Figure 12.- Effect of deflecting the leading-edge flap on the total normal-force and hinge-moment characteristics of the leading-edge flap of the X-3 wing.

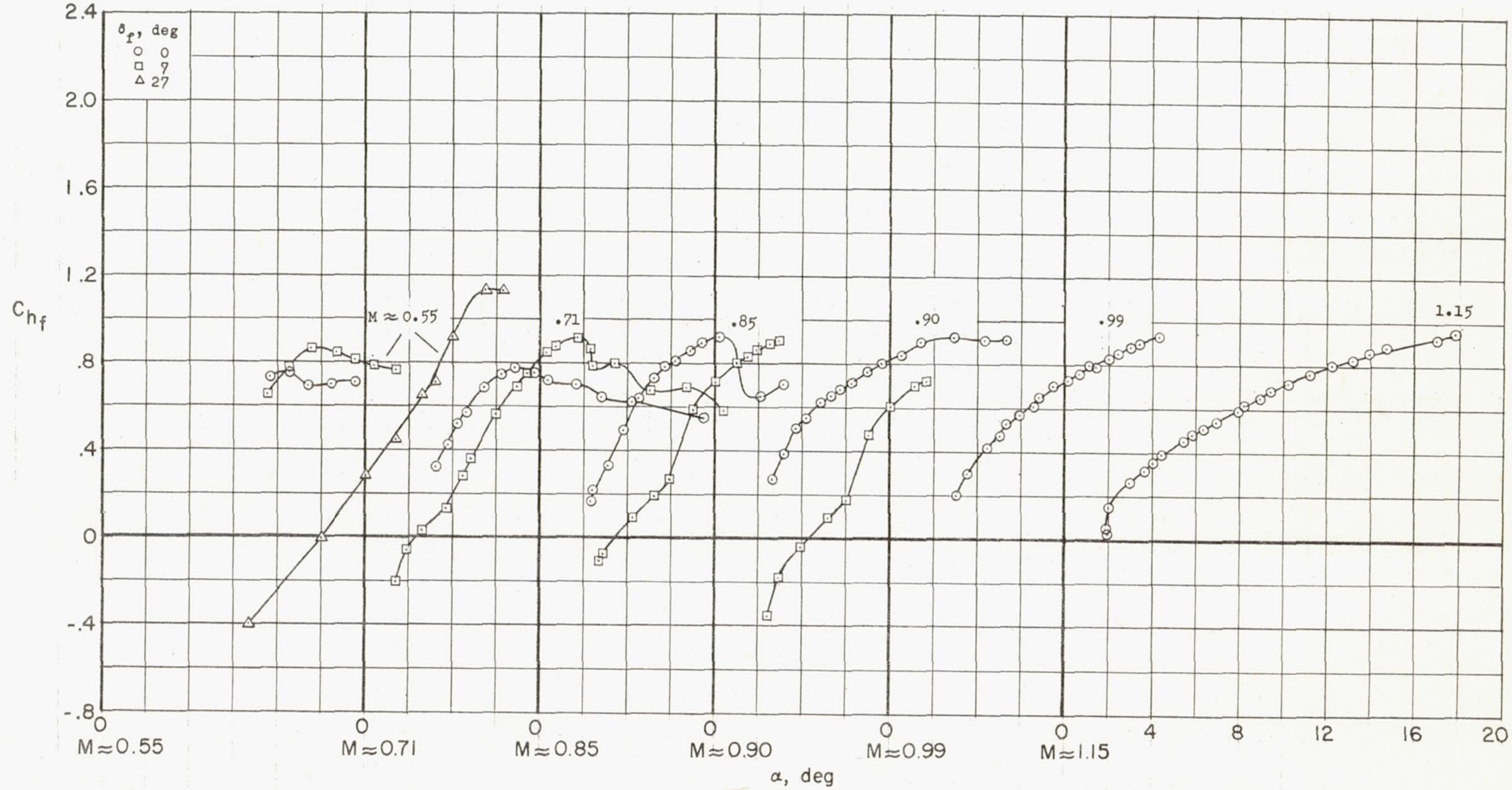

(b) Hinge moment.

Figure 12.- Concluded.

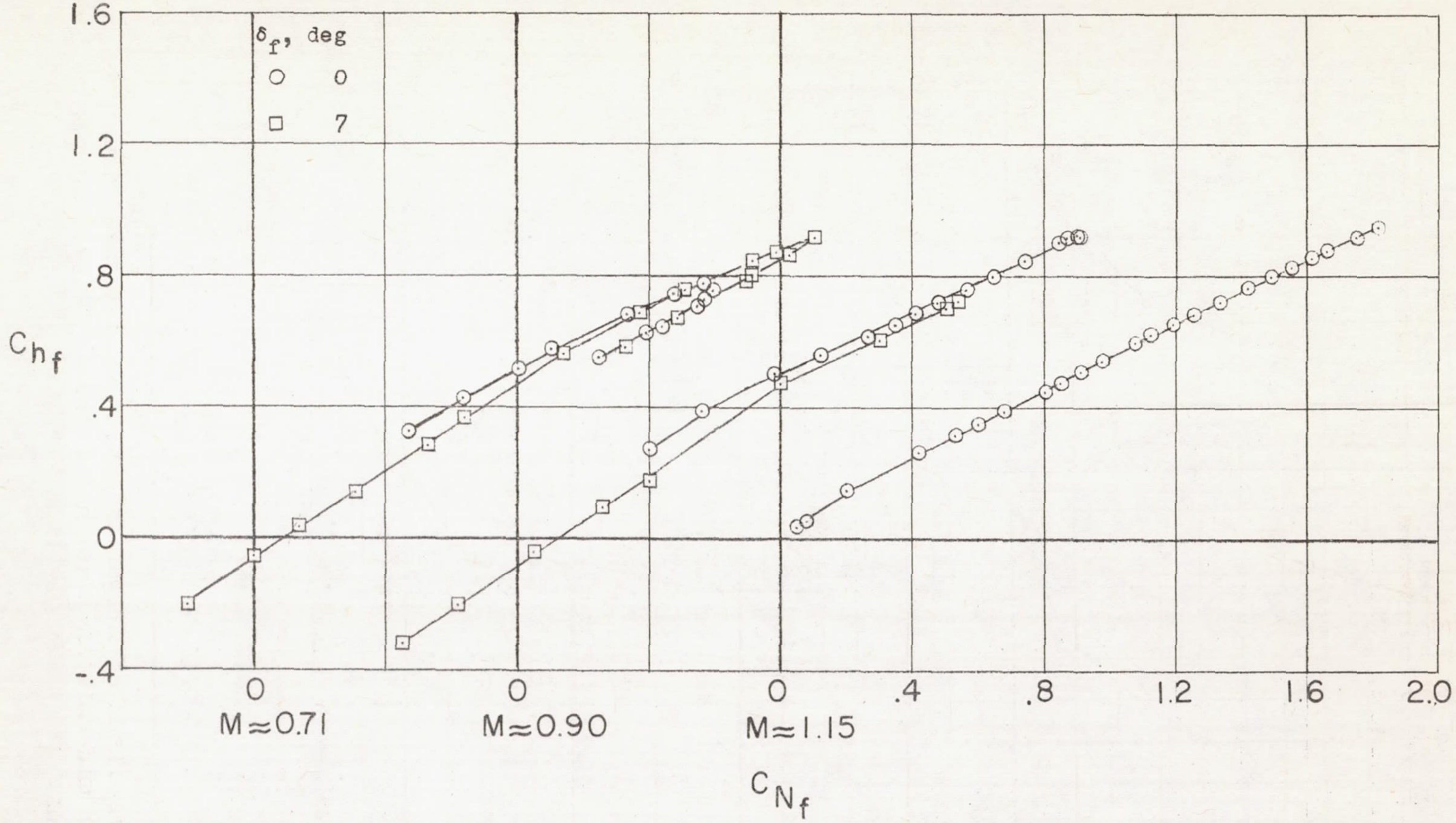

Figure 13.- Variation of hinge-moment coefficient with normal-force coefficient for the leading-edge flap of the X-3 wing.

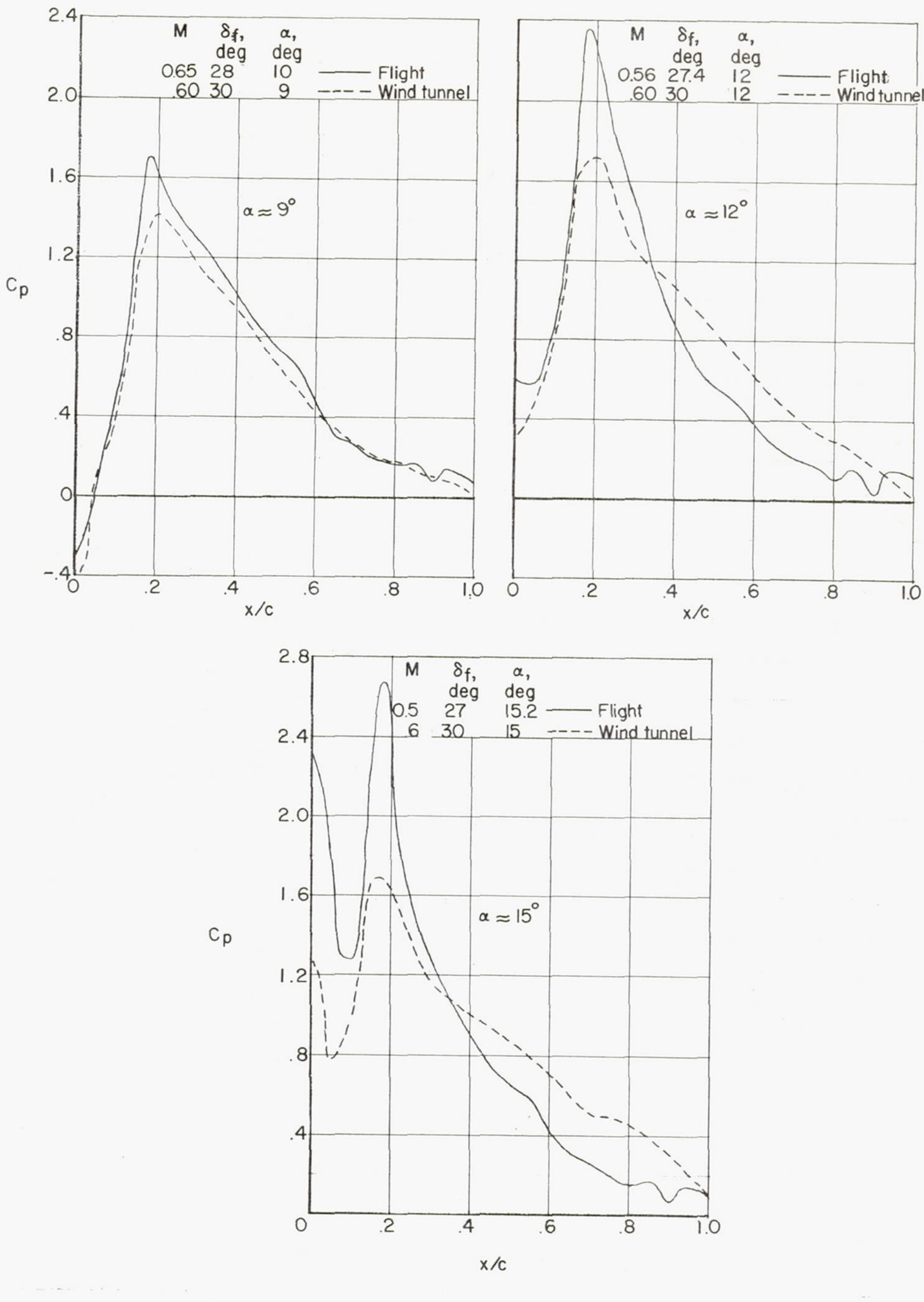

(a) $M \approx 0.55$, $\delta_f \approx 27°$.

Figure 14.- Comparison of flight data with wind-tunnel results of reference 8 for midsemispan stations of the X-3 wing. Chordwise load distributions.

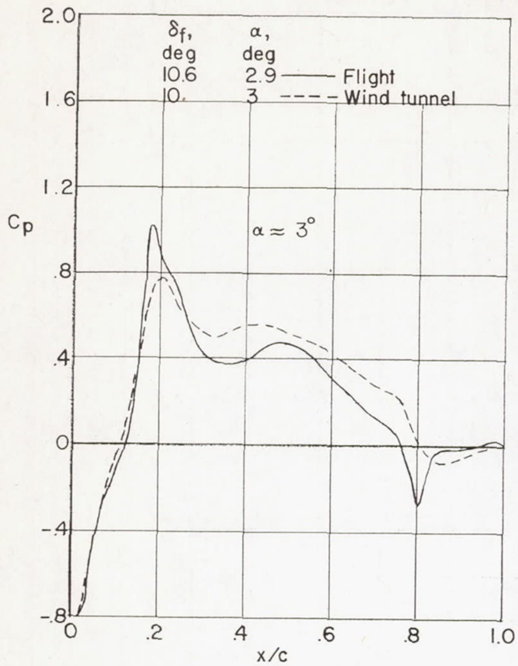

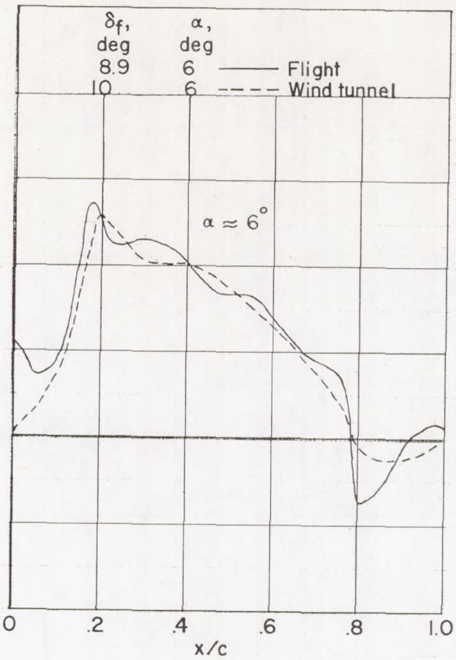

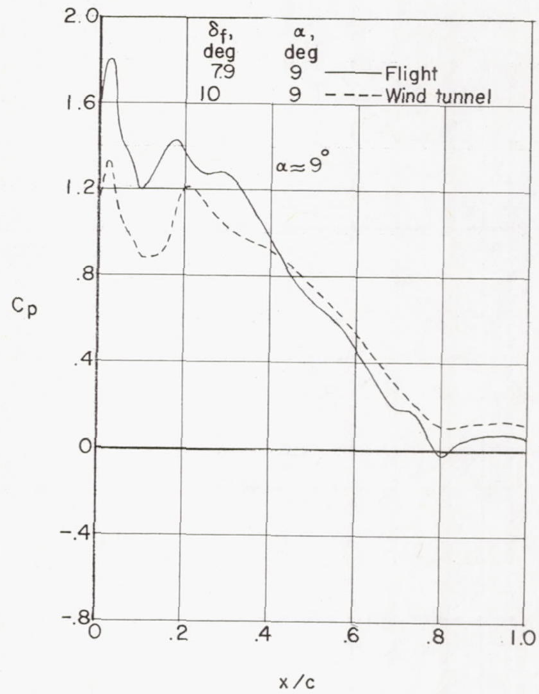

(b) $M = 0.90$, $\delta_f \approx 7^{\circ}$.

Figure 14.- Concluded.

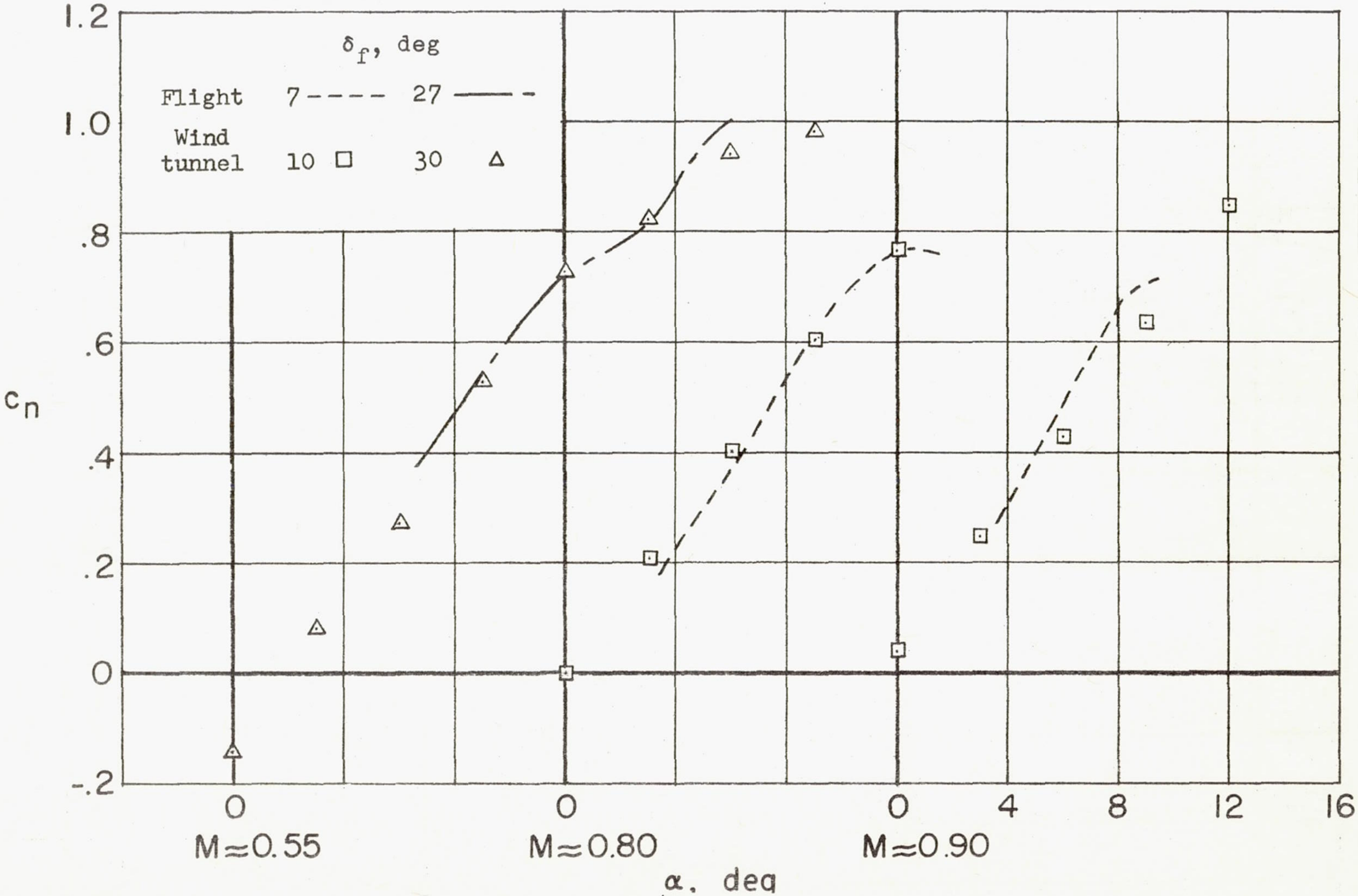

Figure 15.- Comparison of flight data with wind-tunnel results of reference 8 for midsemispan stations of the X-3 wing. Section normal-force coefficient.

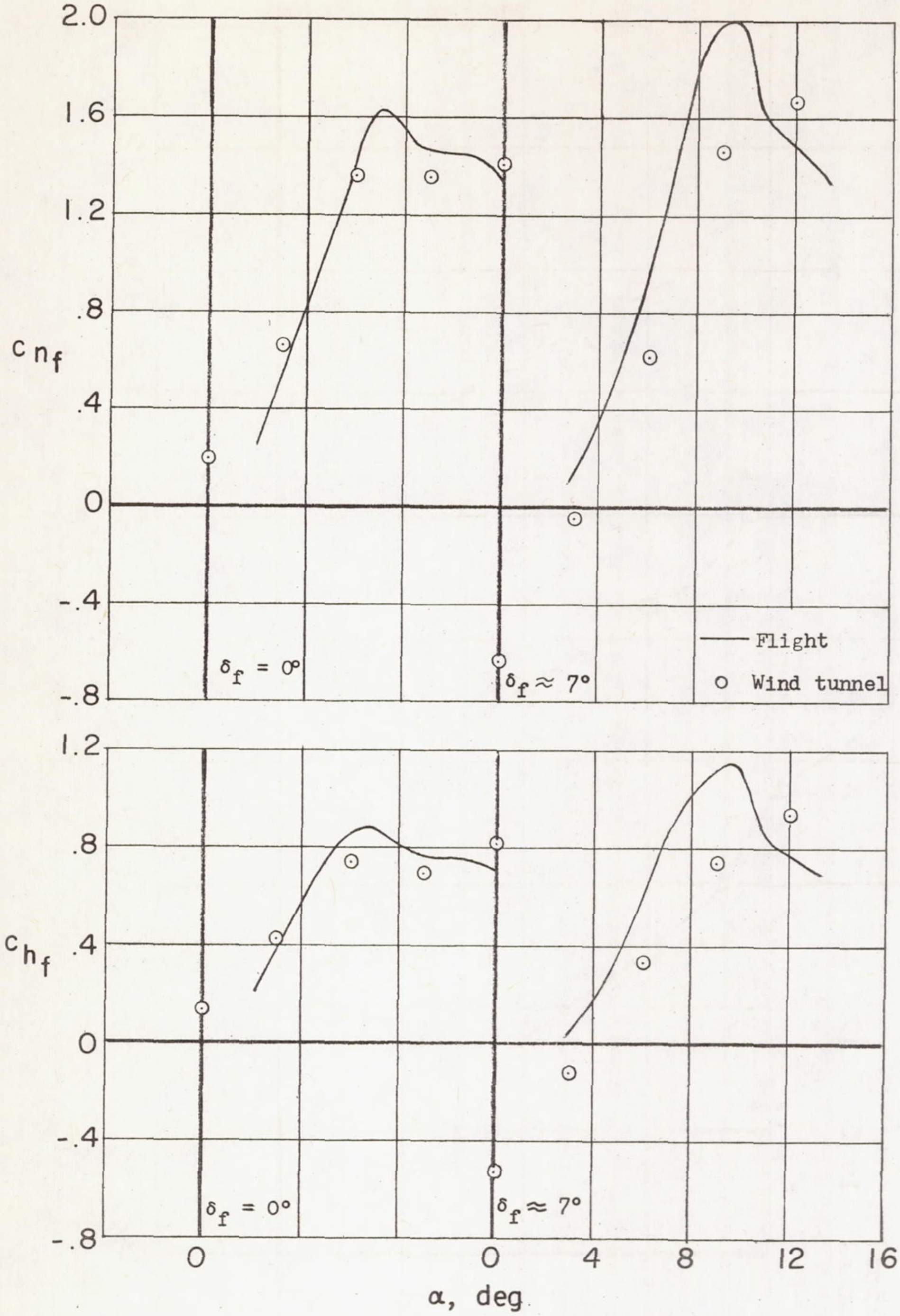

Figure 16.- Comparison of flight data with wind-tunnel results of reference 8 for midsemispan stations of the X-3 wing. Leading-edge-flap characteristics. $M \approx 0.80$.